Synthesis of silica aerogels and their application as a drug delivery system

von Dipl.–Chem. Irina Smirnova

aus Leningrad

von der Fakultät III - Prozesswissenschaften -

der Technischen Universität Berlin

zur Erlangung des akademischen Grades

Doktor der Ingenieurwissenschaften

- Dr.-Ing. -

genehmigte Dissertation

Promotionsausschuss:

Vorsitzender: Prof. Dr.-Ing. M. Kraume

Gutachter: Prof. Dr.-Ing. W. Arlt

Gutachter: Prof. Dr. M. Buback

Tag der wissenschaftliche Aussprache : 26. August 2002

Berlin 2002

D83

Acknowledgements

My student coworkers, Jörg Bläsing, Thinh Nguyen-Xuan, Alfonso Gonzalez, Jozo Mamic, Stefanie Herzog and Elizabeth Willams made the most part of the experimental work. Mihaela Dragan made a systematical investigation of the optimal reaction conditions. I especially appreciate the help of Jozo Mamic, who always showed a strong interest in our work, helped to solve endless technical problems and made a lot of experiments much easier with the useful tricks, that he invented. Jozo and Elizabeth also helped a lot by the fine correction of the text.

The apparatus were constructed with the help of Lothar, Uwe, Dietmar, Shorty and Max. Without them, no experimental work could be possible. Peter Stübing was a "good spirit" of my autoclave during the first year. I learned a lot from him and I am happy that even after retiring he still finds some time to discuss the technical problems that appear. Susanne Hoffmann and Christina Eichenauer helped a lot with the experiments. When the circumstances were not so lucky, Susanne always had some encouraging words for me.

Birgit and Manuela helped me a lot to find a way through the endless forms, invoices, formal letters, etc.

Last but not least, many cordial thanks to my dear parents. Without their help I would never finish my Ph.D. During my whole life they were ready to listen to me any time, gave good advice and were really interested in what I was doing. Also our scientific discussions were always fruitful. Special thanks to my mother, who spent so many hours for the correction of the text of this thesis.

Also, many thanks to all my friends, who supported me psychologically during the writing of this thesis and helped keep me a good mood even in the most difficult moments.

Table of contents

List of abbreviations

Abbreviation

ACN	Acetonitrile
BET	Brunauer, Emmett, Teller method
DDS	Drug Delivery System
DMF	Dimethylformamide
DMSO	Dimethylsulfoxide
EtOH	Ethanol
HMDSO	Hexamethyldisiloxane
HTSCD	High temperature supercritical drying
IR	Infrared region
LTSCD	Low temperature supercritical drying
MeOH	Methanol
MIP	Mercury intrusion
NAD	Nitrogen adsorption/desorption
NIR	Near infrared region
SAXS	Small angle X-ray scattering
SCD	Supercritical drying
SEM	Scannig electron microscopy
TEM	Transmission electron microscopy
TEOS	Tetraethylorthosilicate
TMCS	Trimethylchlorosilane
TMOS	Tetramethylorthosilicate
TPM	Thermoporometry
UV/VIS	Ultraviolet/visual region

Symbols

C	[-]	Constant in BET equation
C_i	[g/g]	Concentration of the substance i, wt%
$C_{CO_2}^{opt}$	[g/g]	Optimal CO_2 concentration in the liquid phase, wt %
D_{AB}	[m²/s]	Diffusion coefficient
γ_{SL}	[J/mol]	Specific energy of the solid-liquid interface
γ_{VL}	[J/mol]	Specific energy of the vapour-liquid interface
γ_{SV}	[J/mol]	Specific energy of the solid-vapour interface
H	[m]	Height to which the liquid rises in the capillary
K	[m⁻¹]	Curvature of the meniscus
M_w	[g/mol]	Mol weight
P	[bar]	Pressure
P^{cr}	[bar]	Critical pressure
P_{cap}	[bar]	Capillary pressure
P^{LV}	[bar]	Vapour pressure of the pure component
q_a	[g/g]	Weight adsorbed per unit of adsorbent
q_m	[g/g]	Maximum load of the adsorbent
R	[nm]	Capillary radius
ρ	[g/cm³]	Density
ρ_{target}	[g/cm³]	Target density of the aerogel
T	[K]	Temperature
T^{cr}	[K]	Critical temperature
t_{gel}	[h]	Gelation time
θ	[grad]	Contact angle
$t_{gel}^{CO_2}$	[h]	Gelation time with CO_2 addition
V	[m³]	Volume
V_a	[m³]	Volume adsorbed by a solid interface
V_{sol}	[m³]	Volume of a sol solution
X	[mol/mol]	Mol fraction

Summary

This work deals with the production of silica aerogels and their potential applications in the pharmaceutical industry.

Synthesis of silica aerogels is rather expensive. A lot of efforts have been made to find a way to decrease the cost of aerogel production. An important factor of the synthesis of low density aerogels is gelation time. Gelation time can be very long, especially in the case of low density aerogels. Different types of catalysts were used in order to accelerate the gelation.

In this work, it is suggested to use CO_2 to enhance the gelation process. It is shown, that the addition of CO_2 during the sol-gel process leads to the fast gelation. The influence of different factors, like temperature, component ratio, and solvent nature on this process is also described. Special attention is given to the experimental determination of the optimal CO_2 concentration needed for gelation at different process conditions. For the evaluation of this process, physical properties of the aerogels synthesized by this method are determined and compared with those obtained by conventional methods.

The second part of this work deals with the application of silica aerogels as a drug delivery system (DDS). Being environmentally benign and non-toxic, silica aerogels can be used in the pharmaceutical industry. Their large surface area and open pore structure make them to an ideal potential carrier material.

In this work, it is suggested the use of hydrophilic silica aerogels as a carrier material for pharmaceuticals. The loading of silica aerogels with pharmaceuticals can be made by different processes, in particular by adsorption. Silica aerogel are loaded with active compounds (drugs) by the adsorption from the supercritical CO_2 solution.

The characteristics of the corresponding aerogel-drug formulations, like drug concentration and stability, are studied in order to prove whether the process suggested in this work is suitable for the pharmaceuticals.

Also, the release of the corresponding drugs from such formulations is investigated. It is expected that the drug release from an aerogel-drug formulation is faster then that of crystalline drugs. Pharmaceuticals adsorbed on silica aerogels get a larger surface area, which should lead to faster dissolution of the compound in water. Moreover, the easily collapsing aerogel structure in water also favors a faster release.

Based on these experiments, the application of silica aerogels as a drug delivery system is discussed.

Kurzfassung

Diese Arbeit beschäftigt sich mit der Herstellung von Silica Aerogelen und deren potentiellen Anwendung als Medikamententräger.

Die Herstellung von Silica Aerogelen ist sehr zeit- und kostenintensiv. Ein wichtiger Parameter des Herstellungsverfahrens ist die Gelierungszeit. Die Gelierungszeit kann, insbesondere bei der Synthese von Silica Aerogelen niedriger Dichte, sehr lang sein. Verschiedene Katalysatoren wurden bereits erprobt mit dem Ziel, die Gelierungszeit zu verkürzen.

In dieser Arbeit wird der Gelierungsprozess in der Gegenwart von Kohlendioxid untersucht. Es konnte gezeigt werden, dass die Gelierung durch die Zugabe von CO_2 während des Sol-Gel Prozesses wesentlich beschleunigt wird. Der Einfluss der Prozessbedingungen, wie Temperatur, Konzentration der Reagenzien und die Art des Lösungsmittels auf die Reaktionsbeschleunigung wird untersucht. Besondere Beachtung wird auf die Abhängigkeit der für die Gelierung benötigten CO_2 Konzentration von den Prozessbedingungen gelegt. Die physikalischen Eigenschaften der nach dieser Methode hergestellten Aerogele werden mit den jeweiligen Eigenschaften der konventionell hergestellten Aerogele verglichen. Anhand dieser Ergebnisse werden die Vor- und Nachteile des vorgeschlagenen Herstellungsverfahrens diskutiert.

Der zweite Teil dieser Arbeit beschäftigt sich mit der Anwendung der Silica Aerogele als Wirkstoffträger. Da Silica Aerogele gesundheitlich unbedenklich sind, werden sie bereits im Bereich der Pharmazie (beispielsweise als Fliesshilfsmittel zur Tablettenherstellung) eingesetzt. Im Rahmen dieser Arbeit wird die Anwendung von hydrophilen Silica Aerogelen als Wirkstoffträger untersucht. Die Beladung der Silica Aerogele mit einem Wirkstoff erfolgt durch Adsorption aus überkritischen Gasen. Die Eigenschaften der resultierenden Wirkstoff-Aerogel Formulierungen, wie die Wirkstoffkonzentration und chemische Stabilität werden experimentell bestimmt. Auch die Freisetzungskinetiken der Wirkstoffe aus solchen Formulierungen werden untersucht. Es konnte gezeigt werden, dass die Freisetzung des Wirkstoffs aus dem Silica Aerogel wesentlich schneller als aus dessen kristalliner Form erfolgt. Die Ursache für die beschleunigte Freisetzung ist die große innere Oberfläche des auf dem Aerogel adsorbierten Wirkstoffs, sowie die augenblickliche Zerstörung des Aerogelgitters in wässrigen Medien.

Aufgrund dieser experimentellen Ergebnisse wird der potentielle Einsatz von Silica Aerogelen als Medikamententräger diskutiert.

1. Introduction and purpose of project

An aerogel is one of the most fascinating solid materials existing. It is a very light and highly transparent polymer material, which is often called "frozen smoke", because of its hazy blue appearance.
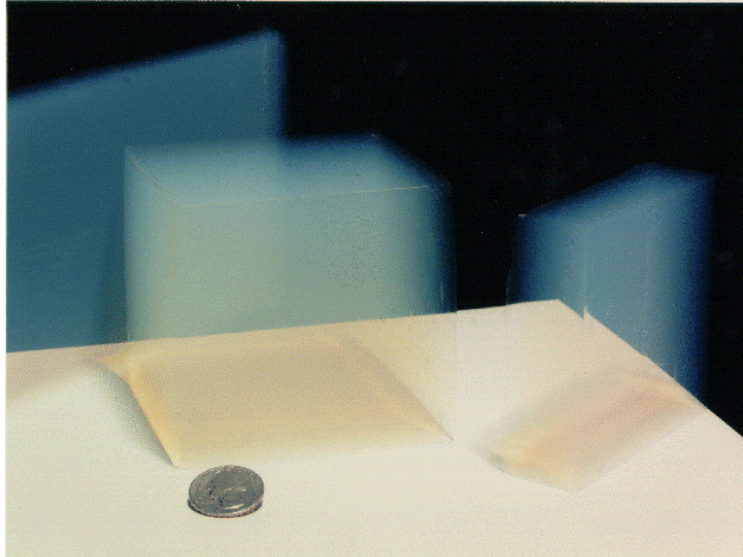
Figure 1-1 Samples of silica aerogels

An aerogel is not conventional foam, but is a special porous material with extreme microporosity on a micron scale. It is composed of individual particles only a few nanometers in size, which are linked in a three - dimensional structure.

An aerogel is made by the so called "sol-gel process". During this process, organic compounds containing silica undergo a chemical reaction producing silicon oxide (SiO_2). This mixture is a liquid at the beginning of the reaction, and becomes more and more viscous as the reaction proceeds. When the reaction is finished, the solution looses its fluidity and the whole reacting mixture turns into a gel. This gel consists of a three-dimensional network of silicon oxide filled with the solvent. During the special drying procedure, the solvent is extracted from the gel body leaving the silicon oxide network filled with air. This product is called aerogel. Aerogels can be synthesized not only from silicon oxide (silica aerogels), but also from different organic and inorganic substances, for example titanium oxide, aluminium oxide, carbon etc.

This novel material has many unusual properties, such as a low thermal conductivity, refractive index, sound speed, along with a high surface area and thermal stability. An aerogel can be made with a density only three times larger than that of air. Aerogels also have many applications in different fields of science and industry. One of the most fascinating

applications is the insulation of space shuttles with aerogels, practiced by NASA (USA). Many scientific groups are currently working with aerogels, which is evident by the International Symposia on Aerogels, taking place every three years [ISA 1-6]. Both synthesis and innovative applications of aerogels are of great interest at the present time.

In this work we will focus on silica aerogels. First, the different methods for synthesizing of silica aerogel, then their properties and applications are presented. The influence of different parameters on the physical properties of silica aerogels is discussed in detail in order to show how the targeted properties of aerogels can be adjusted.

Synthesis of silica aerogels is still very expensive. A lot of efforts have been made to find a way to decrease the cost of aerogel production. An important factor of the synthesis of low density aerogels is gelation time. Gelation time can be very long, especially in the case of low density aerogels. Different types of catalysts were used in order to accelerate the gelation.

In this work, it is suggested to use CO_2 to enhance the gelation process. For several years, CO_2 was used for the supercritical drying of aerogels, but as far as it is known, its influence on the gelation process itself was never reported.

In the first part of this work the gelation process in the presence of CO_2 is investigated. The influence of different factors, like temperature, component ratio, and solvent nature on this process is also described. Special attention is given to the experimental determination of the optimal CO_2 concentration needed for gelation at different process conditions.

For the evaluation of this process, physical properties of the aerogels synthesized by this method should be measured and compared with those obtained by conventional methods. Based on this information the advantages and disadvantages of aerogel synthesis modified by CO_2 – enhanced gelation will be discussed.

The second part of this work deals with the application of silica aerogels as a drug delivery system (DDS).

Being environmentally friendly and non-toxic, silica aerogels can be used in the pharmaceutical industry. Their large surface area and open pore structure make them to an ideal potential carrier material.

In this work, the authors suggest the use of hydrophilic silica aerogels as a carrier material for pharmaceuticals. The carrier material has a strong influence on the mechanism of drug delivery. That is why a variety of different carriers are usually tested for the same drug in order to find the most effective mechanism of drug delivery for every particular application.

The loading of silica aerogels with pharmaceuticals can be made by different processes, in particular by adsorption. Adsorption from the liquid phase is widely used in the pharmacy to load some carrier materials. In the case of silica aerogels adsorption from a liquid phase is not a suitable method, because hydrophilic silica aerogels collapse in water.

It is suggested in the present work to load silica aerogel with active compounds (drugs) by the adsorption from the supercritical CO_2 solution. This process is applied for the loading of porous materials with chemicals, but has been never used for the loading of aerogels with drugs.

The process parameters have to be optimized first. After establishing the procedure for a test substance, different pharmaceuticals are tested. The characteristics of the corresponding aerogel-drug formulations, like drug concentration and stability, are studied in order to prove whether the process suggested in this work is suitable for the pharmaceuticals.

Also, the release of the corresponding drugs from such formulations is investigated. It is expected that the drug release from an aerogel-drug formulation is faster then that of crystalline drugs. Pharmaceuticals adsorbed on silica aerogels get a larger surface area, which should lead to faster dissolution of the compound in water. Moreover, the easily collapsing aerogel structure in water also favors a faster release.

Based on these experiments, the application of silica aerogels as a drug delivery system is discussed.

2. Synthesis and application of silica aerogels: State of the art

2.1. Synthesis of silica aerogels

The synthesis of silica aerogels can be divided into 3 general steps:

a) **Preparation of the gel**. The gel phase is normally obtained by the so-called sol-gel process. In this work, the terms "sol" and "gel" are used as defined in [Gesser 1989]. *Sol*: A sol is a colloidal system of liquid character in which the dispersed particles are either solid or large molecules whose dimensions are in the colloidal range (1-1000 nm). *Gel*: A gel is a colloidal system of solid character in which the dispersed substance forms a continuous, coherent framework that is interpenetrated by a system (usually liquid) consisting of kinetic units smaller than colloidal entities. A gel can be easily imagined as a three-dimensional network filled with a solvent. Gels frequently contain only a small amount of the dispersed phase (1-3%) and exhibit some measure of rigidity and elasticity. The gels are usually classified according to the dispersion medium used, e.g., hydrogel or aquagel, alcogel and aerogel (for water, alcohol, and air, respectively). The most common example of a gel is gelatin. A large variety of chemical reactions can be used to obtain a gel phase. The choice of reaction depends on the desired properties of the final aerogel product.

b) **Aging of the gel.** The gel prepared in the first step is aged in its mother solution. This aging process strengthens the gel, so that shrinkage during the drying step is kept to a minimum.

c) **Drying of the gel.** In this step, the gel should be freed of the pore liquid. To prevent the collapse of the gel structure, drying is made to take place under special conditions such as high temperature or high pressure.

All methods of aerogel production involve these three general steps. Additional procedures can also be undertaken in order to influence the final product structure. There are, currently, a variety of methods for silica aerogel synthesis. This chapter deals with the chronological development of methods for aerogel synthesis.

2.1.1   Process based on sodium silicate: Kistler's work

The first report concerned with the preparation of silica aerogels was published by Kistler in 1931 [Kistler 1931]. Here, removal of the liquid from a gel and its replacement by a gas, specifically, by air, (so as to prevent shrinkage of the gel) was attempted. Hence, the target product was termed an 'aerogel'.

Until Kistler's work, the replacement of the gel pore liquid was performed only through the use of another liquid. Biologists, for example, successfully replaced water from gelatinous tissues by alcohol, xylene and paraffin. The final result was a gel in which an organic solvent was the dispersed phase instead of water. This procedure was used for preparing microscopic sections.

The problem with conventional drying of the gel in air, however, was that it resulted in considerable shrinkage of the gel. This phenomenon can easily be explained by the formation of liquid-vapour interfaces within the gel network that result in large surface tensions, causing a partial collapse of the network. The products of this drying method were hard, glassy masses (xerogels), which were still porous, but where the porosity did not exceed 50% [Fricke 1986].

Kistler`s idea to avoid any collapse can be best understood by his own words: "Obviously if one wishes to produce an aerogel, he must replace the liquid with air by some means in which the surface of the liquid is never permitted to recede within the gel. If a liquid is held under the pressure always greater than the vapour pressure, and the temperature is raised, it will be transformed at the critical temperature into a gas without two phases having been present at any time." [Kistler 1931]. He concluded that it is possible to vent out the supercritical fluid, and to end up with an air-filled non-collapsed gel structure.

The first experiments were done with silica gels filled with water [Kistler 1931].

To synthesize a silica gel Kistler reactedf sodium silicate (water glass) with hydrochloric acid:

$$Na_2SiO_3 + 2\,HCl \quad \rightarrow \quad [SiO_2 \bullet x\,H_2O] + 2\,NaCl \qquad\qquad (1)$$
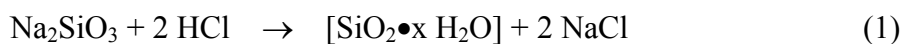
The gels were dried by placing them in an autoclave and raising the temperature until the pressure exceeded the critical pressure and then slowly venting the vapors from the autoclave. The main problem of this process was its high temperatures and pressures ($T^{cr}_{water} = 374°C$, $P^{cr}_{water} = 221$ bar). Furthermore, the corrosivity of the supercritical water is cause to a number of technical problems. To avoid these problems, Kistler extracted the water with ethanol, making use to the fact the two liquids are miscible. In this way, milder process conditions

(T^{cr}_{MeOH} = 243°C, P^{cr}_{MeOH} = 63.8 bar) could be utilized. The aerogels obtained in this manner ranged from transparent to highly opalescent. The density of the aerogel was varied by variation of the silica concentration in the reaction system. Silica aerogels exhibiting densities between 0.02 and 0.1 g/cm^3 were produced in this manner [Kistler 1937].

This method was first extended to other inorganic gels and then to organic materials. Kistler described the formation of aerogels of alumina, ferric oxide, stannic oxide, nickel oxide, cellulose, gelatin etc. The first paper on an aerogel [Kistler 1931] ended very optimistically: "and we see no reason why this list may not be extended indefinitely."

In spite of Kistler's optimistic prognosis, aerogels did not find their application in his time. One of the reasons was surely that the synthesis was highly tedious and time consuming.

The reason for this was that sodium chloride, formed as a by-product in the reaction (1), had to be removed from the gel by several washing cycles. This required more than one week to obtain a small amount of aerogel.

The aerogels were pretty much "forgotten" until the 1960`s, when they were rediscovered.

2.1.2 Processes based on tetraalkylorthosilicate

2.1.2.1 The one-step process

The following publication describing the preparation of an aerogel dates back to 1966 [Peri 1966]. Here, tetraethylorthosilicate (TEOS) is hydrolyzed in ethanol in the presence of hydrochloric acid. This reaction can be summarized as follows:

$$Si(OCH_2CH_3)_4 + 2H_2O \xrightarrow{Cat.} SiO_2 + 4HOCH_2CH_3 \qquad (2)$$
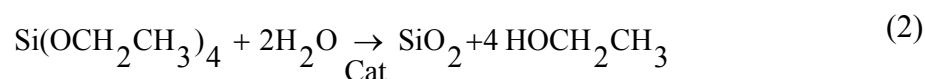
The gel obtained by this reaction was altered in water at 100°C, the water was then replaced by methanol and the gel was dried supercritically.

This method was further developed and silicate gels were synthesized by using different tetrafunctional siliconalkoxide precursors, the general chemical structure of which can be denoted as $Si(OR)_4$, where R denotes an alkyl group ($R=C_nH_{2n+1}$, n=1,2,3....) [Nicolaon 1968 -1], [Nicolaon 1968-2]. The sol-gel process of silicon alcoxides is divided into the following stages:

a) production of monomers (sol solution) by the hydrolysis of precursors;
b) formation of siloxane bonds and oligomers through condensation and polymerization;
c) growth of particles and clusters (aggregation between a cluster and a monomer or between a cluster and a cluster);

d) gelation;

e) aging.

The hydrolysis reaction (3) replaces alkoxide groups (OR) with hydroxyl groups (OH).

$$\equiv Si-OR \ + \ H_2O \ \underset{\text{Esterification}}{\overset{\text{Hydrolysis}}{\longleftrightarrow}} \ \equiv Si-OH \ + \ ROH \tag{3}$$
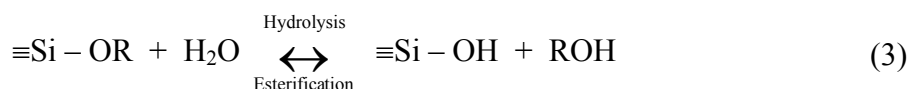
The minimal amount of water for the complete hydrolysis of the ester is determined by the number of groups that can be hydrolyzed.

Water and alkoxysilane are practically immiscible, so additional solvent is needed to homogenize the mixture. A variety of solvents are used for this purpose, alcohols, acetone, dioxane, tetrahydrofurane being a few examples. In the case of alcohols, it should be noted that despite it being used as a solvent, alcohol can participate in an esterification reaction and thus reduce the hydrolysis rate.

The typical phase diagram [Brinker 1990] of the system alkoxylane-water-solvent is shown in Figure 2-1.
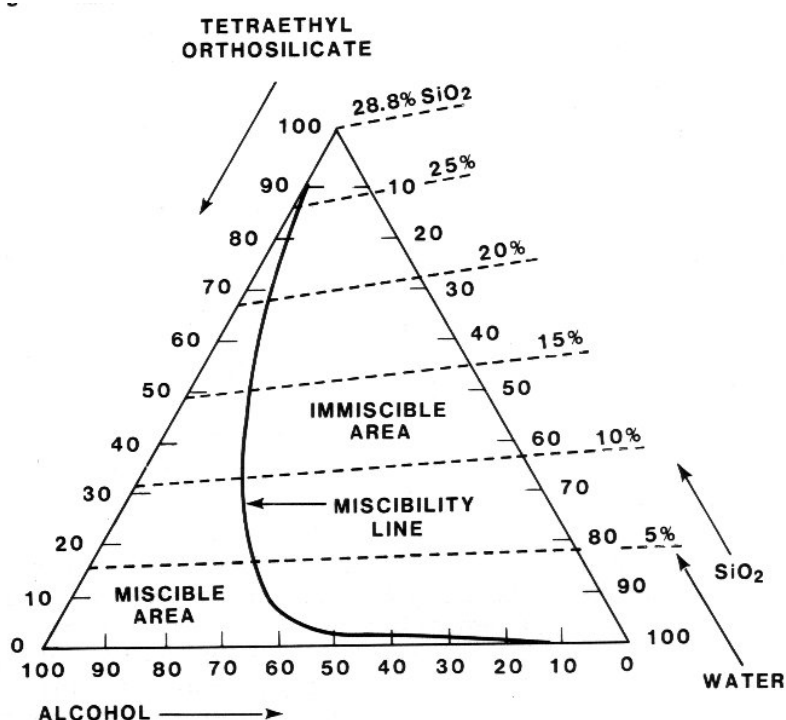
Figure 2-1 Ternary phase diagram of the system TEOS-ethanol-water at 25°C [Brinker 1990]

Simultaneously with hydrolysis (3) the condensation reaction (4),(5) takes place. The product of hydrolysis, silicidic acid (substituted to different degrees), is dehydrated and polymerized through siloxane linkages (Si-O-Si). Polymerization to form siloxane bonds occurs either by an alcohol-producing (4) or a water-producing (5) condensation reaction.

$$\equiv Si - OR + HO - Si \quad \overset{\text{alcohol condensation}}{\longleftrightarrow} \quad \equiv Si - O - Si \equiv + ROH \qquad (4)$$

$$\equiv Si - OR + HO - Si \quad \overset{\text{water condensation}}{\underset{\text{hydrolysis}}{\longleftrightarrow}} \quad \equiv Si - O - Si \equiv + H_2O \qquad (5)$$
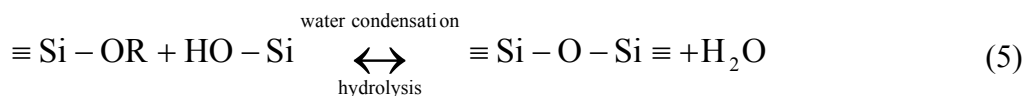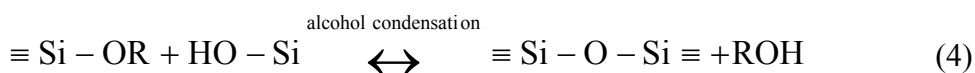
A typical sequence of condensation products is monomer, dimer, linear trimer, cyclic trimer, cyclic tetramer and higher-order rings. This sequence of condensation requires both depolymerization (ring opening) and the availability of monomers, which are in solution together with the oligomeric species and/or are generated by depolymerization (reverse reaction of (4) and (5)). It is important to note that in alcohol-water solutions, normally employed in sol-gel processing, the depolymerization rate is lower than that in aqueous media, especially at low pH.

One of the advantages of the method based on alcoxisilicates is the fact that impurities, such as salts, are not formed as side-products during the reaction. Thus the tedious washing of the alcogel, an essential step in Kistler's method, is not necessary.

In this method, the reaction proceeds in a single step. The initial solvent is alcohol, so no substitution of the solvent is needed. Drying of the silica gels is performed at the supercritical conditions of the corresponding solvent. Using this method, silica aerogels can be prepared in a matter of a few days, in contrast to weeks, required for synthesis using Kistler`s procedure. Several catalysts (acidic and basic) were used in this process and their influence on the physical properties of the aerogels, such as the surface area and pore size has been reported [Nicolaon 1968 -1], [Nicolaon 1968 -2], [Nicolaon 1969].

Since then, various publications have been devoted to aerogel production. Sol-gel processes of silica have been studied in detail and some have even been employed for the production of silica aerogels in industrial scale. In 1984, a pilot plant was built in Sweden featuring a huge autoclave designed to process 100 sheets of aerogel, (measuring 60cm x 60 cm x 3cm) per run [Henning 1981]. The process was based on the alcoxisilicate method described above. Tetramethylorthosilicate (TMOS) was hydrolyzed in the presence of ammonia as catalyst. Methanol was used as solvent, allowing the final gel to be dried at the supercritical conditions of methanol. Highly transparent aerogels were obtained with a density of 70-250 kg/m^3, pore size of 10-20 nm and a specific surface area of 700 m^2/g [Henning 1990].

2.1.2.2   The two-step process

The fundamental study of sol-gel processes in a silicate system was done by Brinker's group (Sandia National Laboratories, Albuquerque). Here the influence of the rate of hydrolysis and gelation on the structure of the silica gels was studied [Brinker 1982]. It was shown, that although hydrolysis and condensation take place concurrently, regulation of the rate of both these processes is possible through changing the amount of water and the pH value of the solution. This conclusion led to the formulation of the two-step sol-gel process.

In the **first step,** TEOS is mixed with a substoichiometric amount of water, solvent and acid, particularly HCl, as catalyst. It was shown, that, at these conditions, hydrolysis proceeds very rapidly and all added water is consumed in the first few minutes of the reaction to produce a distribution of hydrolyzed monomers. Subsequent condensation results in the formation of polymers, i.e. dimers and chain-like or cyclic species. It was supposed that after this step, the water is fully consumed and the resulting polymers are fully esterified. The following net equation was suggested, based on the results of the gas chromatography analysis [Brinker 1982]:

$$n \; Si(OR)_4 + n \; H_2O \xrightarrow[Cat.]{} n \; SiO(OR)_2 + 2n \; (ROH) \qquad (6)$$
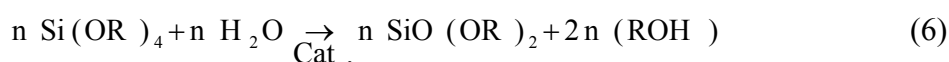
During the **second step** hydrolysis is completed by the addition of water under basic or acidic conditions. A distribution of oligomeric and monomeric species resulting from the first step is hydrolyzed resulting in a condensed gel. Two extreme cases should be considered: the case in which hydrolysis proceeds much more rapidly than condensation and vice versa.

In the first extreme case (rapid hydrolysis, slow condensation), there will be much more hydroxyl groups, as alkoxy groups bond to silicon when condensation begins. The most commonly proposed mechanism under these conditions is a base-catalyzed, nucleophilic attack on silicon [Iler 1979].

$$(RO)_3Si\text{-}OH + OH^- \rightarrow (RO)_3SiO^- + H_2O \qquad \text{(fast)} \qquad (7)$$

$$(RO)_3SiO^- + (RO)_3Si\text{-}OH \rightarrow (RO)_3Si\text{-}O\text{-}Si(RO)_3 + OH^- \; \text{(rate determining)} \qquad (8)$$
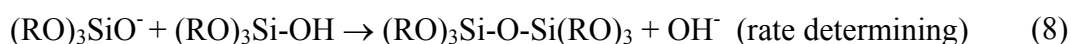
The extent of reaction (7) increases with increase of the acidity of the silanol proton (i.e. the H on $(RO)_3SiOH$). The acidity of this proton increases as the basicity of the other groups bonded to the silicon decreases. For example, the reaction of monosilicic acid to form the dimer, $(HO)_3SiOSi(OH)_3$, results in an increased acidity of the silanol groups remaining in the dimer,

because $(HO)_3SiO^-$ is a weaker base than OH^-. In general, reaction (7) will occur to a greater extent for a polymer in which the silicon atom is cross-linked to another silicon atom via a bridging oxygen than for monosilicic acid. Thus, the more cross-linked species will be most likely to undergo reaction (7) and subsequently be available for reaction (8). In the case of rapid hydrolysis, the larger highly condensed polymers tend to react with feebly acidic monomers to form even more highly condensed species. The larger polymers grow at the expense of the smaller ones. This results in relatively large polymers with extensive cross linking and essentially pure SiO_2.

In the second extreme case (slow hydrolysis, rapid condensation) the formation of polymers is governed by the mechanism of hydrolysis. We consider, for example, the acid-catalyzed hydrolysis, expected to take place by an S_N2 mechanism. Note: The role of the catalyst will be discussed later.
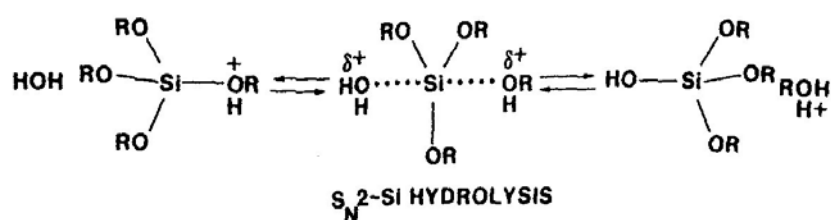
Figure 2-2 S_N2 mechanism of the acid hydrolysis

This mechanism involves the electrophilic attack on the alkoxide oxygen. This step is not principally sensitive to the electronic effects of the other groups bonded to the silicon atom, but is highly sensitive to steric effects. Consequently, monomers are more rapidly hydrolyzed than the end groups of polymer chains. The end groups of a chain are, in turn, more rapidly hydrolyzed than the middle groups of chains [Brinker 1982]. The silanols on these weakly cross-linked units condense more rapidly than silanols on more highly cross-linked species. The resulting polymer is relatively small and not highly cross-linked. These conclusions were also confirmed experimentally [Brinker 1982]. In addition, the authors illustrated that both cases described above, and thus the corresponding microstructure of the gels, can be realized in the two-step process by varying the amount of water and the nature of the catalyst [Brinker 1984]. They also demonstrated that a basic catalyst used in the second step leads to faster particle growth and internal condensation.

Thus, it is highly favorable to run the two-step procedure using an acid catalyst in the first step and a basic catalyst in the second step.

Boonstra et al. studied the two-step procedure further, paying particular attention to the second (base-catalyzed) step [Boonstra 1989]. Investigations were carried out on the influence of the following factors on the rate of gelation, using TEOS as the precursor: HCl concentration, NH_4OH concentration, temperature and hydrolysis time [Boonstra 1988]. The following conclusions were formulated:

-   As the hydrolysis time increases, the gelation time first decreases but then is followed by an increase (see Figure 2-3). A minimum gelation time was found to be achieved at a hydrolysis time of 30 min. This behavior can be explained as follows: initially, the concentration of silanols, which can then participate in the condensation reaction, increases with the hydrolysis time and as a consequence the gelation time in the basic step decreases. When in the first step almost all water added has been consumed, the dimerisation of silanols becomes the dominant reaction, as this results in a decrease of the silanol concentration and, thus, an increase of the gelation time. This result is in agreement with that of [Colby 1986].
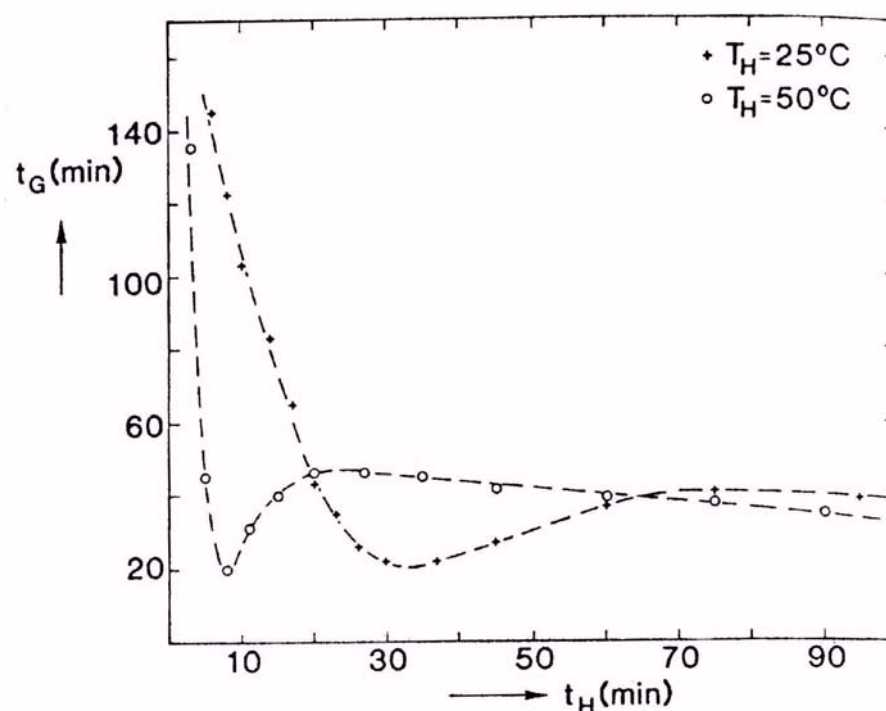
Figure 2-3 Dependence of the gelation time on the hydrolysis time [Boonstra 1988].
Component molar ratio 1TEOS : 4EtOH : 2.5 H_2O

-   The rate of gelation is inversely proportional to both HCl and NH_4OH concentrations. This can be explained by the fact that HCl catalyses the hydrolysis and NH_4OH catalyses

the condensation step. Because the gelation process depends on the concentration of the hydrolyzed TEOS molecules, the higher the hydrolysis rate, the shorter the gelation time.

- The gelation time increases with an increasing ethanol concentration. Ethanol dilutes the initial solution, retarding the condensation process, due to larger distances between the partially condensed species.

These conclusions were taken into consideration during the present work, aiding to find the optimal process conditions.

One of the disadvantages for both the one-step and the two-step procedures is the long gelation time, especially for low-density aerogels ($\rho < 0.1$ g/cm^3). Because of stoichiometric and miscibility conditions, the maximum density of monolithic aerogels cannot exceed 0.3 g/cm^3. Lower densities can be achieved by dilution of initial reactants with additional alcohol. However, the higher the dilution, the longer the time that is required for the gelation to occur. Also, at some maximum dilution level, the reesterification of silicic acid (9) inhibits the gelation, thereby setting the minimum density limit for the low density aerogels.

$$Si\,(OH)_4\ +\ ROH\ \rightarrow\ (HO)_3\,Si\,OR\ +\ H_2O \tag{9}$$

The lowest aerogel density which can be achieved by the single step procedure is 0.02 g/cm^3 [Tewari 1986]. In this case, the gelation process would take as long as 14 days.

2.1.2.3 Further modification of the two-step process

A modified two-step process has been described, in which the alcohol generated by the reactions in the first step, was removed by distillation, leaving a **partly condensed silica intermediate** [Schaefer 1987]. This intermediate was dissolved using another alcohol before completion of the second step, so that the reesterification reaction could be kept to a minimum.

Tillotson and Hrubesh [Tillotson 1992] developed the two-step process further, suggesting a conditions which allow for the production of aerogels with extremely low densities (up to $\rho = 0.003$ g/cm^3) within a reasonable time period. Use of a non-alcoholic solvent in the second step for avoidance of the reesterification reaction was suggested This procedure is as follows:

- In the first step, a non-stoichiometric amount of water and acid catalyst is added to the alkylorthosilicate-alcohol solution. A minimal amount of alcohol is used in this step, enough to keep the solution homogenous. After completion of the first step (the hydrolysis time being approximately 16 hours), the alcohol added in the first step as well as the

alcohol produced during the reaction (2) is removed from the system by distillation. The viscous product remaining after distillation is a partly hydrolyzed and partly condensed silica (**CS**), which can be stored for later use.

- In the second step CS is diluted with a non-alcoholic solvent, such as acetone, ether or acetonitrile. Additional water and basic catalysts (NH_4OH) are added to complete hydrolysis. The gelation time depends on the target density of the aerogel, but even in case of the most diluted samples, it does not exceed 72 hours.

The aerogels produced in this way are transparent and exhibit microstructure characteristics of polymeric gels [Tillotson 1995]. This procedure allows for shorter gelation times, but also has also several disadvantages. Including the necessity of very pure reagents (the authors used triple distilled TMOS) and a long hydrolysis time (16 hours).

2.1.3   Influence of the process parameter of the aerogels properties

Both the one-step and two-step procedure is used today for silica aerogel production. It is expected, that the aerogel properties are strongly influenced by the process parameters. Different synthesis conditions and their influence on the physical properties of the aerogels are discussed in the following chapter.

2.1.3.1   Effect of solvents

The influence of the solvent nature was systematically studied only for the one-step process. In the case of low-density aerogels, the reacting mixture contains up to 95% solvent. Thus, the nature of the solvent used has a great influence on the reaction process.

Solvents may be classified as polar or nonpolar and as protic and aprotic [Morrison 1970].

- **Polarity** largely determines the solvating ability for polar and non-polar species. It can be described by using the dipole moment of the molecule. The dipole moment of a solvent determines the length over which the charge on one species can be "felt" by surrounding species. The lower the dipole moment, the larger this length. This is important in electrostatically stabilized systems (for example, electrostatic stabilization is more effective in systems with a lower dipole moment) and when considering the distance over which a charged catalytic species (OH^-, H_3O^+) is attracted to, or repelled from, potential reaction sites, depending on their charge [Brinker 1990]. Typical polar solvents are water and acetone.

- **Protic** solvents contain at least one hydrogen atom attached to an oxygen or nitrogen atom and, hence, are appreciably acidic. Through hydrogen bonding, such solvents tend to

solvate anions particularly strongly. Although the protic solvents dissolve the reagent and bring it into contact with the organic molecule, they concurrently drastically lower it's reactivity: the anions are less basic and less nucleophilic. Such solvents include water and alcohols.

- **Aprotic** solvents dissolve both organic and inorganic reagents, but, in dissolving ionic compounds, they solvate cations very strongly, and leave the anions relatively unencumbered and highly reactive. Bases become increasingly more basic and nucleophiles, increasingly more nucleophilic. Such solvents have moderately high dielectric constants and do not contain acidic hydrogens. Examples of aprotic solvents are dimethylformamide and dimethyl sulfoxide [Morrison 1970].

The combination of both concepts is possible. Some of the solvents used in the sol-gel process may be categorized as polar protic, polar aprotic and nonpolar. Examples of such solvents are given in Table 2-1.

Protic polar solvent	Aprotic polar solvent	Nonpolar
Methanol	Dimethylsulfoxide (DMSO)	Dioxane
Ethanol	Dimethylformamide (DMF)	Benzene
Formamide	Acetonitrile	Hexane
Water	Acetone	Chloroform

Table 2-1 Classification of solvents

The availability of labile protons also influences the extent of the reesterification (10).

$$\equiv Si - O - Si\equiv \ + \ ROH \ \rightarrow \ \equiv Si - OR \ + \ OH\text{--}Si\equiv \qquad (10)$$

Aprotic solvents do not participate in such reactions because they lack sufficiently electrophilic protons and are unable to be deprotonated to form sufficiently strong nucleophiles (e.g., OH^- or OR^-) necessary for these reactions. Therefore, compared to alcohol or water, aprotic solvents are considerably more inert; however, as discussed previously, they may influence the strength of nucleophiles or decrease the strength of electrophiles.

Systematic investigations of the hydrolysis and gelation time have been conducted by [Berndards 1991]. Here, however, the authors did not apply the results of their study to aerogels synthesis, but concentrated their efforts on sol-gel glasses and films. The influence of

different solvents on the hydrolysis rate was studied by [Bernards 1991]. It was reported, that the gelation time increased in the following sequence:

<div align="center">methanol < ethanol, 1-propanol, < 2-propanol.</div>
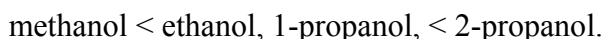
This can be ascribed to differences in proton activity of the catalysts in the solvent. It has been also found [Hasegawa 1988], that the exchange of alkoxy groups occurs when an alkoxy group is different from the alkoxy groups of the silane (Eq.(11)).

$$\equiv Si - O - C_2H_5 \; + \; ROH \; \rightarrow \; \equiv Si - OR \; + \; C_2H_5OH \qquad (11)$$
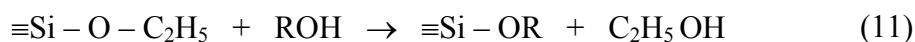
The exchange rate increases when the steric hindrance of the alkoxy group decreases:

<div align="center">methanol > ethanol > propanol > butanol</div>
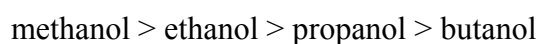
The exchange reactions can also influence the gelation time. This was confirmed by the investigation of the influence of butanol on the hydrolysis-condensation behaviour of TEOS [Bernards 1991]. It was shown, that an increasing butanol concentration results in a longer gelation time, as long as butanol is added in the first step.

Artaki et al. [Artaki 1986] investigated the influence of several protic and aprotic solvents on the hydrolysis and condensation of TMOS.

It was shown, that the gelation time under basic conditions increases in the following sequence [Artaki 1986]:

<div align="center">formamide < methanol < DMF < acetonitrile < dioxane</div>

The aprotic solvent (dioxane) is unable to hydrogen bond to the SiO⁻ nucleophile. Also, being nonpolar it does not tend to stabilize the reactants with respect to the activated complex. Therefore, dioxane results in a significant enhancement of the condensation rate and causes an efficient condensation leading to the formation of large, compact spherical particles. The gelation time required for this process is rather long and the gels show a finer morphology with smaller pores, but a larger average grain size [Artaki 1986].

Both methanol and formamide are protic solvents and they decelerate the condensation rate by deactivating the nucleophile through hydrogen bonding interactions. Moreover, due to their strong dipole moments, they can stabilize the negative charge localized on the reactants, to a greater extent. This results in an increase in the activation energy and consequently, in an

additional deceleration of the rate of condensation. Hydrogen bonding to incompletely condensed $\equiv$Si-O$^-$ groups prevents an efficient condensation process and promotes the formation of large micropores in the polymer network. The polymeric units consist of more highly branched structures rather than spherically condensed particles (as in the case of dioxane). The gelation time in this case is very short.

The dipolar aprotic solvents, (DMF and acetonitrile) also do not hydrogen bond to the nucleophilic silicate involved in the condensation reaction. However, due to their polarity, the anionic reactants are stabilized with respect to the activated complex, slowing down the reaction to some extent. Both the gelation time and grain size are in-between those of dioxane and methanol.

It was also reported [Roig 1998] that in the system TMOS – water – solvent, the gelation time under basic conditions is larger if acetone (polar, aprotic) is used as a solvent than in the case with methanol. This agrees with the results of Artaki et al. [Artaki 1985] and Pajonk et al. [Pajonk 1986].

It should be noticed, that both authors carried out the experiments at a relatively high alkoxide concentration (high target density) – i.e. conditions under which reesterification reactions do not occur to a large extent.

2.1.3.2   Steric effect

Steric hindrance also plays an important role in the sol-gel process.

The effect of the chain length of different alcohols on the gelation time was reported by [Rao 1994]. It was found, that the gelation time increases with an increase in the chain length (thus comparing methanol with butanol, a shorter gelation time is observed for methanol). This can be explained by steric effects: reesterification takes place and the substituents, that increase steric crowding, decrease condensation of the silanol groups and hence result in longer gelation time.

Lee, Kim and Yoo [Lee 1995] used the two-step procedure for the production of silica aerogels and found that one can use **no** solvent during the first hydrolysis step. They found that although alkoxide and water do not form a homogeneous solution at normal conditions, the miscibility could be sufficiently increased by controlling the pH value and process time. A mixture of 10^{-5} moles of HCl and 1.6 moles of water was added to 1 mol of TMOS dropwise under constant stirring. No alcohol was added during this first step. The solution remained homogeneous during the entire process Although the authors give no explanation, it can be supposed, that hydrolysis proceeds simultaneously with the addition of the HCl-water mixture

and the alcohol generated by the reaction dissolves in the water, which appears after the condensation step.

The advantage of using this method is that the mixture contains less alcohol after the first step. Therefore, the distillation time can be reduced or removed all together in the synthesis of low density gels.

2.1.3.3 Effect of catalysts

The fact that the hydrolysis and condensation of alkoxysilicates can be accelerated by using both acids and bases allows for a variety of catalysts to be used in this process.

As mentioned above, both hydrolysis and condensation depend greatly on the pH value of the reacting mixture. It should be noted that the effect of the catalyst must be considered separately for the one-step and two-step process, because of the different natures of the methods.

The one-step process. In the one-step process hydrolysis and condensation take place simultaneously. It is very difficult to separate both processes. The gelation time in this case is the result of both reactions. As already discussed, hydrolysis is accelerated by acid catalysts and condensation, by base catalysts. In the case of acid catalysis, the condensation reaction tends to start at a fairly late stage, whereas with basic catalysts, condensation starts relatively early. The mechanism of the two reactions vary with alteration of the catalysts. For instance, acid catalyzed hydrolysis is an electrophilic reaction (Figure 2-2). In this case, the reaction rate is governed by the concentration of H^+ in the solution. The lower the pH, the faster the reaction proceeds [Aelion 1950]. Hydrolysis of the first OR group on the TEOS molecule is fast, while the subsequent hydrolysis reactions are slow and depend on steric effects. As a result, monomers are hydrolysed more rapidly than chains, which in turn are hydrolysed faster than branches. This type of hydrolysis favours the formation of short linear chains giving rise to a polymer network that is rather weak [Cao 1994]. For base-catalyzed hydrolysis, a nucleophilic substitution of hydroxyl ions for OR groups occurs. Analogous to the acid reaction, the rate of the base catalyzed hydrolysis is a function of the hydroxyl concentration in solution [Aelion 1950]. The hydrolysis reaction is slow and is a rate-determining step, whereas the condensation is relatively fast. This type of reaction favours the formation of highly cross-linked polymers or colloidal particles [Cao 1994].

The influence of the pH on the gelation process was studied by [Brinker 1990]. The general dependence of the relative rate of reaction (v_{rel}) for both hydrolysis and condensation is presented in 2-4.
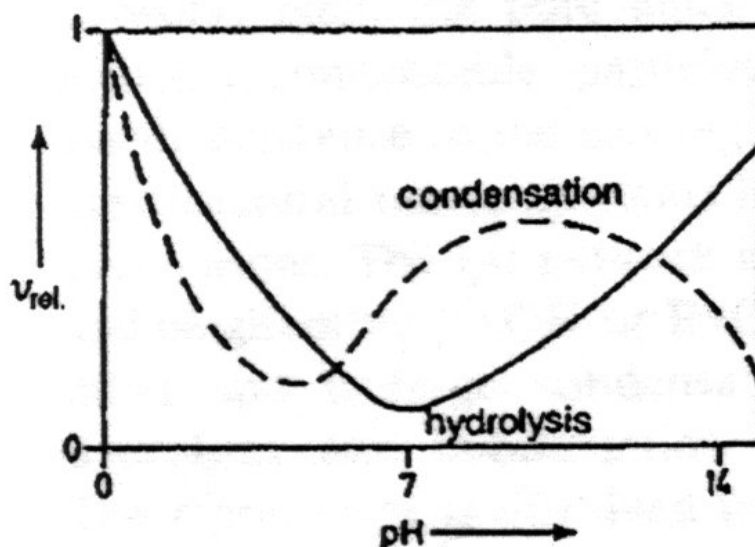
Figure 2-4 Dependence of the hydrolysis and condensation rates on the pH of the solution [Brinker 1990]

However, it was shown [Pope 1986] that the mechanisms described above appear to be applicable only when one considers the HCl versus the NH_4OH catalyzed reaction. Also, pH is not the only factor controlling the hydrolysis and gelation and thus, also the properties of silica gels.

One other factor is the nature of the catalysts. A systematic investigation of 6 different catalysts used in the sol-gel process of TEOS in ethanol was carried out [Pope 1986]. In this investigation, the ratio of other reagents was kept constant (1 mol TEOS: 4 mol water). It was found, that the gelation time increased in the following sequence for the different acids used at the same concentration [Pope 1986]:

$$HF < CH_3COOH < HCl < HNO_3 < H_2SO_4$$

The pH in turn, increases as follows [Pope 1986]:

$$HCl, HNO_3, H_2SO_4 < HF < CH_3COOH$$
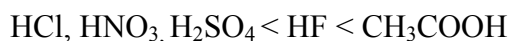
It can be seen that HF, having an intermediate pH results in the lowest gelation time. The same effect can be observed for acetic acid. Thus, the gelation time does not seem to be directly correlated with the pH value and the specific reaction mechanisms should be taken into consideration in every particular case.

Special influence of F^- ions on the sol-gel processes of silica was postulated by early works of Iler [Iler 1979]. It was suggested that F^- influences the mechanism of both hydrolysis and condensation, giving new intermediate complexes, as compared to the H^+ and OH^- ions.

In the case of condensation, the effectiveness of the fluorine anion is due its smaller ionic radius versus that of hydroxyl, which performs the same function of temporarily increasing the coordination of silicon. Other anions such as Cl^-, Br^-, I^-, SO_4^{2-}, NO_3^- are all larger than hydroxyl and hence, are much less effective than hydroxyl in catalyzing the condensation by nucleophilic attack. This result is in agreement with other investigations [Pajonk 1986], where it was shown that NH_4F used as the catalyst allows for an extremely low gelation time.

In the case of acetic acid, this does not solely act as a catalyst, but also leads to anionic substitution of the acetyl radical, forming ether as by-product.

$$\equiv Si-OR \;+\; CH_3COOH \;\rightarrow\; \equiv Si\text{-}OH \;+\; CH_3COOR \qquad\qquad (12)$$

Thus, it is clear that gelation times depend strongly on the catalytic mechanism of the catalyst. Ethanolamines were suggested as basic catalysts for TMOS hydrolysis [Yoda 1996]. It was shown that in the homological sequence of amines, the gelation time decreases with increasing pKa. (In this case, pKa is the measure of the basicity of amines).

Afterward, 17 different catalysts, consisting of acids and bases (strong and weak) and their mixtures were studied [Rao 1994]. It was found that the shortest gelation time could be achieved by using strong bases like KOH and NaOH. This can be due to the fact that these act as strong proton acceptors and, therefore, extremely accelerate the condensation. The longest gelation times were obtained for strong acids (like HNO_3). The gelation times of weak acids, bases and their mixtures are in between those of strong acids and bases. In a later work [Wagh 1997], citric acid was found to be a suitable catalyst for the sol-gel process.

The nature of the catalyst, not only affects the gelation time itself, but also affects the microstructure and optical properties of the aerogels. Rao et al. [Rao 1994] showed that strongly acidic catalysts resulted in transparent but cracked and slightly shrunken aerogels. The acid-catalyzed gels have smaller pores, so the surface tension forces are larger which results in a higher drying stress. On the other hand, the small size of the pores provides the high transparency.

Monolithic and less transparent aerogels were obtained using strong basic catalysts, because the larger pores and highly branched structure of these aerogels allowed for withstanding against the drying stress.

In the case of weak acids, monolithic but semitransparent and shrunken aerogels were obtained. With respect to weak bases, highly transparent and monolithic aerogels could be produced. This can be ascribed to the uniform porosity of such aerogels.

The two-step process. The advantage of the two-step process is the ability to combine both acid and base hydrolysis and, thus, to control the microstructure of the aerogels. After the first step, the condensed silica precursor contains a large number of oligomers and polymers from the partial acid-catalyzed hydrolysis of TEOS. Further hydrolysis of the silica precursor is conducted in a base medium in the second step, where the polymers react or condense much faster than silicic monomers. Many of these polymers have the opportunity to grow further in various directions, eventually forming colloid-like particles that are cross-linked to a gel network. Of course, some of them may not grow substantially except on the two ends. As a result, the two-step gel contains a mixture of linear polymers and colloidal particles in the network, with the network microstructure lying in-between those of acid-catalyzed and base-catalyzed gels. The acid-catalyzed gel has a finer structure but is the most difficult to dry without causing the collapse of the gel body. The two-step gel owns the relatively fine structure due to the presence of polymers from the initial acid-catalyzed hydrolysis of TEOS and yet has enough strength to withstand the small compressive force arising from the non-ideal supercritical drying. Large amounts of polymers in the condensed silica precursor also explain the shorter gelation times necessary in the two-step process [Cao 1994]. This proves that the conditions of the first step may significantly influence the gelation process.

The effect of the pH in both steps of the two-step process on aerogel properties was studied [Stolarski 1999]. It was shown, that the extent of hydrolysis increases with the decrease of the pH of the system, as is the case in the one-step process.

- Under very low pH (less than 2) conditions, the rate of hydrolysis is very high, but practically no condensation takes place. Thus, after the first step, most uncondensed monomers are subjected to further gelation in the second step. Such monomers quickly condense forming large, three-dimensional structures having very large volumes. An increase in the hydrolysis pH results in a lower hydrolysis rate, but the product is partly condensed before the second step.

- If the pH is larger as 2.4, new monomers are additionally formed as a result of dissolution of siloxane. As a result, more branched structures, characterized by an increase pore volume and a lower specific surface area, are formed.

The optimum pH for the first step was found to be 2.4-3.0. The pH during the gelation was found to be the most important parameter with respect to the aerogel structure [Stolarski 1999].

As already discussed, in the case of the one-step process, the gelation rate increases rapidly along with an increase in pH. The same tendency is true for the surface area. It was also found [Stolarski 1999], that the surface area increases with increasing pH only up to the value of pH = 7.3. Further increase of the gelation pH has a reverse effect, namely the surface area decreases. The maximum total pore volume was observed at a gelation pH of 7.7. It was concluded that at the highest condensation and redistribution rates, silica aerogels of the highest specific surface area and pore volume can be obtained [Stolarski 1999].

2.1.3.4   Effect of water content

Water takes part in both hydrolysis and condensation processes. In the case of hydrolysis, water directly participates in the reaction, so the amount of water determines the distribution and number of hydrolyzed monomers formed. Acid-catalyzed hydrolysis of TEOS was found to be first-order in H_2O concentration [Aelion 1950]. A higher value of TEOS : H_2O, causes a more complete hydrolysis of the monomers before significant condensation occurs.

In the case of condensation, water is the reaction by-product. As described above, two different types of condensation can take place: alcohol condensation (4) and water condensation (5). Water condensation takes place if the majority of the Si-OR bonds are hydrolyzed and thus, depends directly on the hydrolysis rate. For the molar ratios TEOS : H_2O (r) < 6, alcohol condensation dominates, while at higher H_2O concentrations water condensation dominates, because more hydrolyzed silanols exist in the system [Sherer 1989]. In the case of water condensation, the increasing H_2O concentration shifts the equilibrium to the reagent; that is the reverse reaction takes place. Thus, increasing the H_2O concentration increases the hydrolysis, but (at a certain level) decelerates the condensation.

Gel times for the acid-catalyzed TEOS system as a function of TEOS : H_2O (r) and TEOS : Ethanol (m) ratios were investigated [Klein 1985]. It was found that at the fixed m value the dependence of the gelation time on r is at a minimum. This minimum shifts to larger values of r if the m value increases. Wagh et al. [Wagh 1998] also found, that the gelation time decreases rapidly with an increase in water concentration in the system. The authors also report the influence of the TEOS: H_2O ratio on the physical properties of the aerogels . They have shown that both density and transparency of the aerogels depend on this parameter, having an optimum at the certain r value.

The dependence of the specific surface area and pore volume of the TEOS aerogels on the water concentration was reported [Stolarski 1999]. The highest surface concentration was obtained using a stoichiometric amount of water. Both a deficiency and an excess of water led to the reduction of surface area. With an increase of water, in excess of the stoichiometric amount, the pore volume decreased.

Their results are in agreement with those of [Yoda 1999], who also reported a decrease in the surface area with an increase in water content.

It was also shown [Cao 1994], that increasing the water content leads to an increase of the dielectric constant of the system, since water has a dielectric constant that is higher than that of any other compound in the sol solution. The dielectric constant of the sol was related to the stability of colloidal particles and their growth. At a constant double layer potential, a higher dielectric constant increases the energy barrier between two primary particles in the sol. As a result, the sol becomes more stable, and a more homogeneous gel structure is obtained. It is of importance to note that the microstructure of the aerogels is also very sensitive to the water concentration in the system.

It can be concluded, that the water concentration should be optimized in every specific case, in dependence of the desired aerogels properties.

2.1.3.5   Effect of the precursor

Various starting compounds can be used to prepare silica gels and aerogels. Usually alkoxysilanes, particularly tetramethoxysilane (TMOS) and tetraethoxysilane (TEOS), are used for both one-step and two-step sol-gel processes. Obviously, the properties of the starting compound have a great influence on the properties of the aerogels. A number of different precursors and their influence on the gelation rate and the properties of the silica gels formed were studied [Chen 1986], among them three alkoxysilanes with different alkyl chain length, silicon tetraacetate and silicic acid.

In the case of acid-catalyzed hydrolysis for different alkoxysilanes it was shown [Aelion 1950], that hydrolysis is a second order reaction with respect to the concentration of alkoxysilane and water:

$$\frac{dx}{dt} = H(C^0_{precursor} - x/2)(2C^0_{water} - x/2) \tag{13}$$

Where $C^0_{precursor}$ and C^0_{water} are the initial concentrations of alkoxysilane and water respectively. X is the decrease in the concentration of water at time t and H is the hydrolysis rate constant of the acid catalysts.

On the other hand, the hydrolysis rate constant (H) is given by [Aelion 1950]:

$$\log H = \log C_{HCl} + \log k \qquad (14)$$

where C_{HCl} is the catalyst concentration in the solution and k is the material hydrolysis rate constant of alkoxasilanes. The material rate constant, k, is an empirical constant determined solely by the characteristics of the starting compound itself. For HCl- catalyzed hydrolysis, k decreases with increasing of the chain length of alkoxy groups [Chen 1986].

The decrease of k with the increasing size of the alkoxide is presumably due to the role of steric hindrance in the hydrolysis mechanism. The hydrolysis rate constant (H) can be calculated from the equation (14). It was demonstrated [Chen 1986], that H decreases with increasing size of the alkoxide, just as k does. The hydrolysis time was estimated using this data and compared with the gelation time. It was shown [Chen 1986], that under the employed conditions, the calculated times for 95% completion of the hydrolysis process is less than ten minutes, compared to the much longer gelation times of 44 to 550 hours.

Condensation starts as soon as the alkoxy group is hydrolyzed. The initial condensation rate is very high and short chains (or oligomers) are formed at this stage. At a later state, further condensation is possible only through the cross-linking of already formed chains, which are separated from one another by alcohols and water molecules. The cross-linking of these chains eventually leads to the formation of a gel. Since the cross-linking requires diffusion and collisions between chains, it is expected, that as their concentrations increase, the probability of collisions also increases. Because of the difference in the sizes of the alcohols formed during the hydrolysis of different precursors, the average separation of the chains in solution will be different if all alcohols are retained. Chen et al [Chen 1986] proved this suggestion and showed that when different starting compounds are used in the same solvent, longer gelation times are observed when using starting compounds with larger volumes.

The relation between the gelation time (t_{gel}) and initial concentration of the monomer C_0 can be expressed as [Bechtold 1968]:

$$t_{gel} = 1/C_0 \, K'(f^2 - 2f) \qquad (15)$$

where K' is the polymerization rate constant and f is the apparent functionality of the monomer, which is the average number of effective functional groups per monomer molecule participating in the polymerization.

The precursor nature and concentration not only influence hydrolysis and condensation, but also the properties of the aerogels. The concentration of the precursor is directly connected with the target density of the aerogels, which is defined as:

$$\rho_{target} = \frac{m_{SiO_2}}{V_{sol}} \qquad (16)$$

where m_{SiO_2} is the mass of the SiO_2 that can be produced by the given amount of the precursor, and V_{sol} is the volume of the sol solution.

At present, TMOS and TEOS are the most widely used precursors. The influence of the precursor nature on the properties of the aerogels were studied for 3 different precursors: TMOS, TEOS and polyethoxydisiloxane (PEDS) [Wagh 1999]. It was found that the monolithicity of aerogels depends strongly on the catalyst used for each precursor. TEOS and PEDS precursors acid catalysts and TMOS precursor base catalysts result in monolithic aerogels. The pore size distribution for TMOS and PEDS aerogels was found to be narrow and uniform. The particles are spherical in shape and smaller in size than those of TEOS aerogels. These smaller pores and particles result in better optical transmission (93% for TMOS and PEDS aerogels and only 70% in the case of TEOS aerogels). Also the pore size distribution for TEOS aerogels is broaded and shifted towards smaller pore radii.

It has been also found that TMOS and PEDS aerogels have greater surface areas than aerogels. This is due to the fact that both the TMOS and PEDS aerogels consist of a network of a smaller sized SiO_2 particles [Wagh 1999]. As a result, one may conclude that TMOS and PEDS are better than TEOS as precursors for silica aerogels.

2.1.3.6   Processes based on other precursors

Tetraalkylorthosilicates, widely used as precursors for the sol-gel process are rather expensive. Hence, considerable efforts have been undertaken in aim of developing a more cost-effective procedure.

BASF modified Kistler's procedure, and used an aqueous sodium silicate as a starting material. In the production of Basogel, the aerogel product of BASF, a solution of sodium silicate is mixed with sulfuric acid and the sol is sprayed in order to form small droplets of the gel. The metal salts, produced by the reaction, are extracted and the water is exchanged for an organic solvent followed by the supercritical drying [Materials of ISA-5].

Heley et al. [Heley 1995] used $SiCl_4$ as a precursor to produce a low-density aerogel powder. Gels were produced by hydrolyzing $SiCl_4$ in water in the presence of an inert solvent.

The gelation takes place very rapidly giving an opaque gel. After solvent transfer, the gels are supercritically dried in a particulate state giving an aerogel powder with a density of 0.04 g/cm^3 as the final product. It was also shown, that both the reaction rate and the transparency of the final product may be regulated by the addition of an inert solvent (for example,

tetrahydrofurane). Thus, $SiCl_4$ seems to be a possible alternative to alkoxysilanes for the synthesis of aerogel particles.

2.1.4 Aging process

Gelation is a spectacular event that occurs when a solution suddenly loses its fluidity and takes the appearance of an elastic solvent. The gel point represents the moment when the last link is formed in the chain of bonds that constitutes the spanning cluster. This network restrains the flow of the pore fluid. The chemical reactions are not finished, when the gel point is reached - the chemical evolution of the system continues also after the gelation. This post-gelation process is termed **aging**.

In a wet gel, chemical processes during aging are categorized as syneresis and Ostwald-ripening [Brinker 1990].

- Syneresis is characterized by a shrinkage of the gel network, caused by further condensation reactions after gelation. Condensation in silica gels continues long after gelation because of the large concentration of active hydroxyl groups. If two neighbouring hydroxyl groups condense on a network surface, the newly formed siloxane bond (Si-O-Si) takes up less space than the two Si-OH groups and, as a result, liquid is expulsed from the pores. This causes the pore size to decrease to some extent. This process is schematically shown in Figure 2-4.

Figure 2-4 Syneresis in silica gel [Brinker 1990]
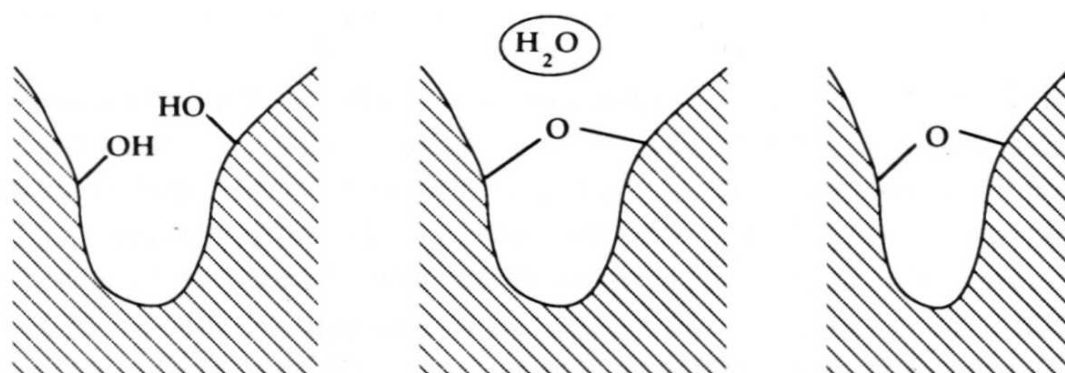
- Ripening is a process of dissolution and re-precipitation driven by the different solubilities between surfaces with different radii of curvature. It can be shown [Brinker 1990], that the smaller the particle, the greater its solubility. Therefore, smaller particles dissolve and the solute particles precipitate onto larger particles. The result of this dissolution-precipitation

is the reduction of the net curvature of the solid phase: small particles disappear and small pores are filled in, so the interfacial area decreases and the average pore size increases.

The structural changes that occur during aging have an important effect on the drying process. The stiffer and stronger the gel network becomes, the better it can withstand the capillary pressure. Thus aged gels shrink and crack to a lesser degree than their non-aged counterparts.

The strengthening of the gel network can be favoured by different methods [Rolison 2001]. Strengthening involves either aging the wet gel in its mother liquor or soaking the gel in a silicon alkoxide during the aging step. For example, the stiffness of TEOS-based gels can be increased by aging in TEOS-ethanol solution [Haereid 1995].

Also, stiffness of the gels prepared by other precursors, for example polyethoxydisiloxane, can be increased by soaking in the polyethoxydisiloxane solution [Einarsrud 2001]. It was observed that such aging increases both cluster and particle dimensions. Low-density aerogels with a surface area of ~ 700 m^2/g have been reported [Einarsrud 2001].

Influence of the aging process on the microstructure of NH_4OH- and NH_4F-catalyzed gels was studied [Suh 1999] and it was shown that the aging procedure allows for the reorganization of the structure, resulting in a unimodal pore size distribution. The pore volume and mean pore diameters of the resulting aerogels increases, whereas the surface areas remain virtually unaffected. The rate of such aging was found to be much slower than that of gelation. The stable porous texture of corresponding aerogels for given sol-gel conditions can be finally obtained by prolonged aging [Suh 1999].

During the aging process, the solvent evaporates, causing a slight shrinkage of the network before the aging process has actually been completed. Thus, if solvents with a low vapour pressure are used, this kind of shrinkage can be eliminated. Ionic liquids were used for this purpose [Dai 2000]. Ionic liquids are a class of solvents that have extremely low vapour pressures and possess versatile solvent properties. As a consequence, they offer an attractive method for achieving longer gelation times without shrinking of the gel network. The gels synthesized by this method are so stable, that even conventional drying causes just a little shrinking. This method can be helpful for the preparation of aerogels and aerogel film having a moderate density.

2.1.5   Drying methods

The wet gel is a three-dimensional porous structure filled with pore fluid and can be schematically represented in Figure 2-5. When removal of the liquid from such a structure by simple evaporation is to be conducted, capillary forces must be considered.
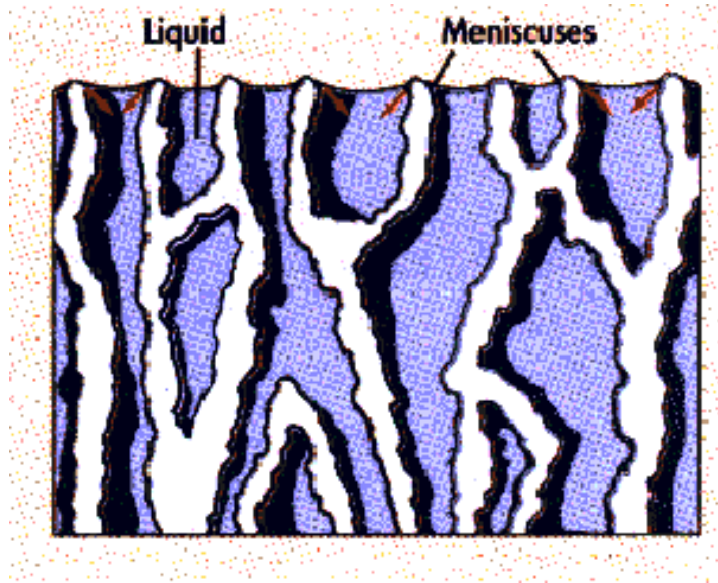
Figure 2-5 Distribution of the solvent in the pores of the aerogel

The parameter that causes liquids to rise in a capillary or spread out onto a solid surface is the difference in the specific energy of the solid-vapour interface (γ_{SV}) and the solid-liquid interface (γ_{SL}). The liquid film of a plane solid surface has two interfaces, solid-liquid and liquid-vapour, so the energy change is [Brinker 1990]:

$$\Delta E = \gamma_{LV} + \gamma_{SL} - \gamma_{SV} \tag{17}$$

If $\Delta E < 0$, the liquid spreads spontaneously and forms a film. If, on the other hand, $\Delta E > 0$, a droplet is formed (Figure 2-6).
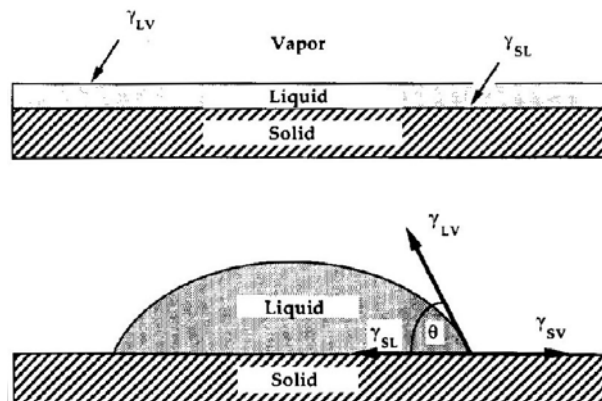
Figure 2-6 Liquid film and a droplet on solid interface [Brinker 1990]

The form of the droplet is characterized by the contact angle, θ. The balance of tensions is given by:

$$\gamma_{SV} = \gamma_{SL} + \gamma_{LV} \cos (\theta) \tag{18}$$

In the case of a liquid in a solid, cylindrical capillary, the liquid rises and causes replacement of the solid-vapour interface with a solid-liquid interface. The energy gained by this process is:

$$\Delta E_{cap} = 2 \pi r h (\gamma_{SV} - \gamma_{SL}) \tag{19}$$

where r is the capillary radius and h is the height up to which the liquid rises. The work performed by the liquid to move against gravity is equal to the product of the capillary pressure (P_{cap}) and the volume of liquid moved, $\Delta V = \pi h r^2$. Taking into account Eq.(19), the capillary pressure can be expressed by:

$$P_{cap} = -2\pi h (\gamma_{SV} - \gamma_{SL})/r = -2\gamma_{LV} \cos (\theta)/r \tag{20}$$

Figure 2-7 schematically illustrates the forces acting within the capillary.
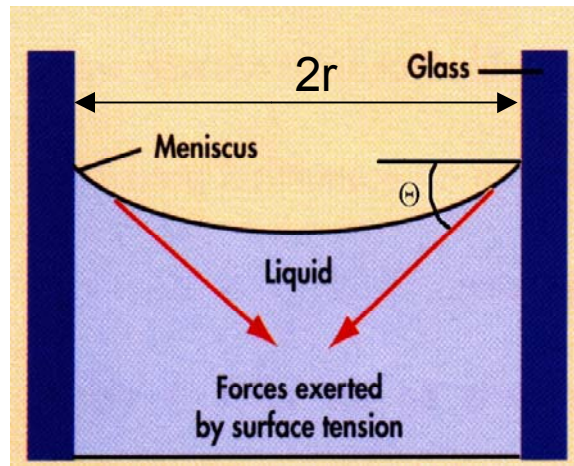
Figure 2-7 Illustration of the capillary forces in the meniscus

Capillary pressure in the cylindrical capillary can be expressed as:

$$P_{cap} = \gamma_{LV} k \tag{21}$$

where k is the curvature of the meniscus formed in the capillary.

The significance of the capillary pressure in the drying of gels, however, is not its effect on the vapour pressure; but, rather, its effect on the solid phase. This is because the gel contracts as the liquid evaporates from its pores due to the considerable stresses generated by the menisci in the tiny pores. These stresses can exceed the strength of the network by a

substantial margin. The capillary pressure of several solvents typically used in aerogel production are presented in Figure 2-8. Here a relation between the capillary pressure and the size of the pore is demonstrated. It is important to note that a pore-size distribution causes additional problems. This is because when pores of different sizes exist in the gel body, large pressure gradients may develop throughout the mass, resulting in cracks.
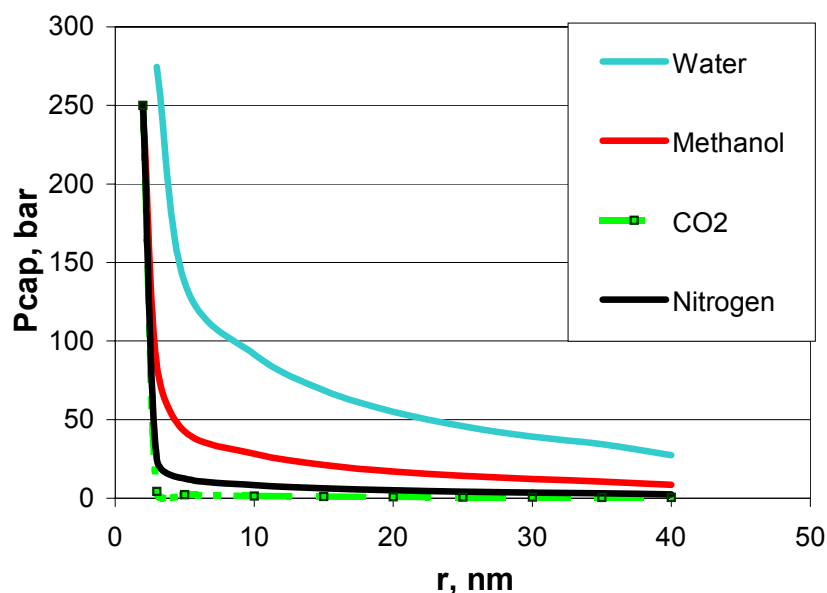
Figure 2-8 Dependence of capillary pressures on pore radius for four different solvents calculated using $\theta = 0$

2.1.5.1   Supercritical drying

Since shrinkage and cracking are most likely the result of capillary forces, they may be avoided by removal of the pore liquid above the critical temperature (T^{cr}) and critical pressure (P^{cr}) of the concerned liquid. At this point there is no distinction between the liquid and vapour phases i.e. the densities become equal - there is no liquid-vapour interface and, thus, no capillary pressure [Brinker 1990]. This drying process is termed supercritical drying (SCD).

High temperature supercritical drying (HTSCD)

There are two different methods of supercritical drying: high temperature supercritical drying (HTSCD) and low temperature supercritical drying (LTSCD).

HTSCD is schematically represented in Figure 2-9. The process is carried out as follows:

- The wet gel, together with a sufficient amount of solvent (e.g. methanol) is placed in an autoclave and the temperature is slowly raised. This causes a pressure increase (step 1 in Figure 2-9). Both the temperature and pressure are adjusted to reach values above the

critical points of the corresponding solvent. On attaining the set temperature and pressure, the conditions are kept constant for a certain period of time. This ensures that the autoclave is completely filled with the supercritical fluid, and therefore, ensures the absence of liquid - gas interfaces in the pores during drying.

- The fluid is then slowly vented at constant temperature, resulting in a pressure drop (step 2 in Figure 2-9).

- When ambient pressure is reached, the vessel is cooled to room temperature (step 3 in Figure 2-9). Thus, the phase boundary between liquid and gas has not been crossed during the drying process.
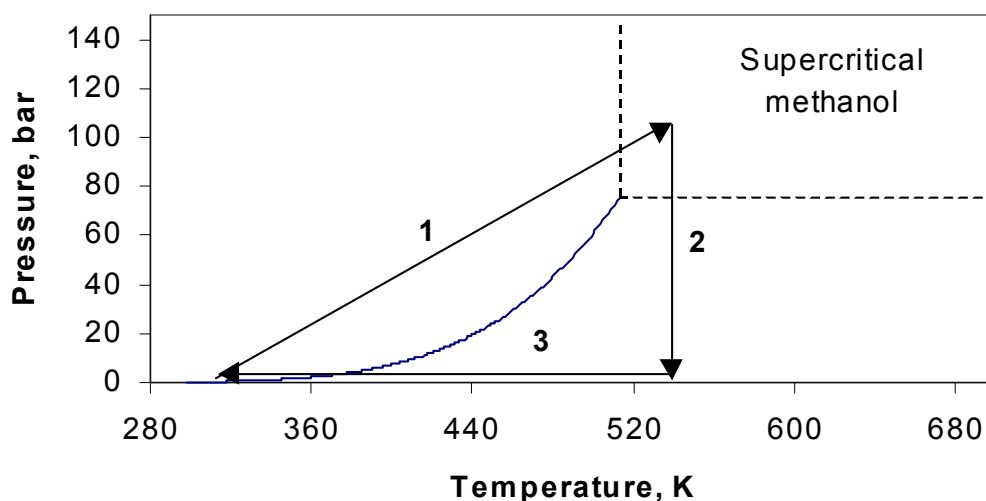
Figure 2-9 High temperature supercritical drying

This process was applied by Kistler [Kistler 1931] and is still widely used for silica aerogel production. It is of impotance to note that supercritical drying in organic liquids leads to rearrangement reactions in the gel network due to the high temperature conditions. For example, under supercritical conditions, the silica aerogel surface is reesterified, making the material hydrophobic and stable when exposed to atmospheric moisture. Processes such as aging and ripening of the gels are accelerated, small pores are filled and particle necks become strengthened.

J.Gross et al [Gross 1998] conducted a "rapid supercritical extraction process" where the rates of the condensation reactions were increased due to the increased temperature.. Sol was poured directly into a container and heated immediately to supercritical conditions in an autoclave. Gelation and aging occurred during heating and the reaction rates were found to be very high due to the high temperatures. Also, the gel filled the container completely, which

enabled relatively fast venting of the supercritical fluid. This process seems to be an interesting and practical modification of normal high temperature drying.

This method, however, may present problems due to the combination of high temperatures and high pressures as well as the flammability of the solvents.

On August 27, 1984, the pilot plant of the firm Airglass in Sjöbo, Sweden, experienced a terrible incident when the main gasket of a pressure vessel gave way, causing 3000 liters of methanol (at 260°C and 86 bars) to leak out and explode. The building and most of the equipment was completely destroyed [Henning 1990].

Many efforts have been undertaken in aim of establishing a drying procedure that can be carried out at moderate temperatures and pressures. Kirkbir et al. [Kirkbir 1998] have managed to reduce the drying pressure (but not the temperature). Several different solvents such as ethanol, butanol, pentanol and isooctane were tested and, in each case, it was found that the drying pressure can be reduced to a certain value, so that shrinkage of the aerogels does not exceed 5%. For example, in the case of isobutanol the critical pressure is 48.5 bar. Drying was carried out at 18 bar with 2 % shrinkage. Reduction of the process pressure not only reduces accidental risk but also lowers the production costs.

Low temperature supercritical drying (LTSCD)

An alternative method for aerogel drying was suggested in 1985 [Tewari 1985].

The solvent present in the gel before drying (generally alcohol) is replaced by a liquid having a critical point close to ambient temperature. Liquid CO_2 was found to be the most practical choice. Other substances which seem applicable are freons (R13, R23 and R116), but these are more expensive and are hazardous for the environment. Low temperature SCD has the advantage of being implemented at a low temperature (< 40°C) and moderate pressure (< 80 bar).

The whole process is shown schematically in Figure 2-10. The experimental procedure is as follows:

- The gel containing excess amount of solvent (e.g. CH_3OH) is placed in an autoclave (an excess amount of the solvent is used so that evaporation during transfer does not lead to gel shrinkage). The vessel is sealed and liquid CO_2 is pumped in at 4-10°C until the pressure reaches about 100 bar (step 1 in Figure 2-10). The outlet valve is then opened so that the solvent extracted by the liquid CO_2, is able to flow out. When the solvent is completely replaced by CO_2, the pump is turned off, the temperature is raised to 40 °C

(i.e. above the critical temperature of CO_2, $T^c = 31°C$) and the pressure is kept constant at 100 bar (step 2 in Figure 2-10).

- On reaching 40°C, and thus ensuring the transition of CO_2 into the supercritical state, the system is slowly depressurized under natural flow (step 3 in Figure 2-10).

- When ambient pressure is reached, the system is cooled down to the room temperature (step 4 in Figure 2-10). Aerogels obtained by this method are hydrophilic.
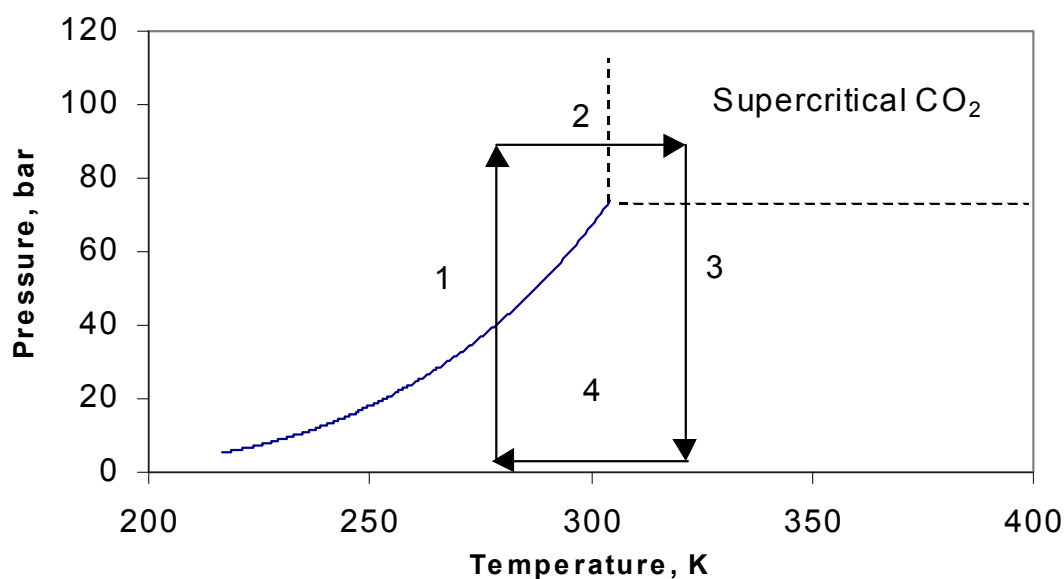
Figure 2-10 Low temperature supercritical drying

Ten years later, the LTSCD process was modified such as to involve the use of supercritical CO_2 as compared to liquid CO_2 [van Bommel 1995]. In this case, the heating and cooling steps can be eliminated. A continuous process of aerogel production including the recycling of CO_2 was also suggested.

The LTSCD process also involves an extraction step, which strongly depends on the diffusion of CO_2 in the solvent. The two main transport mechanisms of the alcohol and CO_2 are Knudsen diffusion and surface diffusion [van Bommel 1995].

It is difficult to predict the duration of the drying step, because in most cases the diffusion coefficients of the liquid in the sample are unknown. If the duration of diffusion is not long enough, a non-transparent area inside the gel is observed, or in the worst cases, cracking of the aerogel occurs. In order to describe the extraction process, binary diffusion coefficients of methanol-liquid CO_2 and methanol-supercritical CO_2 were determined [Novak 1999]. The experimental data are presented in Table 2-1.

It can be seen that the diffusion coefficient increases with increasing temperature, as is expected.

By using this experimental data it is possible to predict the drying time for the production of transparent aerogel monoliths.

Van Bommel [van Bommel 1995] has optimized the drying process and showed that for plate-shaped aerogels, the drying time is strongly dependent on the plate thickness. The relationship is such that the drying time increases exponentially with an increase in the plate thickness.

Temperature, (°C)	D_{AB} x 10^9 (m^2/s)
20	4.37
40	5.52

Table 2-1 Binary diffusion coefficient for the system MeOH - CO_2

Comparison of HTSCD and LTSCD

A comparative study of aerogels dried by the HTSCD and LTSCD methods was performed by [Ehrburger-Dolle 1995]. It was shown that the microporosity of CO_2-dried aerogels is significantly larger than that of the corresponding MeOH-dried aerogels. However, the micro- and mesoporous textures of the CO_2-dried aerogel are equivalent to those of the alcogel. These results are in agreement with those of other authors [Yoda 1999], [Wang 1993].

Shrinkage of the CO_2-dried aerogel is probably due to the reorganization of aggregates during the exchange of alcohol with liquid CO_2. The aggregate arrangement is very similar to that observed in gels formed with pyrogenic silicas. In contrast, after HTSCD, the structure collapses at a short length scale and thus, the initial aggregate network is strengthened.

Dieudone et al [Dieudone 2000] illustrates by SAXS experiments, that the aerogels obtained by methanol supercritical drying show a smooth surface, whereas the CO_2-dried aerogels have tough solid particles. However, transparency of the CO_2-dried samples is comparable with that of alcohol-dried samples [Tewari 1985]. This agrees with the results of Tajiri [Tajiri 1998], who also studied the transmittance of aerogels, dried in different supercritical media. It was reported, that for the high-temperature SCD, isopropanol seems to be the most favoured medium.

A model relating the drying stress to the thermal expansion and flow of the pore liquid has been designed for comparison of the two drying techniques [Unsulu 2001]. This model suggests that the CO_2 exchange method results in smaller stresses and that these stresses are of

such a small magnitude that crack-free gels result. In the case of thin circular plates, stress development during both drying methods, is about three to four orders of magnitude less than the stress formed in cylindrical silica gels

2.1.5.2   Subcritical drying

In spite of the differences between the HTSCD and LTSCD process, both are considerably expensive due to the high pressures involved. For this reason there is a great interest in subcritical or ambient pressure drying.

Ambient pressure methods for the preparation of aerogels are have began to emerge. These approaches offer great promise to lower costs for aerogel production and thus represent an important consideration for the future development of these materials. Ambient-pressure methods for silica aerogels include both surface modification and network strengthening. Additionally, the contact angle between the pore liquid and the pore walls has to be influenced so as to minimize capillary forces. Brinker and Desphande [Desphande 1992] described a drying method based on the so-called "spring-back effect". This involves chemical modification of the inner surface, e.g. via silylation. The water-alcohol mixture in the pores of the gel is first exchanged for a water-free solvent. Then, reaction with chlorotrimethylsilane takes place so that SiOH groups are silylated. This causes the surface of the aerogels to become hydrophobic. After another solvent exchange, drying takes place by evaporation. During drying the silyl-modified gels begin to shrink due to the development of capillary forces. However, a "springback" effect is observed when the liquid phase starts to form isolated droplets within the gel network. Since neighboring surface silyl groups are chemically inert and detach with little activation energy, the gel body is able to re-expand. Densities for subcritically dried gels are as low as 0.150 g/cm^3. It has been showed that the total pore volume obtained by this method is even larger than that of CO_2-dried samples of the same composition [Land 2001].

Hoechst developed this method further [Schwertfeger 1998] suggesting a novel cost-effective method of subcritical drying, avoiding solvent exchange using waterglass as a cheap silica source and employing a silylation agent. This silylation agent not only achieves the desired surface modification, but also reacts with the water in the pores of the hydrogel to form a low-tension organic solvent, suitable for ambient drying conditions. The hydrogel is placed into a solution of hexamethyldisiloxane (HMDSO) and trimethylchlorosilane (TMCS). TMCS reacts with the hydroxyl groups on the gel surface yielding the preferred $-O$-Si-R_3 surface groups, while HCl is released in the water phase. Furthermore, TMCS reacts with the water at

the HMDSO-water interface to form HMDSO and HCl. As HMDSO is poorly miscible with water, phase separation occurs and the aqueous HCl phase is expelled from the pores. Finally, the HMDSO soaked gel is dried at ambient pressure [Schwertfeger 1998]. The reactions which occur are illustrated in the Figure 2-11. Such aerogels are normally hydrophobic. The Hoechst group has also shown that such aerogels can turned into hydrophillic materials by oxidation of the surface groups [Schwertfeger 1996].
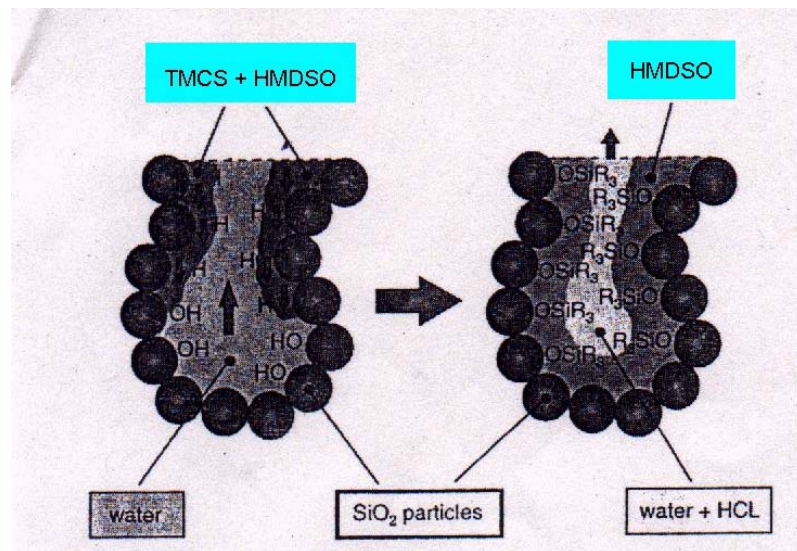
Figure 2-11 Schematic presentation of the reactions occurring during the silylation process

Loy et al [Loy 1997] tried to solve the shrinkage problem by synthesizing silica aerogels directly in supercritical CO_2, making solvent exchange unnecessary. In this case, the standard reactions cannot be applied, because water is produced and water is poorly miscible with CO_2 under normal conditions.

This problem was avoided by applying the "water-free" sol-gel polymerization technique, described by Sharp [Sharp 1993], who applied the technique for aerogel production with following supercritical drying. Loy [Loy 1997] reported that TMOS reacts with formic acid in the presence of CO_2 as a solvent. The reaction can be summarized as follows:

$$n\,Si\,(OR) + 4\,n\,HCOOH \rightarrow (SiO_2)_n + 4\,n\,HCOOR \qquad (22)$$
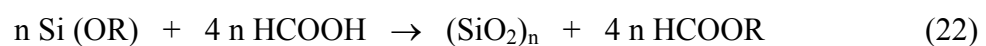
After 8-18 hours of aging, the pressure was slowly released and white, opaque silica aerogels were obtained. The white color and opacity of the aerogels can be explained by the relatively high acid concentration.

Direct formation of silica aerogel powders in supercritical CO_2 and acetone was reported by [Moner-Girona 2000]. Unfortunately, until now no detailed information on the properties of the resulting aerogels have been reported.

All subcritical drying processes result in aerogels with densities not lower than 0.1 g/cm^3. Up to the present time, there is no way to produce low density aerogels other than using supercritical drying.

2.1.5.3 Freeze - Drying

Another drying method where the phase boundary between the liquid and gas phase does not exist and thus the capillary pressure does not play an important role, is **freeze-drying**. Here, the solvent must be exchanged for another with a low expansion coefficient and a high pressure of sublimation and then the pore liquid is frozen and sublimed under vacuum [Hüsing 1997]. Material obtained by this way is called a cryogel.

Unfortunately, freeze drying has many disadvantages including the fact that the aging period has to be prolonged for stabilization of the network and, in some cases, the network may be destroyed by crystallization of the solvent in the pores. Cryogels are therefore only obtained as powders.

2.2. Properties of silica aerogels and methods of determination

The extensive interest in aerogels, particularly silica aerogels, is due to their unusual solid material properties. In the following chapter, the properties of silica aerogels and the methods used to determine such properties, are presented.

Table 2-2 provides an overview of the most important physical properties of silica aerogels.

Property	Value	Comments
Apparent density	0.003-0.35 g/cm^3	Most common density is ~0.1g/cm^3
Internal surface area	600-1000 m^2/g	As determined by nitrogen adsorption/desorption
% Solids	0.13-15%	Typically 5% (95% free space)
Mean pore diameter	~20 nm	As determined by nitrogen adsorption/desorption (varies with density)
Primary particle diameter	2-5 nm	Determined by electron microscopy
Refractive index	1.0-1.05	Very low values for a solid material
Thermal tolerance	> 500°C	Shrinkage begins slowly at 500°C, increasing with increasing temperature. Melting point is >1200°C
Coefficient of thermal expansion	2.0-4.0 x 10^{-6}	Determined using ultrasonic methods
Dielectric Constant	~1.1	For a density of 0.1 g/cm^3. Very low for a solid material
Sound Velocity	100 m/s	For a density of 0.07 g/cm^3. One of the lowest velocity values for a solid material

Table 2-2 Physical properties of silica aerogels

2.2.1   Pore structure

The IUPAC has recommended a classification for porous materials where pores of less than 2nm in diameter are termed "micropores"; those with diameters between 2 and 50 nm are termed "mesopores", and those greater than 50 nm in diameter are termed "macropores". Silica aerogels possess pores of all three sizes. However, the majority of the pores fall in the mesopore regime, with relatively few micropores. The approximate values of the pore size are between 5 and 100 nm, with an average pore diameter between 20 – 40 nm and a BET surface area between 600 and 1000 m². Porosity can be as high as 99%.

One important aspect of the aerogel pore network is its "open" nature and interconnectivity. Pores in various materials are either open or closed depending on whether the pore walls are solid or porous themselves. A macroscopic example of an open-pored material is a common sponge. In a closed-pore material, gases or liquids cannot enter the pore without breaking the pore walls. In open-pore structures, however, fluids (gases and liquids) can flow from pore to pore, although with limited restriction, and eventually travel through the entire material. It is this property that makes silica aerogels effective materials for gas phase catalysts, microfiltration membranes, adsorbents, and substrates for chemical vapor infiltration.

It is of extreme importance to state the method of determination used when stating porosity data. Aerogels have an unusual combination of high porosity and small pore size, making porosity characterization by conventional techniques such as mercury intrusion (MIP), thermoporometry (TPM), and nitrogen adsorption/desorption (NAD), difficult. All these techniques are based on the application of capillary pressures on the aerogel network, which may cause large volumetric compressions, leading to incorrect values for pore size and volume [Scherer 1998].

The most widely utilized method for determination of aerogel porosity is the nitrogen adsorption/desorption technique. Here a gas, usually nitrogen, is adsorbed at its boiling point onto the solid sample. The amount of gas adsorbed depends on the size of the pores within the sample as well as on the partial pressure of the gas relative to its saturation pressure.

High resolution scanning electron microscopy (SEM) and transmission electron microscopy (TEM) are techniques that may provide information on the microstructure of aerogels. These methods also present difficulties, mainly related to sample preparation, for, during the experiment, the fine aerogel powder may become electrostatically loaded and thus altered, in some way. These methods, however, allow a direct examination of the aerogel structure allowing the particle size and pore size to be approximately estimated. A SEM picture of a

silica aerogel can be seen in Figure 2-12. Quantitative information about the pore size cannot be obtained from SEM.
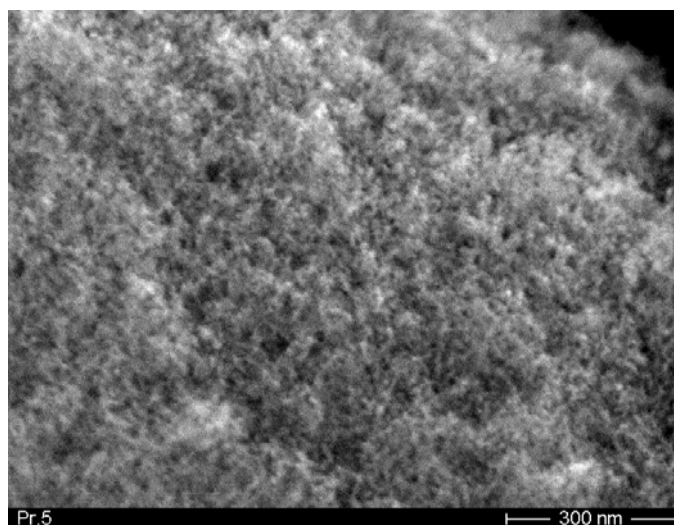
Figure 2-12 SEM picture of silica aerogel sample

Small-angle light scattering has been found to be a good solution to the problem of pore structure characterization in aerogels. This technique is not destructive, and neither sensitive to pore connectivity. By simple alteration of the instrumental set-up and wavelength, one is able to sample a considerably large size range [Hua 1995].

2.2.2   Density of silica aerogels

Two different terms are used to characterize silica aerogels: bulk density and skeletal density. **Bulk density** is defined as the relation of the aerogel's mass to its volume. This value can be as low as 0.003 g/cm^3 (the density of the air is 0.001 g/cm^3). This makes aerogels the lightest solid material known at present. The bulk density is normally measured as follows: a sample of known volume is weighed and thus the bulk density is calculated. The volume can be obtained either using Archimedes' law for those aerogels which are wetted with a certain liquid, or the sample is simply cut into a regular form (normally rectangular or cylindrical) and its volume is measured directly. Bulk density can be controlled during aerogel synthesis. The target value can be achieved by dilution of the initial sol with a known volume of the solvent. It should be noted that this value (known as the target density) cannot be obtained exactly, because of the shrinkage during drying, but the accuracy has only a marginal error of up to 5%.

The texture of the solid part of aerogels is made of ultrafine particles. The **skeletal density** of these particles is supposed to be very close to that of the bulk solid (2.2 g/cm^3 for silica gel). These values were obtained by using helium picnometry [Woigner 1987].

2.2.3   Optical properties

The optical properties of silica aerogels are best described by the phrase "silica aerogels are transparent". This may seem obvious, for silica aerogels are made of the same material as glass. However, the situation is not as simple as the comparison. While distant objects can be viewed through several centimeters of silica aerogel, an illuminated material displays a slightly bluish haze when viewed against a dark background and the transmitted light is slightly reddened. The scattering in the aerogel can be divided into two different types: bulk scattering and exterior surface scattering. The bulk scattering can be described by Rayleigh theory.

Rayleigh scattering is the scattering effect observed by small dust particles in the atmosphere. The actual entity that causes scattering, called the scattering center, can be as small as a single large molecule (with an inherent inhomogeneity) or clusters of small molecules arranged in a non-uniform way. However, scattering becomes more effective when the size of the scattering center is similar to the wavelength of the incident light. This occurs in small particles (~400-700nm in diameter for visible light), or by larger, macroscopic, particles that have inherent irregularities. When scattering centers are smaller in size than the wavelength of the incident light, scattering is much less effective. In silica aerogels, the primary particles have a diameter of ~2-5 nm, and do not contribute significantly to the observed scattering. However, scattering does not necessarily arise from solid structures. In silica aerogels, a network of pores can act themselves as scattering centers[1]. The typical UV/VIS spectrum of silica aerogel is shown below. There is then a "visible window" of transmission through the silica aerogel that is an attractive feature of this material for daylighting applications.

---

[1] Taken from the homepage of Berkely National Laboratory, USA [http://eetd.lbl.gov/ECS/aerogels/satoc.htm]

UV-VIS-NIR Spectrum of Silica Aerogel
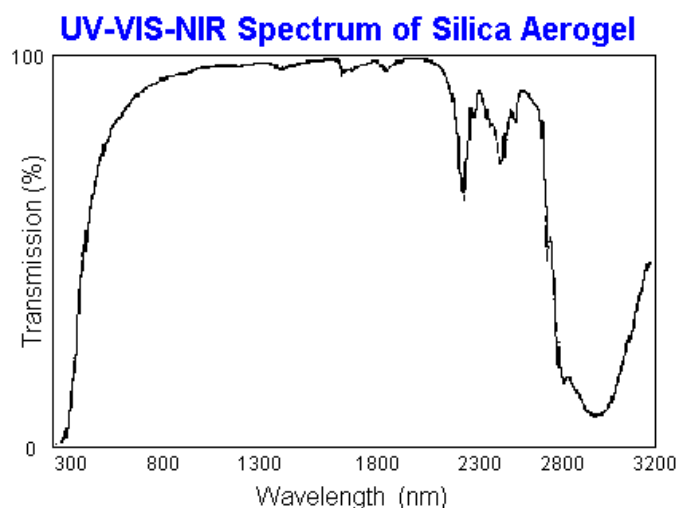
Figure 2-13 UV-VIS spectrum of silica aerogel[2].

In many applications of silica aerogels, their transparency plays an important role. Thus, multiple efforts have been undertaken so as to improve this characteristic of silica aerogels. Initially, various physically oriented approaches where taken to solving this problem, such as investigation of the influence of the drying process, of water adsorbed to Si-OH groups, or of absorbed organic components. Heating the aerogels improves their transparency due to the desorption of water and burning of organic components [Buzykaev 1999]. Also, the sol-gel process parameters greatly influence the optical properties of aerogels. Bulk scattering can be minimized by the selection of optimal synthesis parameters. A review of the works devoted to this problem was published by Pajonk [Pajonk 1998]. It has been shown that the two-step synthetic method resulted in more transparent aerogels than those obtained by one-step synthesis.

2.2.4 Thermal conductivity

Thermal conductivity is one of the widely studied properties of silica aerogels. Kistler demonstrated that the thermal conductivity of an aerogel is on the order of 0.02 W/mK at ambient pressure in air and on the order of 0.01 W/mK when evacuated [Kistler 1931].
If one also considers the transparency of aerogels, one may recognize a enormous potential for the reduction of heat losses in all kinds of window systems. A group at Würzburg University, headed by Prof. Fricke and the Berkeley Lab Group have conducted studies on the thermal conductivity of different aerogels.

---

[2] Taken from the homepage of Berkely National Laboratory, USA [http://eetd.lbl.gov/ECS/aerogels/satoc.htm]

The passage of thermal energy through an insulating material occurs through three mechanisms: solid conductivity, gaseous conductivity and radiative (infrared) transmission. The sum of these three components gives the total thermal conductivity of a material [Fricke 1986].

- Solid conductivity is an intrinsic property of a specific material. For dense silica, the solid conductivity is relatively high (a single window pane transmits a large amount of thermal energy). However, silica aerogels possess a very small (~1-10%) fraction of solid silica and thus exhibit a lower solid conductivity and hence, transmit a lower thermal energy. The higher the porosity of the lower the density, the lower the thermal energy contribution.

- The space that is not occupied by solids in an aerogel is normally filled with air (or another gas) unless the material is sealed under vacuum. Gases are also able to transport thermal energy through the aerogel. The pores of silica aerogel are open and allow the passage of gas through the material.

- The final mode of thermal transport through silica aerogels involves infrared radiation. Radiative heat transport proceeds via emission and adsorption of infrared photons. An important parameter that influences this transfer route is the optical thickness of the sample, given as the product of the geometrical thickness and the optical extinction coefficient of the aerogel. At low temperatures, the radiative component of thermal transport is low, and not a significant problem. At higher temperatures, radiative transport becomes a dominant mode of thermal conduction, and must be dealt with accordingly.

An attempt to calculate the total thermal conductivity arising from the sum of these three modes can prove to be difficult becasue the modes are coupled (e.g. a change in the infrared absorbency of the aerogel also results in a change in the solid conductivity). For measurement of the thermal conductivity, a Vacuum Insulation Conductivity Tester -VICTOR- may be employed. This was constructed at the Berkely Laboratory and is composed of a thin-film heater-based device that is able measure the thermal conductivity of panels with a maximum length of 26 cm, using pressures of various gases down to 0.01 Torr. Other authors reported the use of a hot wire method [Lee 1995]. Typical values of silica aerogel thermal conductivity are quoted in Figure 2-14.
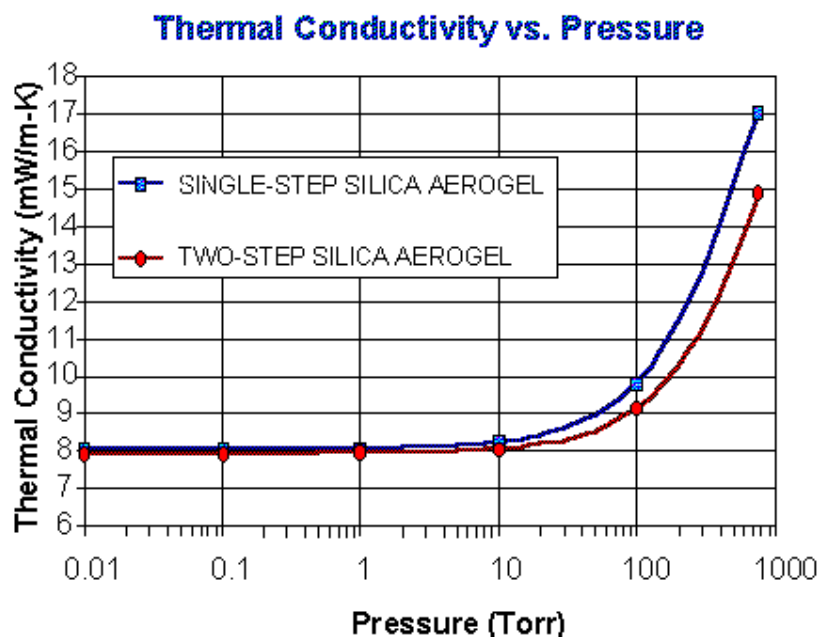
Figure 2-14 Thermal conductivity of silica aerogels at various pressure[3].

2.2.4.1   Velocity of sound and mechanical properties

The sound velocities in SiO_2 aerogels with values between 100-300 ms^{-1} are among the lowest for inorganic solids. The sound is carried solely by the delicate SiO_2-structure, and not by the air within the porous body. The reason for the extremely low sound velocity is the exceptionally small Young´s modulus ($10^6...10^7$ N/m^2). This can qualitatively be demonstrated by merely compressing a piece of aerogel between one's finger tips. Pieces of aerogel can be loaded up to pressures of about 3 bar without destruction. The absorption of sound up to the MHz-range is small in the aerogel. The rigidity shows a continuous increase with the TMOS concentration for alcogels and aerogels [Hafidi 2000].

The elastic properties of an aerogel powder has been studied by Stark et al [Stark 1998] using atomic force microscopy (AFM). This method allows for the direct measurement of local elastic sample properties.

2.2.4.2   Hydrophobicity

Silica aerogels can either be hydrophilic or hydrophobic, depending on the conditions during synthesis. Generally, aerogels synthesized by unmodified hydrolysis and condensation of alkylorthosilicates and dried by high temperature SCD are hydrophobic, and those dried by CO_2 are hydrophilic. This difference is due to the different surface groups formed during the supercritical drying process. LTSCD results in hydroxyl groups (-OH) on the surface of the

---

[3] Taken from the homepage of Berkely National Laboratory, USA [http://eetd.lbl.gov/ECS/aerogels/satoc.htm]

aerogel and, thus, in hydrophilic aerogels. Adsorption and capillary condensation of the water in the aerogel takes place, eventually resulting in cracking of the gel body. HTSCD allows for the reaction of the surface hydroxyl groups with the solvent to form methoxy groups (-O-CH_3)v and thus results in hydrophobic aerogels (Figure 2-15).
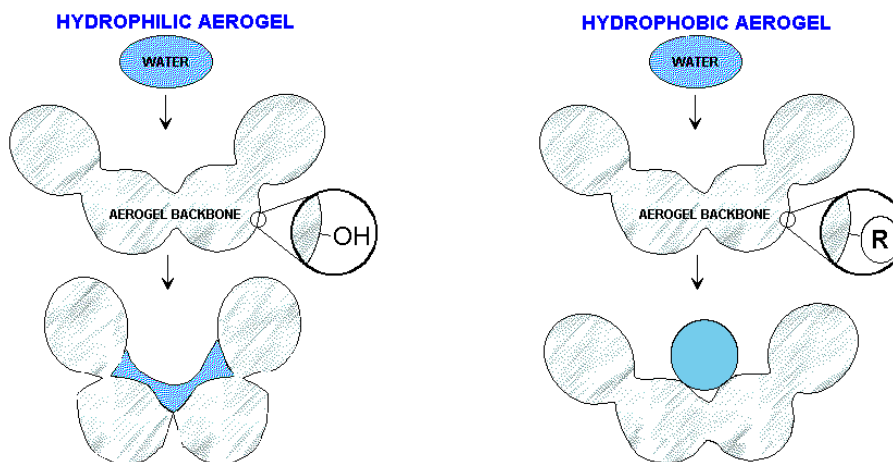
Figure 2-15 Hydrophilic and hydrophobic aerogels [Schwertfeger 1996].

Hydrophobic gels exhibit hydrophobicity only for a certain period of time. Their being exposed to air over a long time results in their adsorbing water, a characteristic that is not typical of hydrophobic materials [Schwertfeger 1996].

There are two different routes to increase the hydrophobicity of an aerogel:

-   The hydrophobic character can be increased by the addition of a silylating agent during the sol-gel step. This principle is used in ambient-pressure drying [Deshpande 1996]. The method is rather time consuming because the diffusion rate of the silylating agent into the pores is the limiting step. Schwertfeger et al [Schwertfeger 1996] synthesized hydrophobic aerogels by the one-step procedure using a mixture of alkylorthosilicate and an organically substituted trialkoxysilane as precursor. The inner surface of the aerogels were modified without alteration of the typical aerogel properties.

-   A second approach for increase in hydrophobicity is the modification of the aerogel surface after drying. The surface of hydrophilic aerogels can be modified by reaction with gaseous methanol [Lee 1995]. It has been shown that after a ten-hour reaction time at a temperature of 200°C, the surface was made to be completely hydrophobic.

Hrubesh et al [Hrubesh 1999] produced permanently hydrophobic aerogels. Here the aerogels were left into contact with the vapours of a surface modifying agent containing trimethylchlorosilane (TMCS), that reacted with the surface silanol groups to form Si-O-Si bonds and a protective "umbrella" of methyl groups linked to the silica surface.

2.3. Aerogel applications

The combination of such an extensive range of unusual solid material properties enables the application of aerogels in many different areas of technology. Some of these areas are presented in Figure 2-16.
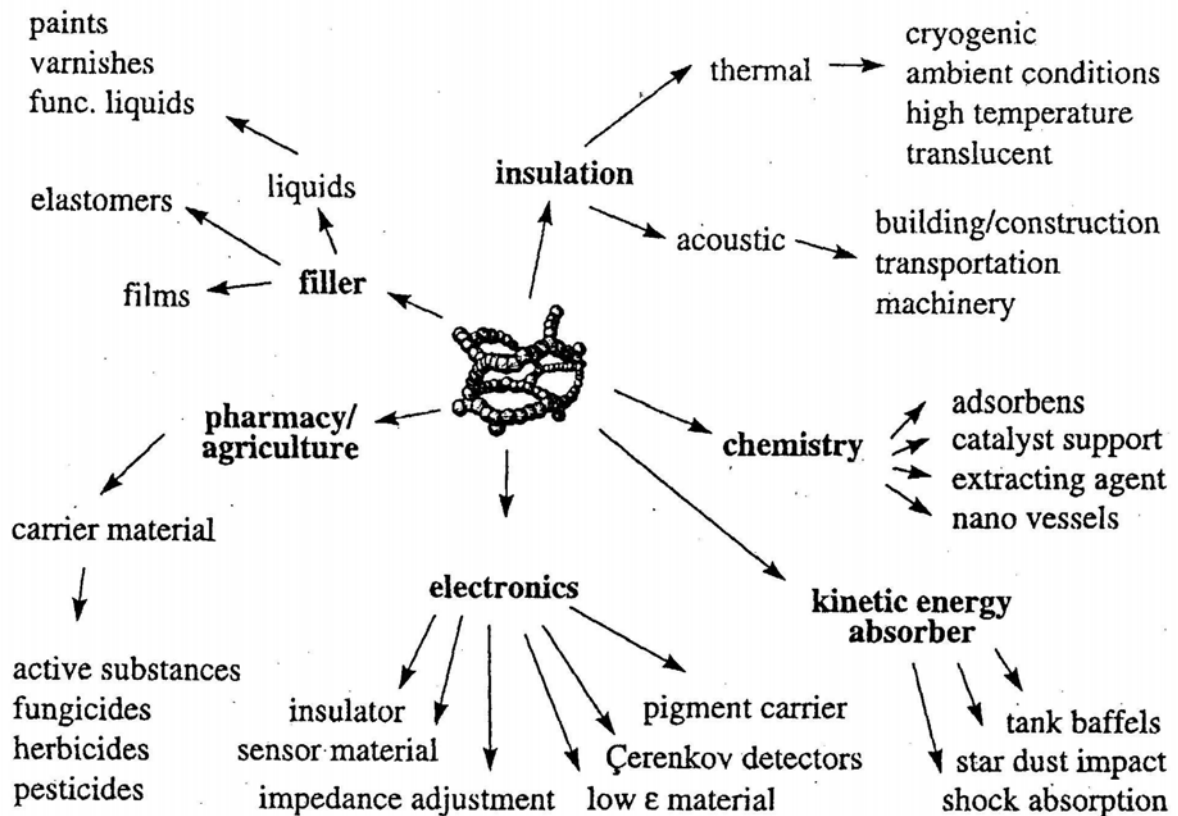
Figure 2-16 Aerogel applications [Schwertfeger 1998]

There are vast amounts of literature describing already existing and potential applications of aerogels [Hüsing 1997], [Schwertfeger 1998], [Rolison 2001]. It is unfeasible to describe all applications, but those that are viewed to be the most promising, will be discussed.

2.3.1 Applications based on low thermal conductivity

The translucency and good thermal conductivity of aerogels makes them promising materials for window insulation. Thanks to the low extinction coefficient in the visible and near-infrared region of the spectrum, aerogels are highly transparent to solar radiation. Together

with their large thermal resistance, aerogels may be suitable for transparent insulation in passive solar use.

An example of an aerogel as an insulating device is shown in Figure 2-17.
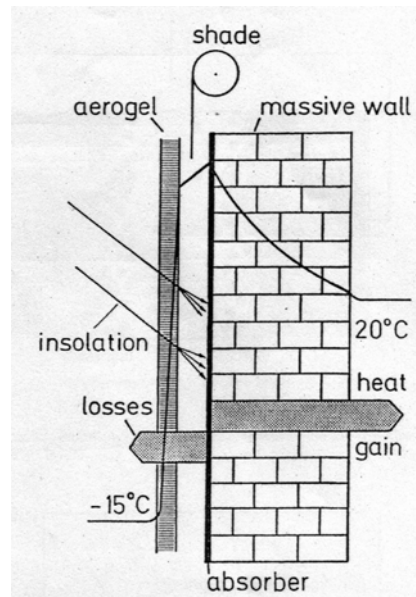
Figure 2-17 Transparent insulation (TI) is installed in front of a massive, black-painted wall. TI consists of granular silica aerogel between two protective glass panes. The solar radiation transmitted through the TI is absorbed by the black surface and most of the produced heat is transferred into the building, only little heat is lost. To prevent overheating, a shading device is necessary [Fricke 1986].

The solar radiation is transmitted through the aerogel and absorbed by the black wall surface which heats up as a result. Due to the efficient thermal insulation of the aerogel layer only a small amount of heat is needed for heating the building. Overheating during the summer months has to be prevented by using a shading device. For some specific applications the granulated form of the aerogel is favoured. The physical properties of this granulate hs been thoroughly investigated [Schmidt 1998].

The thermal properties of aerogels may be improved by addition of an opacifer (carbon black) to the silica sol which then becomes integrated into the gel. Thus, opacified granular or powdered aerogels are promising as substitutes for glass fiber or foam insulation, refrigerators or to heat storage devices [Burger 1998]. It is also possible to mix the aerogel powder or granulate with other materials such as polymers in order to improve the stability of the final product.

The application of aerogels as thermal insulators has awakened great industrial interest. The German companies Cabot and Axiva have begun the commercial production of translucent wall panels for passive lighting systems [Ackerman 2001].

Kamiuto et al [Kamiuto 1999] demonstrated the application of silica aerogels for the solar tank (shallow solar-pond water heater) surface insulation. They have shown that the temperature drop of water within the solar tank after sunset can be appreciably suppressed by introducing the aerogel surface insulation system. The theoretical model they proposed, can predict sunny-day hourly variations in the hot-water temperature within the solar tank.

NASA has used aerogels for the insulation of the Mars Rover, which collects information on the surface of Mars since the Pathfinder landing in 1997.

Another application based on the low thermal conductivity of silica aerogels is the furnace for high temperature experiments. The group of the German Aerospace Center (Deutsches Zentrum für Luft- und Raumfahrt) in Köln studies the direct solidification of metals in a silica aerogel furnace. Due to the high transparency of the aerogels the direct optical investigation of the solidification process is possible. It hs been demonstrated that silica aerogels are stable enough for this purposes and are not wetted by the metals alloys employed [Alkemper 1998]. An aerogel mold for the metal alloys is shown in Figure 2-18.
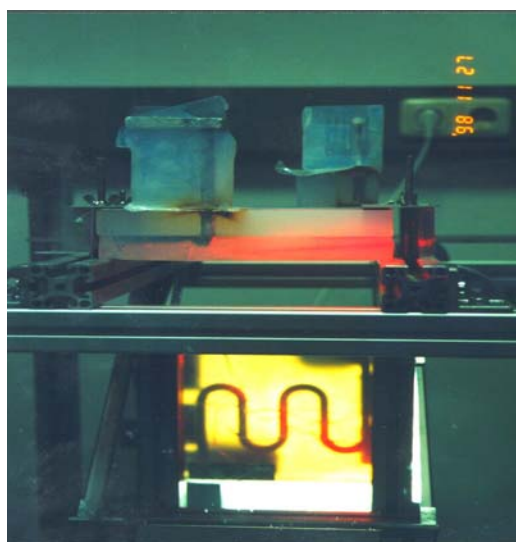

Figure 2-18 Aerogel mold for the metal alloys[4].

Such an application requires the aerogel to posses a well-defined geometrical form. Due to the shrinkage during the drying procedure, aerogels are normally cast into simple shapes, such as

---

[4] Taken from the homepage of Institut für Raumsimulation, Deutsches Zentrum für Luft- und Raumfahrt, Köln

plates or cylinders. Because of their brittle structure, it is extremely difficult for areogels to be re-formed. Traditional operations such as like cutting, milling and grinding are very difficult in this case. Sun et al. [Sun 2001] considered the laser micromaching of silica aerogels. This process allows for the formation of holes and channels with specific diameters to be integrated into the aerogel at ambient temperature.

2.3.2   Aerogel for Cherenkov counter

A crucial idea that strongly promoted the further development of high quality transparent silica aerogels, was the use of this low-density material in Cherenkov counters in high-energy physics. Cherenkov radiation occurs if a charged particle penetrates a medium (index of refraction, n) with a velocity (v), that is faster than the velocity of light (c/n) in this medium. The medium is polarized in such a way that light is emitted at an angle θ_c with respect to the momentum vector comparable to a super-sonic shock wave. The angle is given by

$\cos(\theta_c) = (\beta n)^{-1}$, with $\beta = v/c$. For the detection of fast pions, kaons or protons, a medium with an index of refraction close to unity is required. Aerogels just happen to fit into the range of n-values which cannot be covered by gases or liquids. It can be made with a refractive index of 1.007-1.06, corresponding to densities of 50-300 g/l [Fricke 1986]. Such a low refraction index can otherwise be achieved only through the use of compressed gases. The use of aerogels eases the detector fabrication processes.

Another application of silica aerogels in fundamental physical research is the study of phase transitions in super-cooled helium and neon [Tan 2000].

2.3.3   Dust capture

One of the most fascinating applications of silica aerogels is the capture of extraterrestrial grain ("cosmic dust") traveling at hypervelocities (> 3 km/s). Because of their porous structure, silica aerogels are able to dissipate the kinetic energy of the cosmic particles and catch the particles. The high transparency of silica aerogels enables direct observation of the final position of the captured particles [Tsou 1995].

Doping of silica aerogels with metal ions make aerogels fluorescent, allowing these materials to serve as a calorimeter for retardation of the grains. In such a way, the extraterrestrial grains can be distinguished from numerous other grains of terrestrial origin, such as alumina grains from solid rocket engines [Westphal 1998].

Figure 2-19 Tracks in aerogel mark the particle entry[5].

STARDUST, a NASA spacecraft, currently on a mission to encounter the comet Wild 2 is equipped with an aerogel aimed to encapsulate interstellar and comet dust particles and bring them to Earth in the year 2006.

Information regarding this mission is available under *http://stardust.jpl.nasa.gov/.* Figure 2-19 shows a photograph of particles captured within a silica aerogel.

Due to their porous structure, silica aerogels can be used as a chemically inert matrix, as demonstrated by Woigner et al [Woigner 1998-1], who used sintered silica aerogels as a host matrix for long life nuclear waste, in particular for the fixation of actinide. It has been shown, that silica aerogels can absorb around 10 wt% of the oxides (a model substance, neodymium oxide was used for these experiments).

Another field of technology where the highly porous morphology of aerogels is generating enormous interest is in microelectronics. Opportunities here should have a widespread impact because interlayer dielectrics (ILD) with a dielectric constant less than that of dense silica ($\varepsilon = 4$) are critical for high speed devices. There is a vital need for a new generation of low dielectric constant materials in order to improve device performance as smaller feature sizes in integrated circuits are developed. Silica aerogels represent one of the most promising of all

---

[5] **Taken from http://www.jpl.nasa.gov/technology/features/aerogel.html**

materials for ILD because of their low dielectric constant ($\varepsilon < 2$), thermal and dimensional stability, and compatibility with semiconductor processing [Rolison 2001].

2.3.4   Aerogel catalysts

Catalysis is the area which has strongly promoted the synthesis of metal oxide aerogels. Metal oxides, such as Fe_2O_3, Al_2O_3 and V_2O_5 are traditionally used in the chemical industry as heterogeneous catalysts. One of the most well known examples is the Fisher-Tropsch synthesis of hydrocarbons:

$$3H_2 + CO \xrightarrow{Fe_2O_3, Al_2O_3} H_2O + CH_4 \tag{23}$$
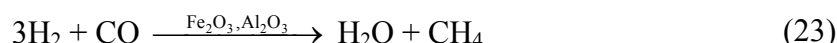
It is well known that the activity of heterogeneous catalysts depends strongly on the surface area of the catalyst. As a consequence, the extremely large surface area of aerogels makes them promising catalyst material. Unlike usual catalysts, for instance zeolites, aerogels do not have a microporous, but rather a mesoporous network, which favours the transport of reagents and/or products inside the catalyst body. Since many catalytic reactions are transport-limited, the use of an aerogel may enhance the reaction.

Many different types of aerogels have been developed for this function. Several reviews exist concerning this topic, for example the articles of Pajonk [Pajonk 1997], [Pajonk 1999] and Baiker [Baiker 1998]. The group of Prof. Baiker in Zürich has synthesized numerous binary oxide aerogels.

Table 2-3 presents several aerogel-catalyzed reactions, intended to give an impression of the immensity of this field. Several new types of metal oxide aerogels as well as mixed organic-inorganic aerogels are reported annually, making novel catalytic applications highly anticipated.

Aerogel catalyst	Reaction	Reference
V_2O_5 -TiO_2	Selective Catalytic Reduction of NO with NH_3	[Schneider 1994-3], [Zegaoui 1996]
Pt-TiO_2	Hydrogenation	[Schneider 1994-1]
Pd- TiO_2	Hydrogenation	[Schneider 1994–2]
SiO_2 - TiO_2	Epoxidation of cyclic olefins	[Hutter 1995]
Cu-ZrO_2, Ag-ZrO_2	Methanol synthesis	[Koeppel 1998]
Fe_2O_3, Al_2O_3	Fisher-Tropsch synthesis	[Bianchard 1982]
SiO_2 - TiO_2	Photocatalitic oxidation of $Fe(CN)_3$ in water	[Ahmed 1995]
Nb_2O_5	C_4 Hydrocarbon isomerization	[Maurer 1993]
MgO	Alkene isomerization	[Sun 1999]
$TiCl_4$-Al_2O_3	Ethene polymerization	[Fanelli 1989]
Ru-SiO_2	Synthesis of N,N-Diethylformamide from CO_2, H_2 and diethylamine	[Schmid 1999]
BaO•6Al_2O_3	Methane combustion	[Arai 1991]
CuO	Nitrophenols degradation	[Bandara 1996]

Table 2-3 Aerogel catalysts

2.3.5 Aerogel as a host matrix: synthesis and applications of composite aerogel materials

At present, an interest has grown in the field of composite aerogel materials. Thee final product consists of a silica aerogel and one or more additional phases (of any composition or scale). The aerogels, doped with a second organic or inorganic material (hybrid aerogels) posses a number of novel properties. All the materials considered here have a silica aerogel substrate and, thus, at least one phase has a physical structure with dimensions on the order of nanometers (the particles and pores of the aerogel). The aerogel composites (hybrid aerogels) can be prepared in two different ways:

1. Through chemical reaction during the sol-gel process or

2. By post-treatment of the dried aerogels (for example through the vapour phase after supercritical drying or through reactive gas treatment).

Using the first method, a variety of composites can be produced. Normally a non-silica material is added to the silica sol before gelation. This added material be of various natures including soluble organic or inorganic compounds, insoluble powders, polymers and biomaterials. In all cases, the additional components must be able to withstand the subsequent steps in aerogel synthesis. The most critical step is the supercritical drying process. The added material may be destroyed by the high temperatures or in the case of low temperature SCD, may simply be washed out with the CO_2.

If the added components are bulk, insoluble materials (such as carbon fibers or mineral powders), the settling of the insoluble phase before gelation should be prevented by special treatments. Also, it is important that the added component does not influence the gelation chemistry of the silica precursor. This general approach has been used by several research groups in order to prepare nanocomposites of silica aerogel.

The Group of Prof. Baiker, Zürich, [http://www.baiker.ethz.ch/] incorporated different metals including Pt and Pd into metal oxide aerogels. These doped materials were then used as catalysts in different reactions.

The use of SiO_2 aerogels doped with PbS nanocrystals has been reported [Yao 2000]. These products can be used as narrow-band semiconductors. Merzbacher et al [Merzbacher 1999] described the morphology of nanoscale deposits of ruthenium oxide in silica aerogels. Ruthenium oxide was deposited in the internal surface of the aerogel by impregnation with a Ru(III)tris-acetylacetonate followed by reduction and oxidation. The final product exhibited a particular electrical conductivity. Casas et al. [Casas 2001] synthesized magnetic nanocomposites formed by iron particles hosted in silica aerogels pores by the sol-gel route. They underline that such products are good candidates for applications in the field of magneto-optical sensors and magnetic devices due to their attractive properties, including soft magnetic behaviour, low-density and electric resistivity. Leventis et al. [Leventis 2002] reported a different formation of an iron-silica network by use of a magnetic field during the sol-gel step. A certain degree of anisotropy could be achieved by this method.

The Microstructured Materials Group at Berkeley National Laboratory studied different methods for synthesis of aerogel nanocomposites, including carbon-silica aerogels. Recently, they reported a new route for the manufacture of main-group and transition metal oxide aerogels using inorganic salt precursors [Gash 2001]. In particular, chromina aerogels were

synthesized from a chromium nitrate ethanol solution. Propylene oxide was used to promote the gelation process. This method is much more cost effective than that using conditional precursors and presents the novel possibility for the synthesis of both pure mono- and binary oxide aerogels and aerogel nanocomposites.

Ayers and Hunt [Ayers 2001] described the synthesis of silica aerogels doped with chitosan, a polymer derived from chitin, a natural polyglycosamide. Chitosan was brought into the aerogel matrix by soaking of the silica gel in a hexamethyldisilazane solution followed by supercritical drying. Composite aerogels with a surface area of 470-750 m^2/g were obtained. The biocompatability screening showed a very high value for hemolysis, but a low value for cytotoxicity. These hybrid aerogels may find use in diverse applications such as drug delivery or wastewater treatment using the chelating effect of the included chitosan.

A French group [Buisson 2001] reported the encapsulation of lipases in silica aerogels.

An enzyme suspension was added to the silicon precursor and then allows to form a gel. This was followed by supercritical drying with CO_2, which resulted in an aerogel containing the corresponding enzyme. The biocatalytical activity of the final product was studied using the esterification reaction of 1-octanol by lauric acid. In all cases, the aerogels exhibited very good catalytic activity. Immobilization of three other enzymes (PGA, thermolysin and chymotrypsin) in silica aerogels was studied by Basso et al. [Basso 2000]. However, loss of their catalytical activity in water was reported.

Large pore aerogels can be used as a host matrix for bacteria, as demonstrated by Power et al [Power 2001]. They showed that it is possible to immobilize the microorganisms within an aerogel to facilitate the detection of chemicals and organisms within the environment.

The same group showed that the pore size of the aerogels can be enlarged by the incorporation of water-soluble organic polymers (PEG) in the sol [Martin 2001].

All samples described above include the embedding of molecules into the gel without chemical bonding. The group of Prof. Fricke in Würzburg investigated the modification of silica aerogels on a chemical level in order to obtain functionalized aerogels [Hüsing 1997].

A number of modified aerogels having different physical properties was synthesized by using a mixture of organically substituted tri-alkoxysilane and TEOS as precursors.

The second method for the production of aerogel composite materials is based on the fact that the open pore network of silica aerogels facilitates the transport of vapours through the entire volume of the material. Theoretically, any compound with at least a slight vapor pressure can be deposited throughout a silica aerogel. Lamb et al. [Lamb 1997] exposed a silica aerogel to

fullerene vapour (300-700 °C) and obtained a fullerene/aerogel hybrid that can be used for energy storage applications. Hunt et al [Hunt 1995] deposited nanolayers of different materials (Fe, Ni, carbon etc.) on silica aerogels, using chemical vapour infiltration. They used the thermal decomposition (500-750 °C) of the corresponding hydrocarbon gas in the pores of silica aerogel. Silicon-silica composites were prepared by catalytic decomposition of dilute silane gas followed by a post-deposition heat treatment to induce crystallinity in the silicon. The resulting composites photoluminesce when illuminated by UV radiation. This effect is believed to be due to quantum confinement effects originating from extremely small silicon crystals. Composites of silica, iron and various iron oxides were also produced by this method, resulting in ferro- or paramagnetic materials [Cao 1999].

Borsella et al. [Borsella 2001] synthesized silicon-silica composites following the sol-gel route. These aerogels, however, did not show the same luminescence properties as in the case of Hunt et al [Hunt 1995].

The Microstructured Materials Group has recently discovered a process that can alter the chemical structure of the silica (or other oxide) backbone of an aerogel. This process utilizes an energized reducing (or other) gas to form thin films of new material on the interior surface of the aerogel. The techniques used in this case are similar to standard plasma methods. However, the nanoscale pore structure of the silica aerogels prohibit the formation of a plasma within the aerogel. Nevertheless, the centers of thick monoliths are affected by this process. In the simplest case, silica aerogel monoliths are partially reduced by energized hydrogen. The resulting composite consists of a silica aerogel with a thin layer of oxygen-deficient silica (SiO_x) on the interior surface. As with other reduced silica materials, this material exhibits strong visible photoluminescence at 490-500 nm when excited by ultraviolet (330 nm) light. However, the process used in this case is relatively gentle, and does not alter the physical shape or optical transparency of the original aerogel. This composite is the basis for the aerogel Optical Oxygen Sensor [http://eetd.lbl.gov/ECS/aerogels/sacomp.htm].

An especially interesting application of both pure aerogels and aerogel composites is their use as adsorbents. Due to their high porosity, aerogels can adsorb different chemical compounds. The adsorption of different gases including SO_2, CO, NO and H_2S in multi-metal oxide aerogels has been studied in aim of their usage in the capture of waste gases from air [Ahmed 1998], [Khaleel 1998]. It was shown [Ahmed 1998] that the $CaO-SiO_2$, $MgO-SiO_2$ aerogel nanocomposite sorbents can be efficiently used to adsorb and thus, capture waste

gases through both physical and chemical sorption mechanisms. The authors suggest the use of these aerogels as filters in the workplace and indoor living spaces.

Yoda et al. [Yoda 2000] used titania-impregnated silica aerogels to remove VOC's from air. Applying benzene as a typical VOC, they demonstrated that these aerogels possess excellent benzene adsorption capabilities. The adsorbate could then be decomposed to CO_2 by photocatalytic reaction.

Adsorption of water vapour on modified silica aerogels was reported by Mrowiec-Bialon et al [Mrowiec-Bialon 1998]. They have shown that $CaCl_2$-SiO_2 and $LiBr$-SiO_2 hybrid aerogels exhibit outstanding adsorption capacities of water vapour (up to 100 wt%). Knez and Novak [Knez 2001] obtained similar results for pure silica and mixed SiO_2-Al_2O_3 aerogels. They highlighted the fact that these aerogels remain stable even after 25 repeated adsorption/desorption cycles.

Hrubesh et al [Hrubesh 2001] investigated the adsorption of different organic solvents by hydrophobic silica aerogels. They demonstrated that the adsorption capacity of these materials exceeds that of activated carbon by 30 times. Thus hydrophobic silica aerogels can be used in the removal of solvents like toluene and chlorbenzene from water. Similar results were also reported by the Hoechst group [Sievers 1998].

In the present work, the high adsorption capacity of silica aerogels is exploited, in the aim of incorporating pharmaceuticals into aerogel materials.

2.3.6 Aerogels as carriers for active compounds and pharmaceuticals

Being chemically inert and non-harmful to the human body, silica aerogels may easily find an application in the pharmaceutical industry and agriculture.

Golob [Golob 1997] described the application of fine silica aerogel powders for the storage protection of grains in the agricultural industry. Having a small particle size and very large surface area, aerogel powders can absorb the protective lipid layer of insects causing the organisms to lose body fluid and, consequently, die.

The chemical composition of silica aerogels is identical with that of fumed silicon oxide, produced by combustion of silicon chloride. Amorphous silicon oxide has been used in the pharmaceutical industry for many years. The corresponding product is called "Aerosil" and has been an exclusive product of the German company "Degussa" since 1940. Aerosil has passed all clinical tests and has been found to be non-harmful to the human body [Degussa 2001]. It has been shown that orally administrated Aerosil passes through the gastrointestinal tract without being resorbed in detectable quantities. It is expected that silica

aerogels having the same chemical composition and amorphous structure as Aerosil would have similar clinical characteristics. Aerosil has an average surface area around 200 m^2/g [Degussa 2001]. Aerogels have much larger internal surface (500-1000 m^2/g), enabling them to exhibit superior properties to Aerosil, in particular applications. Several principle ideas for the use of aerogels in pharmaceutical and agricultural applications already exist.

It has been reported [DE 19653758 A1] that aerogel powder can be used as a free flow agent. The flow characteristics of powder are especially important in the pharmaceutical industry for pellet production. It has been shown that the addition of 0.5 % aerogel powder to lactose powder improves the flow properties of the resulting powder, compared to the addition of the same amount of the conventional products used for this purpose (Aerosil and Sipernat).

Schwertfeger et al [Schwertfeger 2001] reported the use of silica aerogels as potential carrier materials in medicine and agriculture. Here both hydrophobic and hydrophilic aerogels were loaded with pharmaceuticals by means of adsorption from corresponding liquid solutions. By choosing a suitable hydrophilic or hydrophobic aerogel, the substance with which the aerogel is loaded can be released in an accelerated or a delayed form. Ambient dried aerogels, having a relatively high density (ρ >0.1 g/cm^3) were used for this purpose. The authors dispersed the aerogels in a solution of the target substance. The loading with the target compound took place and then the resulting mixture was filtered in order to yield the loaded aerogel. The resulting powder was dried and could be used as a drug delivery system (DDS).

One of the most important characteristics of a DDS is the release rate of the loaded substances. "Release" descibes the dissolution of the corresponding substance with particular attention to its time dependence.

Depending of the medicament type, different drug release rates are desirable. In some cases (e.g. pain killer) an immediate release of the active substance is favourable. In other cases (e.g. anti-flammatory drugs) controlled release is important in order to support the constant concentration of the active substance in the body. Formulations of the same active agent can be prepared in a different way in order to achieve the desirable dissolution rate. [Stricker 1998]. This fact was demonstrated for the drug *metoprolol tartrate,* being prepared in 3 different formulations giving correspondingly fast, moderate and slow release [Sirisuth 2000]. Release of the *metoprolol tartrate* is shown in Figure 2-20.
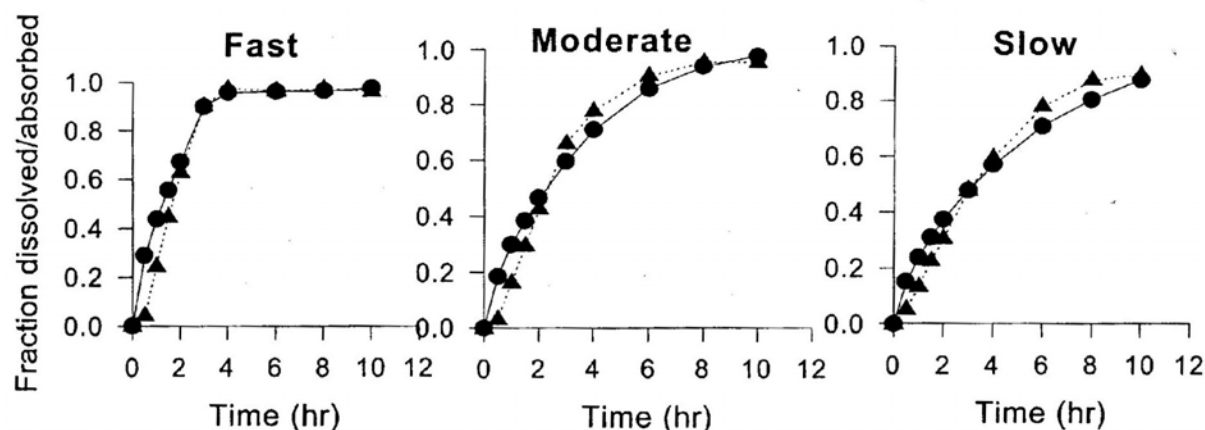
Figure 2-20 Different release profiles of *metoprolol tartrate:* fast, moderate and slow [Sirisuth 2000].

The dissolution rate can be altered by different mechanisms: variation of (1) filler content, (2) compression force used in formation of a pellet, (3) carrier material and (4) surface area of the drug, are but a few. Specific surface area is one of the very important parameters controlling both the dissolution rate of drug and its absorption in the body. A large specific surface area allows for a fast dissolution and thus, an effective absorption in the body [Stricker 1998]. For instance, it was shown that *griseofulvin* having a specific surface area of 1.5 m^2/g (corresponding to a mean particle size of 2.7 μm) is twice as effectively absorbed as *griseofulvin*, having a specific surface area of 0.4 m^2/g (corresponding to a mean particle size of 10 μm) [Atkinson 1962]. The specific surface area of the active component may be increased either by particle micronization, or by increasing the surface area adsorption of the drug on the carrier. Since aerogels have an extremely large surface area, we could expect that its use as a carrier can improve the dissolution and adsorption of drugs.The application of aerogels as carriers of pharmaceuticals is one of the topics of the conducted work.

3. Aerogel production: Experimental results

As discussed in section 2.3, the structure and properties of aerogels depend strongly on the synthetic conditions (e.g. amount of water, catalyst nature and concentration, solvent and temperature). An important factor in the sythesis of low density aerogels is the gelation time. In the one-step process, the gelation of a sample having a density of 0.02 g/cm^3 requires a relatively long time (approximately 14 days). In the two-step process, the gelation time of such samples can be as short as 3 days, but this process includes several tedious steps e.g. special purification of the reagents and distillation of the alcohols after the first step [Tillotson 1992]. Different types of catalysts have been utilized in order to accelerate the gelation process.

In the conducted work, the use of CO_2 is suggested as an accelerator of the gelation process. CO_2 has been used for the supercritical drying of aerogels over several years, but as far as literature is concerned, it seems as though its use as a gelation accelerator has never been reported. In this project, the gelation process in presence of CO_2 has been studied. Special attention has been given to the influence of various factors (temperature, component ratio, solvent nature) on this process.

Initially, the experimental methods used in this work for the synthesis of aerogels and their characterization are described. The experimental results are subsequently presented and the advantages of the proposed method, discussed.

3.1. Methods and apparatus for silica aerogel production

A high pressure autoclave was constructed for the aerogel synthesis. This autoclave was used for both aerogel production and drug loading.

The calculations required for the autoclave construction were performed according to the German high pressure vessels standard (Druckbehälterverordnung). The principle scheme of the autoclave is as shown in Figure 3-1. The detailed version of this diagram can be found in the Appendix.
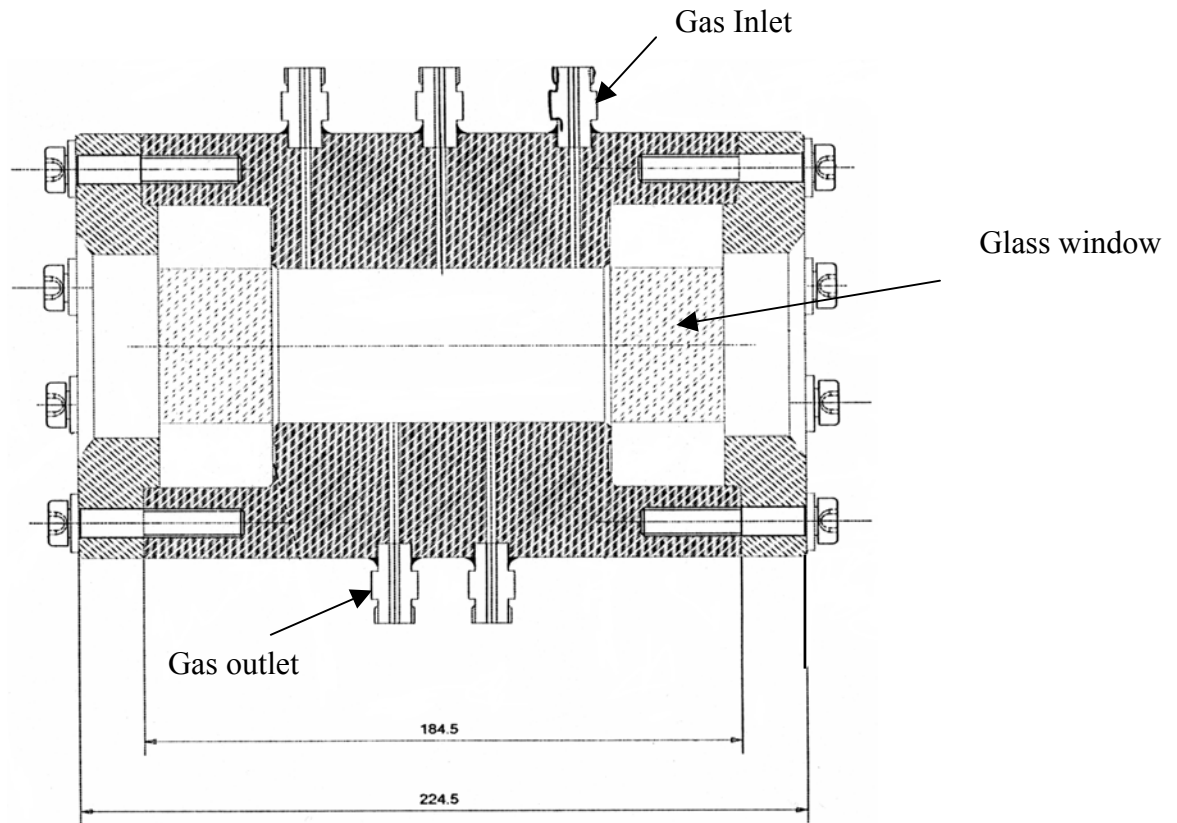
Figure 3-1 Autoclave for the aerogel production

The view cell consists of a stainless steel (V4A) cylinder, 2 viewing glass windows (stainless steel 1.4462 and borosilicate glasses DIN 7080, Herbert Ind., Wuppertal), and 2 flanges, which are sealed with Teflon rings. The maximal working pressure of the autoclave is 200 bar, maximal working temperature is 100 °C. For the extraction of the solvent, the autoclave has 3 inlets and 2 outlets for CO_2. During the extraction of the solvent from the gel the optimal mixing between the gas and the solvent in the pores of the gel should be achieved. To reach this purpose the ideal number and position of the inlets and outlets were simulated using "Fluent/3D". Several possible combinations of the number and position of inlets and outlets were considered.

The following assumptions were made for the simulations:

- Autoclave is filled with the aerogel
- Porosity of the aerogel is 95 %

The flow in the presence of 3 inlets and 2 outlets was found to be optimal. The results of the simulations for this specific case are presented in Figure 3-2. The arrows represent the gas moving through the aerogel. In the simulation, it can be seen that there are practically no dead zones in the autoclave.
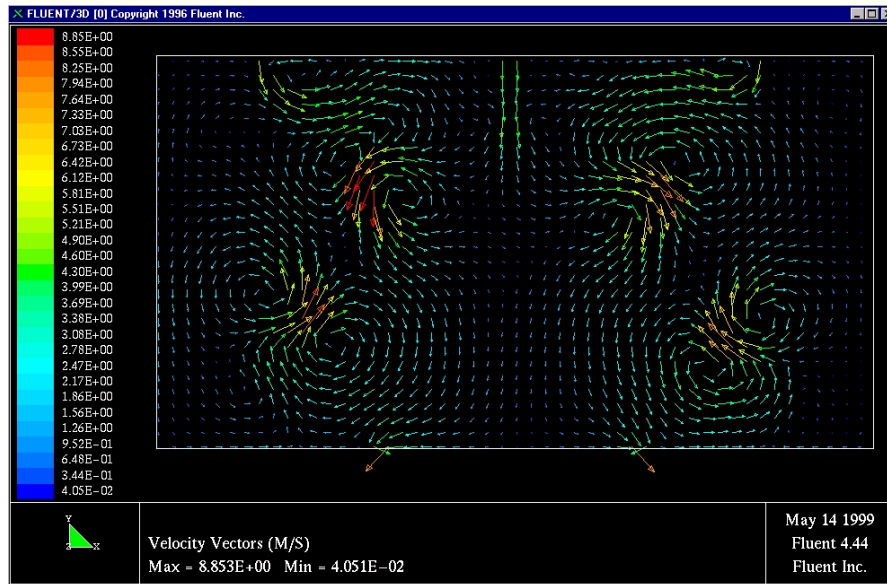
Figure 3-2 CO$_2$ flow in the autoclave filled with aerogel

The calculated position of the inlets and outlets was realized in the autoclave with an accuracy ± 4 %.

The volume of the autoclave is 249.5 ml. The diameter of each inlet and outlet is 1 mm. For better mixing in the liquid phase, the autoclave can be rocked with constant velocity. In the case of very viscous fluids and/or the presence of a solid phase, steel balls with a diameter of 10 mm can be introduced in the autoclave to enhance the mixing. The temperature is regulated by means of a heating jacket and temperature controller with an accuracy of ± 1°C. The temperature is measured with a Pt100 thermometer calibrated by two point measurements (ice water and boiling water). The periphery pipelines are constructed to enable gas support of the system. The flow sheet of the apparatus is shown in Figure 3-3.

Figure 3-3 Flow sheet of the apparatus for aerogel production and adsorption measurements

For the main part of the experiments, CO_2 support was needed. The gas originating from the tank (1) is compressed in the gas pump (3) (membrane compressor, Whitey Model LC-10) and heated up to the target temperature in the heat exchanger (5). The pump pro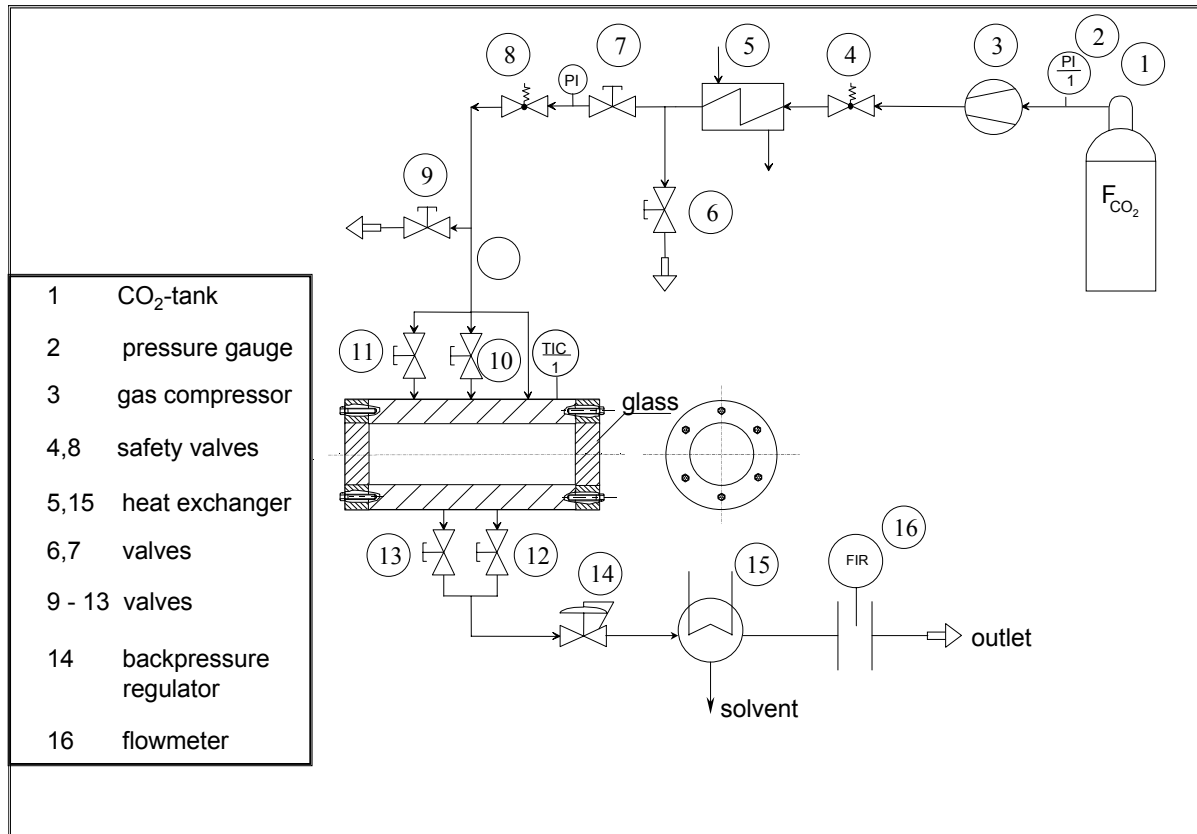vides a constant flow rate, which can be regulated additionally by the back pressure regulator (14), (TESCOM Vordruckregler 26 - 1700). The solvent, eventually present in the outlet gas stream can be condensed in a heat exchanger (15). The flow rate of CO_2 is measured by the flow meter (Brooks Schwebekörper Durchflußmesser, Serie GT 1350), which is calibrated using the air stream.

3.1.1   Selection of the synthesis method

The aim of the project was to find conditions that enhance the gelation process and thus, reduce the gelation time. As mentioned in section 2.1.2.2, the two-step process provides shorter gelation times than the one-step process. However, the two-step process, as described in [Tillotson 1992] includes several time consuming steps, like special purification of the reagents and distillation of the alcohol. The distillation of alcohol can be eliminated if the aerogel with a density higher than 0.01 g/cm^3 is to be produced, as achieved by [Lee 1995] (see also section 2.1.2.3). The same approach was employed in the conducted work. The

principle scheme of the 2-step method and the component ratio as recommended in [Tillotson 1992] was followed (see also section 2.1.2.2). Hydrochloric acid and ammonium carbonate were chosen as catalysts, as defined in the common 2-step procedure (section 2.1.2.3). The concentration of both catalysts was varied in aim of finding the optimal conditions, but no distillation of alcohol or purification of the reagents as suggested in [Tillotson 1992] was performed. The goal of the project was to allow for reaction enhancement, which would provide the same short gelation time as in the conventional two-step method, without having to perform the tedious operations characteristic of this method.

3.1.2   Synthesis of a silica aerogel by the two-step method

Silica aerogels were made following the modified two-step procedure described in [Tillotson 1992]. In the first step TMOS was mixed with water, methanol, and hydrochloric acid. The molar ratio of the components during the hydrolysis was as follows:

$$1 \text{ mol TMOS} : 2.4 \text{ mol MeOH} : 1.3 \text{ mol } H_2O : 10^{-5} \text{ mol HCl}$$
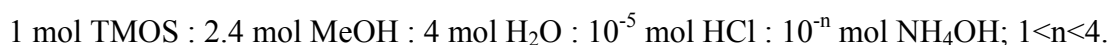
The reaction mixture was stirred for 30 minutes. The distillation of alcohol was not performed after the first step.

After that acetonitrile, water, and ammonia solution were added to the initial mixture (second steo) . The amount of acetonitrile was calculated to get the desirable concentration of TMOS (target density). Different mole ratios (to TMOS) of the ammonia base catalyst was used for the condensation reaction as noted below:

$$1 \text{ mol TMOS} : 10^{-n} \text{ mol } NH_4OH; \, 1 < n < 4.$$
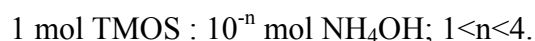
The final molar ratio of the components after the second step was as follows:

$$1 \text{ mol TMOS} : 2.4 \text{ mol MeOH} : 4 \text{ mol } H_2O : 10^{-5} \text{ mol HCl} : 10^{-n} \text{ mol } NH_4OH; \, 1 < n < 4.$$

The water containing in the catalysts solutions was also taken into account. The resulting mixture (70-150 ml) was poured into a mold and stored for gelation at the target temperature (25°C < T < 70°C). Note: The gelation time depends on the target density. After gelation, the resulting gel was aged for a period 10-24 hours. The gel was then placed in the autoclave, together with some additional acetonitrile to prevent evaporation of the solvent from the gel. Supercritical drying was then performed following the principles of the low temperature SCD, as described in section 2.1.5.1. CO_2 was preheated to the target temperature (20-70°C) by means of a heat exchanger (Pos. 5, Figure 3-3) and slowly introduced into the autoclave so that the gel was not damaged by the sudden pressure change. After the pressure in the autoclave was equal to that in the gas tank, the compressor was switched on and the pressure

was slowly increased to 100 bar. The outlet valve was then opened and the CO_2 flowed through the gel. During this process, some cracks were seen to appear within the gel body due to the sudden gas flow. The flow rate was maintained at a constant value. The value of 20 NL/h was found to be an optimal flow rate for the drying process. The outgoing stream was then passed through pure water and analyzed by GC after 1-hour intervals. In cases where traces of acetonitrile were found, the water was changed and the extraction process was continued. The extraction process was continued until no more solvent (acetonitrile or TMOS) was detercted in the outgoing stream. For the given gel volume and flow rate, the optimum extraction time was found and used in the following experiments, so that the GC analysis was no longer necessary.

3.1.3   Synthesis of a silica aerogel modified by CO_2 addition

In the case of aerogel synthesis modified by CO_2 addition, the initial sol solution was prepared as described in section 3.1.2. The volume of the solution was between 80ml and 150 ml. A small amount of the initial solution (~5 ml) was poured into a glass vial and stored separately at the same temperature (control sample). The rest was poured directly into the autoclave which was then heated to the target temperature (25°C < T < 70°C).

While heating, the autoclave was rocked so as to allow for better heat transfer. When the target temperature was reached, the CO_2 (preheated to the same temperature) was added to the solution in small portions. CO_2 was first pumped into a small gas vessel, this vessel was weighed and then CO_2 was added into the rocking autoclave. The amount of CO_2 added to the system was determined by weighing the gas vessel before and after such gas addition. Typically 2-3 g of CO_2 were added at once. After the addition of each portion of the gas, the pressure increased quickly and then decreased slowly due to the dissolution of CO_2 into the solution. The mixture remained colourless and transparent and no phase separation was observed. Figure 3-4 portrays a photograph of the autoclave filled with the sol.
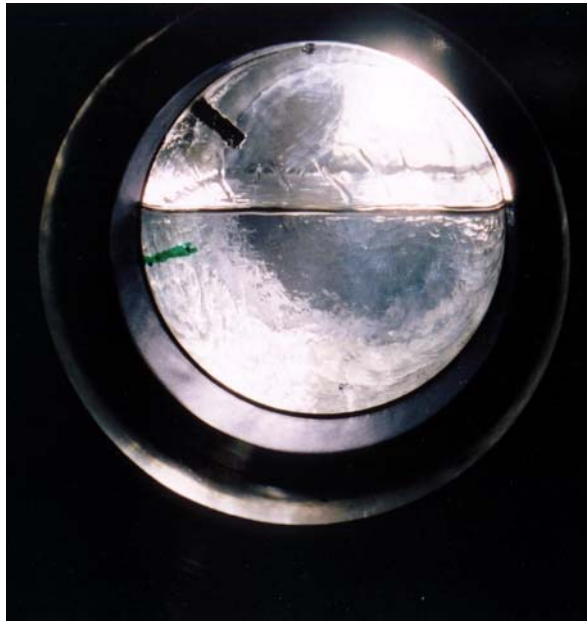
Figure 3-4 Sol solution during CO$_2$ addition (before gelation).

The liquid phase (sol and CO$_2$ dissolved therein) occupies approximately half of the autoclave volume. The upper phase is a gas phase, containing CO$_2$ and a small amount of solvent. On the left upper side of the autoclave, and thus in the gas phase, is a thermocouple. The solution is not quite homogeneous, because of the dissolution of CO$_2$ in the liquid phase. CO$_2$ was further added to such a solution. The viscosity of the liquid phase increased continuously with increasing CO$_2$ concentration. When a certain concentration of CO$_2$ was reached, the solution lost its fluidity and became a gel. The viscosity of the gel was so high that it no longer moved when the autoclave was rotated by a considerable angle.

This state can be seen in the photograph depicted in Figure 3-5, where the autoclave is rotated to the right by 90°. The change in the position of the autoclave can be observed by the thermocouple, which now occupies a position on the right upper side of the picture. The gel phase on the left side of the image shows that the gel does not move during the rotation of the autoclave.

Figure 3-5 Gelation occurs (autoclave is rotated to the right by 90°).

At this point, no more CO_2 was added. The final pressure above the solution was between 30 and 50 bar.

In a few experiments the solutions either did not form a gel at all or the gelation process required long periods of time. In these cases, this occurrence prevailed for both the samples containing CO_2 and the control samples. These cases were not taken into account during this work. To avoid the large uncertainty in the experimental data, all experiments were repeated at least twice.

The resulting gel was aged in the autoclave during 1 - 72 hours. The volume of the gel did not change significantly and its appearance did not alter during the aging procedure. This state can be seen in Figure 3-6. This gel looks very similar to that shown in Figure 3-5, but, in this case, the autoclave is not rotated.

The supercritical drying procedure was then carried out as described in section 3.1.2. The only difference was that the initial pressure in the autoclave was around 30 bar, because of the CO_2 addition during the gelation. The pressure was slowly increased up to 100 bar and then the extraction was carried out as described in section 3.1.2. The extraction process was maintained as long as no solvent was found in the outgoing stream. After the extraction was completed, CO_2 was slowly vented out from the autoclave (flow rate being equal to 20 Nl/h). The autoclave was then cooled down to room temperature The final state of the drying procedure is shown in Figure 3-6. The volume of the resulting aerogel compared to that of the gel has decreased a little (i.e. shrinkage took place), but the aerogel still possesses a half-

cylindrical form, like that of the corresponding gel. At this point the aerogel synthesis is completed and the product aerogel can be removed from the autoclave.
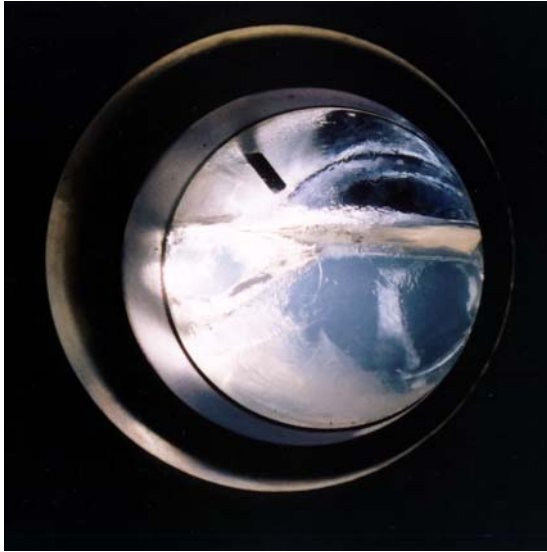

Figure 3-6 Gel before drying
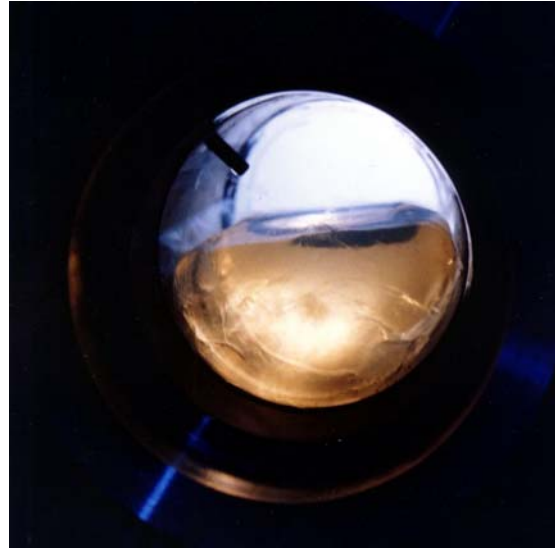
Figure 3-7 Aerogel after the supercritical drying

3.1.4   Characterization of the aerogel properties

3.1.4.1   Bulk density

The bulk density of an aerogel was determined by weighing a sample of known volume. It was rather difficult to manually cut the aerogels in such a way as to obtain a regular geometric shape. A cutting cylinder was therefore used for this purpose. This allowed for accurate cylindrical pieces of the aerogel to be produced allowing for the accurate calculation of the volume through measurement of the length and diameter of the cylinder. The density of the aerogel was determined as a mean value of at least two measurements.

3.1.4.2   Pore size and surface area

Both pore size and surface area were measured by the nitrogen adsorption/desorption technique. The adsorption isotherm, in this case, depends on the molar quantity of nitrogen (or it standard volume, V_a) adsorbed by the solid surface as a function of gas pressure. Plots of V_a against the reduced gas pressure, P/P_0, (P_0 is the vapor pressure of nitrogen at 77K) reveal much about the structure of the adsorbing material simply by its shape and the presence of a hysteresis between the adsorption and desorption curves. The theory of Brunauer, Emmett and Teller (BET) enables the calculation of the specific surface area of the

adsorbence, its pore size and volume from the adsorption/desorption data. This theory is based on the Langmuir adsorption theory, but, whereas Langmuir assumed that the gases form only one monolayer on the solid, Brunauer, Emmett and Teller suggested a multilayer adsorption mechanism. The BET theory is based on the assumption that the forces active in the condensation of gases are also responsible for the binding energy in multi-molecular adsorption. By equating the rate of condensation of gas molecules onto an already adsorbed layer to the rate of evaporation from that layer and summing for an infinite number of layers, the following expression can be obtained:

$$\frac{P}{V_a(P^{LV} - P)} = \frac{1}{V_m C} + \frac{C-1}{V_m C}\left(\frac{P}{P^{LV}}\right) \tag{24}$$

C is the constant, resulting from the difference between the enthalpy of adsorption of the first layer and enthalpy of condensation of nitrogen. The values of V_m and C may be obtained from a straight-line plot of $\dfrac{P}{V_a(P^{LV} - P)}$ vs. $\dfrac{P}{P^{LV}}$. The volume of the monolayer, V_m having been determined, allows the surface area of the sample to be determined using the area occupied by a single nitrogen molecule (16,2 A^2 at 77K) [Micrometrics 1998]

This method was successfully applied to determine the specific surface area of silica aerogels. A typical adsorption isotherm is shown below.

The adsorption isotherm shows a hysteresis loop, typical for mesoporous materials, having the pores with a diameter of 2-50 nm. The reason for the hysteresis is the difference between the evaporation from the pore and the condensation within it. When gas condenses in a pore, the condensate travels on the walls inwards toward a central core of decreasing diameter. The decreased diameter leads to retards the evaporation process and causes the decreasing portion of the loop to lag behind until all pores have emptied [Micrometrics]. The specific surface area of silica aerogels is around 500-1000 m^2/g. The value of the constant C is between 100 and 150. As discussed in the previous section, the determination of the pore volume by nitrogen adsorption is not an accurate method, because of the shrinkage of the aerogel during the condensation and the following evaporation of the nitrogen. However, the surface area is calculated in the region of relatively low pressures, where the shrinkage still does not play an important role. The measurements were carried out at the Institut für Technische Chemie, Technische Universität Berlin.
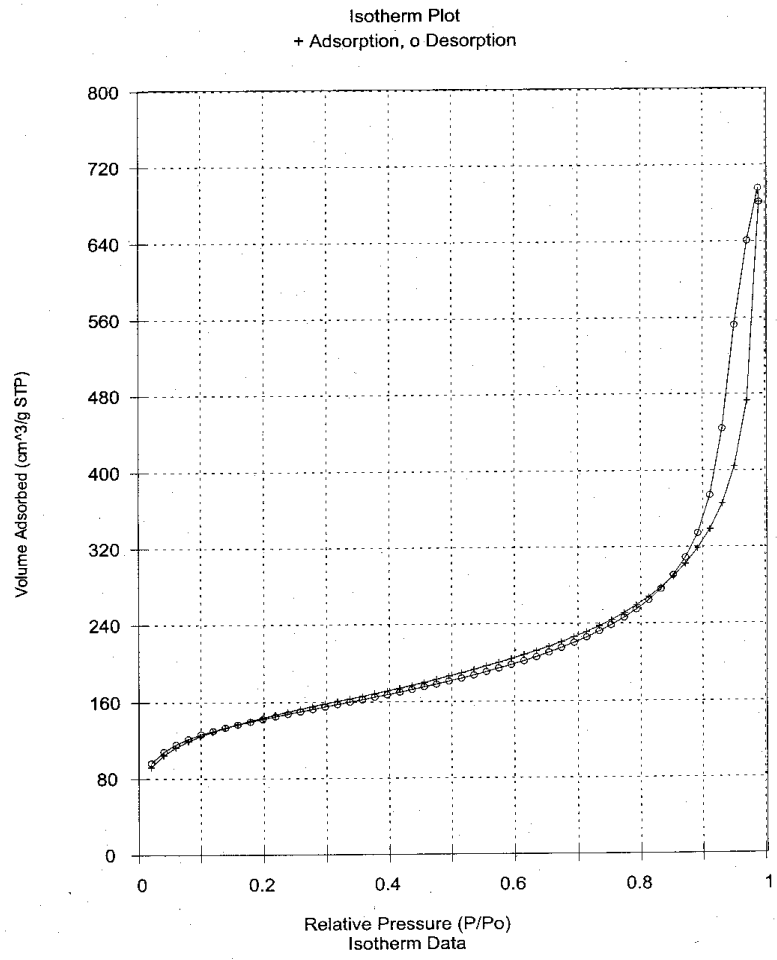
Figure 3-8 Adsorption isotherm of nitrogen on silica aerogel

3.1.4.3   Spectroscopic measurements

The optical properties of a silica aerogel as well as its chemical composition may be investigated by IR spectroscopy. In this work, IR spectroscopy was used for the qualitative characterization of the aerogel composition. For the spectroscopic measurements, the silica aerogels were used in the powdered form, compressed with wax and KBr. The adsorption spectra were measured in the region of 600-4000 cm^{-1}. An IR Spectrometer Magna System 750 was used for these measurements. The measurements were carried out at the Institut für Anorganische Chemie, Technische Universität Berlin.

3.2. Gelation enhancement by CO_2 addition

Two-step process was modified by the addition of CO_2 to the sol solution during the second step. The experimental procedure is described in section 5.3. Astonishingly, it was found that the addition of CO_2 leads to a fast gelation of the solution. This fact has never been reported in the literature [Arlt 2000].

In order to characterize the gelation enhancement, gelation times were measured for the samples prepared by CO_2 addition and for the control samples, that were allowed to form a gel without CO_2 addition.

To determine the gelation time the experimental procedure was slightly different to that described in section 5.3. CO_2 was added to the solution, not in the small portions, but the whole amount needed to reach the predetermined CO_2 concentration in the mixture was added at once. The gelation time ($t_{gel}^{CO_2}$) was determined as a time interval from the moment of the CO_2 addition to the moment when the solution lost its fluidity. The gelation time of the control sample (t_{gel}) was determined as the time interval between the point at which the target temperature was reached and the point at which the solution was completely altered into a gel. The time period needed for the CO_2 addition (normally around 5 minutes) was subtracted from the results. In Table 3-1, the results for the solution with a target density of 0.03 g/cm^{3}are presented. One can see that the gelation time decreases drastically with CO_2 addition. For example, the gelation time at 25°C is 161 hours for the conventional sol, but only 1 hour in the sase of CO_2 addition. At higher temperature the difference in gelation times is not as large, but still significant (21 hours compared to 53 minutes).

It should be noted, that the gelation process takes place at an even faster rate when CO_2 is added in portions. However, in this case, the gelation time can not be determined accurately, because the procedure depends on the operator's handling (e.g. closing and opening the valve, stirring time between the steps etc.). All this factors cause a large uncertainty in the calculated gelation time. On the contrary, if CO_2 is added at once, the gelation time is well defined and, thus, can be measured reliably.

t_{gel} , 25°C	t_{gel}, 40°C	$t_{gel}^{CO_2}$, 25°C	$t_{gel}^{CO_2}$, 40°C
161 h	21 h	60 min	53 min

Table 3-1 Gelation times at 25 and 40°C. Component molar ratio:

1 mol TMOS : 2.4 mol MeOH : 4 mol H_2O : 10^{-5} mol HCl: 10^{-2} mol NH_4OH.

It is supposed that the gelation time depends strongly on the CO_2 concentration. To study this effect, the gelation time was measured as a function of the CO_2 content in the system. The experimental results are presented in Figure 3-9. The solid line represents the trend line fitted to the experimental data. The trend parameters are noted in the legend.

It can be seen that the gelation time decreases rapidly with increasing CO_2 content and approaches a constant value when the total CO_2 concentration reaches 20 wt %. Further addition of CO_2 does not enhance the reaction significantly.

As CO_2 was added to the sol solution, it dissolved partly therein. Just after the CO_2 addition, the pressure increased and than decreased rapidly because of the dissolution of CO_2 in the liquid phase. Generally, equilibrium was reached within 15-30 min, depending on the total amount of CO_2 added. After equilibrium was reached, the pressure remained constant and this value was taken for evaluation. The final pressure above the sol determines the CO_2 solubility. The dependence of the CO_2 concentration on the final pressure in the system is shown in Figure 3-10.
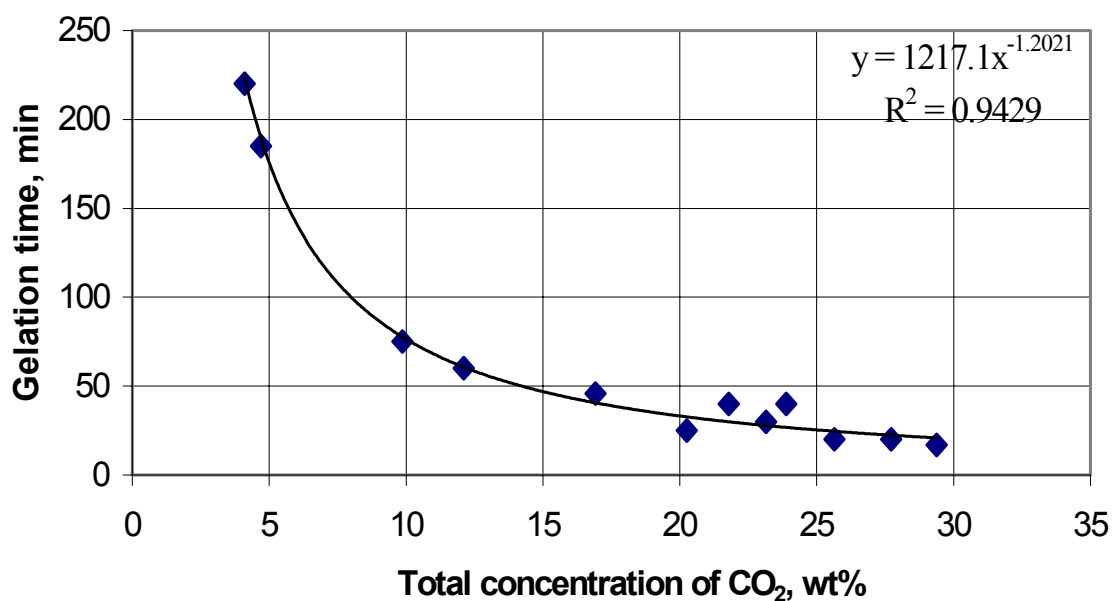
Figure 3-9 Dependence of the gelation time on the amount of CO_2 added to the system at 40°C. Component ratio: 1 mol TMOS : 2.4 mol MeOH : 4 mol H_2O : 10^{-5} mol HCl: 2×10^{-3} mol NH_4OH. Solvent – acetonitrile; $\rho_{target} = 0.04$ g/cm^3
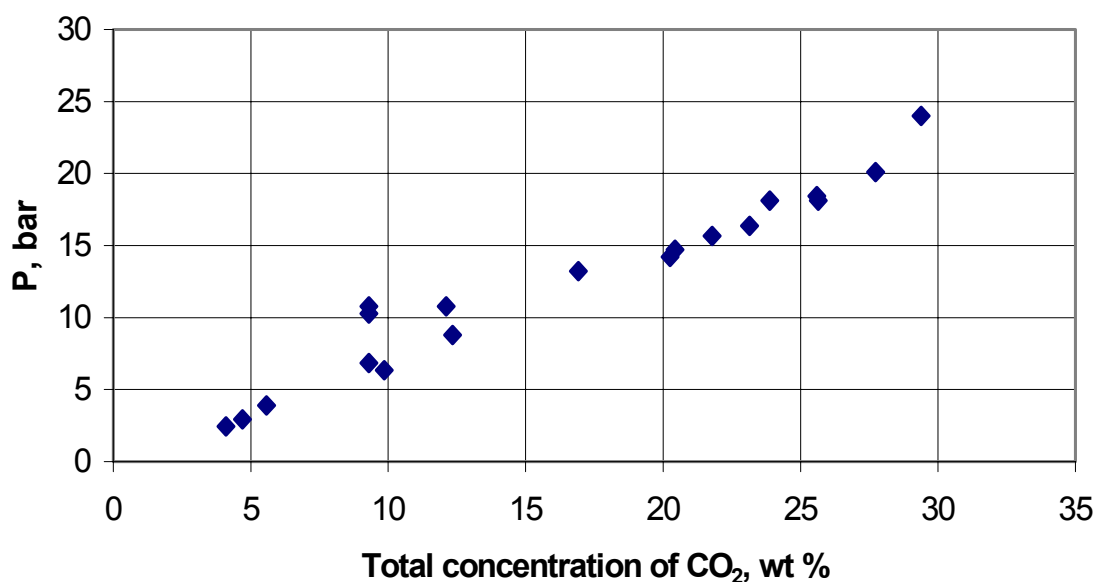

Figure 3-10 Pressure – concentration dependence in the system CO_2 – sol.

Considering that the reaction takes place in the liquid phase, we can expect that the reaction rate depends on the concentration of CO_2 in the liquid phase rather than on the total CO_2 concentration in the system. It is difficult to estimate the concentration of CO_2 in such a reacting system directly, because the composition of the liquid phase changes continuously. In the case of slow reactions several methods which allow measurement of the liquid phase concentration are known. In our case, the addition of CO_2 leads to an acceleration of the reaction, so that the whole process can be completed within several minutes. Thus, reliable measurement of the concentration of CO_2 in the liquid phase during the reaction cannot be achieved. However, it is possible to estimate this value from the experimental results on the basis of some assumptions. The initial solution consists of several components, including TMOS monomer, water, catalyst and acetonitrile as solvent, the main component being the solvent. When the reaction has initiated, the solution also contains the reaction products: partly hydrolyzed TMOS, methanol and a variety of polymer chains. But at the very beginning of the reaction (reaction time = 0) we can assume, that the volume of the mixture is a sum of the volume of all components (under neglect of the excess volume). In this case the volume of acetonitrile is proportional to the target density (25).

$$V_{acetonitrile} = \frac{m_{SiO_2} - \rho_{target} V_{sol}}{\rho_{target}} \qquad (25)$$

Knowing the volume of the mixture and the target density of the solution, the acetonitrile concentration can be calculated. The calculation for several target densities is given in Figure 3-11. Because most of the experiments were aimed to obtain target densities less than 0.04 g/cm^3, the concentration of acetonitrile was always greater than 75 wt%, as can be seen from the Figure 3-11. The reactions are therefore conducted in very diluet solutions. The solubility of CO_2 in the reacting mixture can, therefore, be expected to be close to the solubility of CO_2 in acetonitrile.
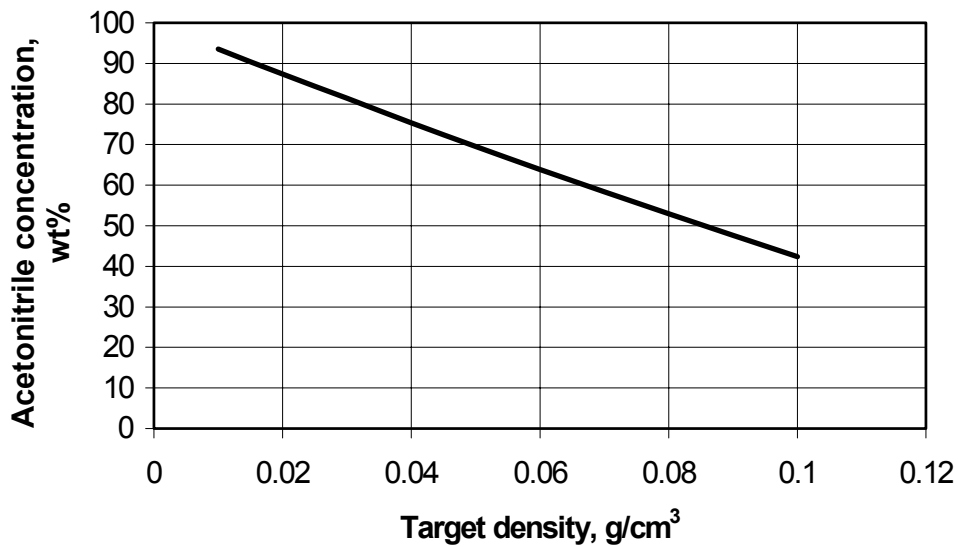
Figure 3-11 Dependence of the acetonitrile concentration on the target density of the solution

The vapor-liquid phase equilibria of the acetonitrile-CO_2 mixtures has already been studied [Bendale 1994], [Kordikowski 1995]. No liquid-liquid separation has been observed. The experimental results taken from this work are shown in Figure 3-12.
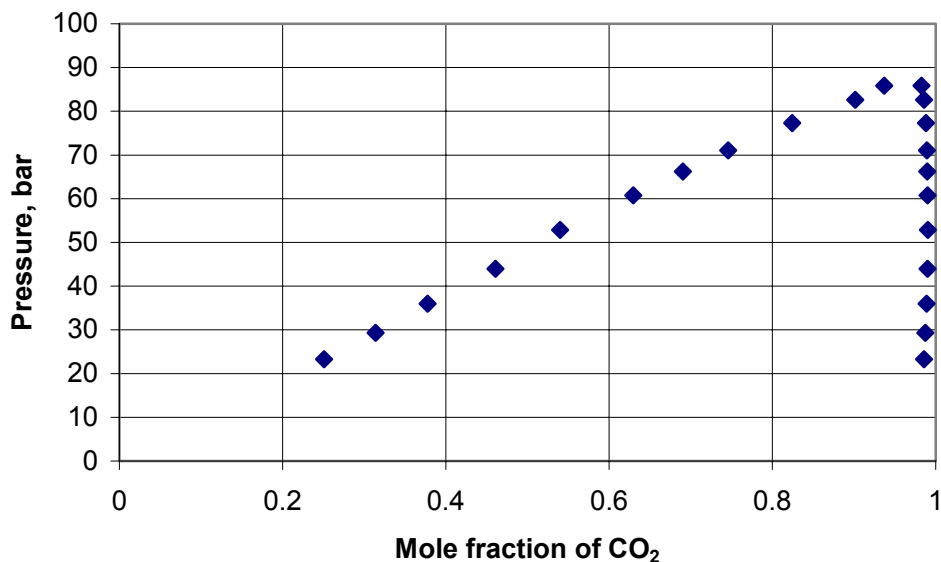
Figure 3-12 P-x-y diagram for the system CO_2-acetonitrile at 45°C [Bendale 1994]

It is clear that the concentration of acetonitrile in the vapor phase is very low (mole fraction of CO_2 is close to unity). Thus, it may assumed that the concentration of CO_2 in the gas phase is 100%. Using this assumption it is possible to estimate the concentration of CO_2 in the

solutions studied. The estimation procedure is based on the iteration method and is composed of the following steps:

a) The volume of the liquid phase is calculated using the experimentally determined mass of the solution in the autoclave and the density of the liquid phase. The densities of the corresponding solutions were measured using a pycnometer with an accuracy ±1%. The results are summarized in the Table 3-2.

b) The volume of the vapor phase is calculated as the difference between the total volume of the autoclave and the volume of the liquid phase.

c) The CO_2 mass in the gas phase is determined using its density under the experimental conditions. The pressure for every composition is identical with that presented in Figure 3-10. Fluid properties of CO_2 were taken from the NIST database [NIST].

d) The amount of CO_2 in the liquid phase was calculated by subtraction of the CO_2 amount calculated in step (c) from the total CO_2 amount added to the system.

e) A new liquid phase volume was calculated under the assumption that the density of the liquid phase does not change significantly. This iteration procedure was repeated until the concentration of CO_2 in the liquid phase remained constant.

ρ_{target}, g/cm^3	$\rho_{solution}$, g/cm^3 (23 °C)	$\rho_{solution}$, g/cm^3 (33 °C)
0.03	0.8079	0.7934
0.04	0.8184	0.8086
0.05	0.8267	0.8174

Table 3-2 Densities of the sol solutions studied

Using this method, the CO_2 concentration in the liquid phase was calculated for all experiments. The diagram constructed in this way for the sol-CO_2 system is presented in Figure 3-13. Another set of experimental data measured by Kordikowski et al [Kordikowski 1995] for the binary system CO_2 − acetonitrile is also presented in Figure 3-13.
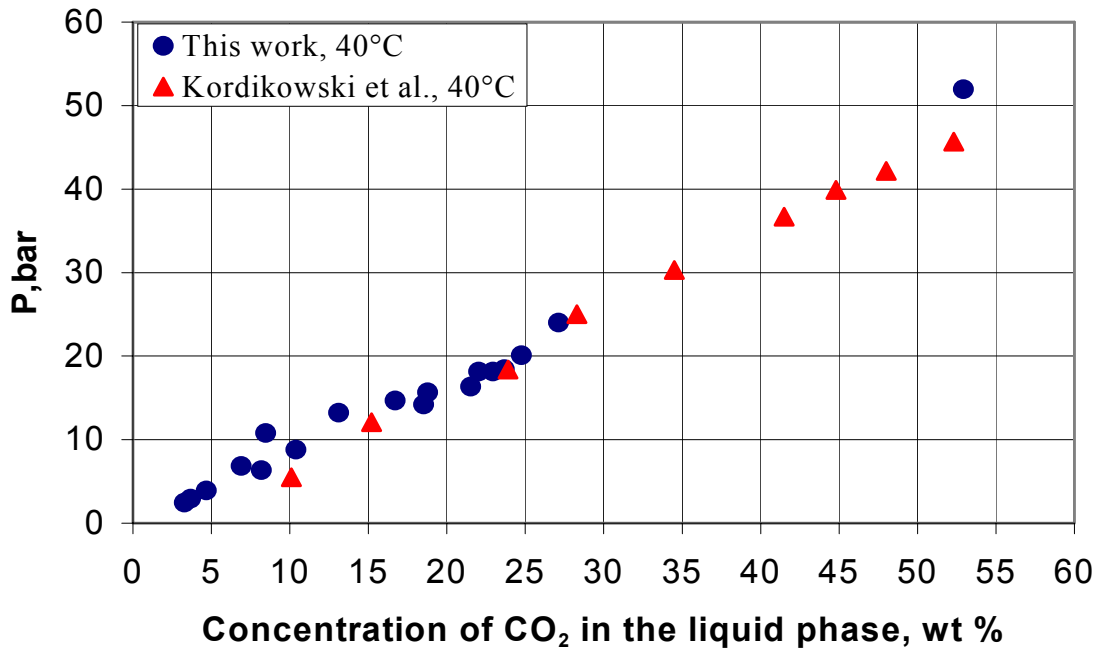
Figure 3-13 Solubility of CO_2 in sol solution at 40°C. Component ratio in the sol solution: 1 mol TMOS : 2.4 mol MeOH : 4 mol H_2O : 10^{-5} mol HCl: $2X10^{-3}$ mol NH_4OH. Solvent-acetonitrile; ρ_{target} = 0.04 g/cm^3.

From the plots, it can be seen that the solubility of CO_2 in the sol is very close to that in acetonitrile. It is expected that in the case of solutions of lower target densities, the solubility of CO_2 in such solutions is even more close to it solubility in acetonitrile. Thus, the data of CO_2 solubility in acetonitrile can be used to make the first rough estimation of the CO_2 content in the liquid sol phase, since this cannot be measured directly.

No liquid-liquid phase separation was found in the CO_2-sol system by visual observation even in the case when the CO_2 concentration in the system was 50 wt% as long as gelation did not take place. The volume of the system increased by 10-40 % depending on the CO_2 amount added. After gelation took place, further CO_2 addition lead to the formation of another liquid phase, directly over the gel phase.

Using the procedure described above, the calculation of the CO_2 concentration in the liquid phase for the experimental data shown in Figure 3-9 can be performed. The results are presented in Figure 3-14. The solid line represents the trendline fitted to the experimental data. The trend parameters are noted in the legend. It can be seen that this dependence exhibits a similar trend to that presented in the Figure 3-9. This indicates that the total concentration of CO_2 in the system is a suitable parameter for the characterization of this phenomenon. The dependence of the gelation on the corresponding values of the total concentration of CO_2 in the system and its concentration in the liquid phase will be further presented.
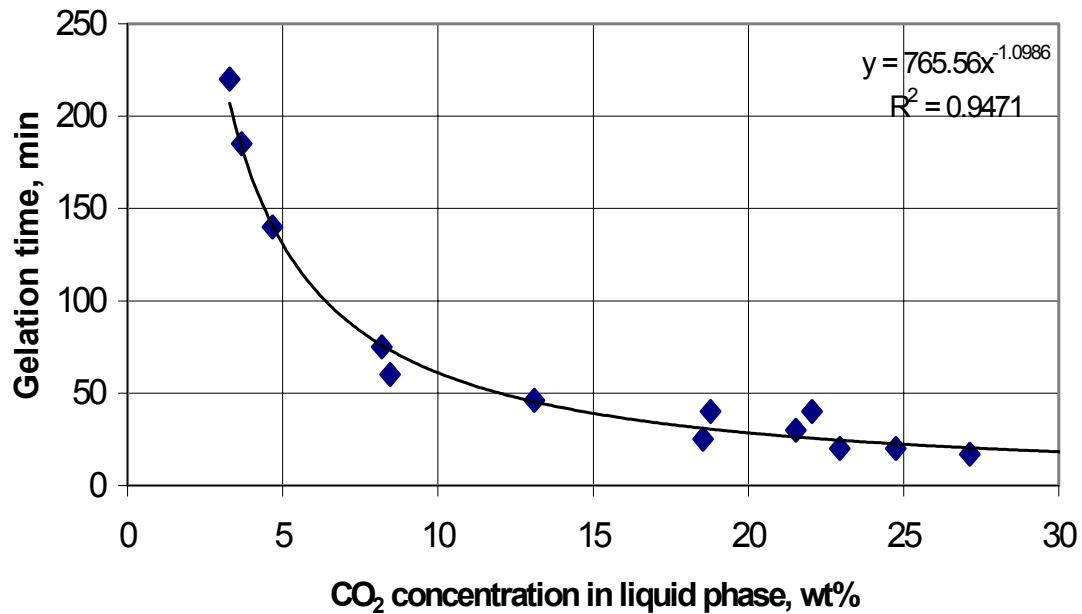
Figure 3-14 Dependence of the gelation time on the CO_2 concentration in the liquid phase

3.2.1 Determination of the optimal CO_2 concentration required for gelation

As indicated in section 3.2, addition of CO_2 always leads to a faster gelation process. However, the gelation time is dependent on the CO_2 concentration in the solution. It was of interest to find an optimal CO_2 solution concentration for fast gelation.

This was conducted following the procedure described in section 5.3. CO_2 was added to the solution in small portions every 5 minutes until gelation took place. The concentration, reached in the liquid phase at this point ($C_{CO_2}^{opt.}$) was considered to be an optimal value.

Further CO_2 addition led to the formation of a second liquid phase on the gel surface. The optimal concentration in the liquid phase ($C_{CO_2}^{opt.}$) was determined experimentally for every solution. Once determined, this value can be used for the further experiments. In this case, the corresponding amount of CO_2 can be added to the initial mixture at once, instead of in small portions, to save time. If the optimal concentration is exceeded by more than 10 %, gelation also takes place, but precipitation of colloidal particles may occur during aging. It was found that the aerogels obtained in this case are less transparent, or, indeed, completely opaque. This

phenomenon will be discussed in detail later (see section 3.3). Thus, if a transparent aerogel is desired, $C_{CO_2}^{opt.}$ must be determined experimentally for every specific case.

3.2.1.1   Influence of the aerogel's target density

It was found that $C_{CO_2}^{opt.}$ has a constant value for a solution of given concentration, but varies with the TMOS concentration (or target density) of the solution. This effect was studied for the solution of different target densities. All other parameters were kept constant (component ratio: 1 mol TMOS : 4 mol H_2O : 10^{-5} mol HCl: 10^{-3} mol NH_4OH; t = 25°C). The dependence of $C_{CO_2}^{opt.}$ on the target density of the aerogel is shown in Figure 3-15.

One can see that with increasing target density, the $C_{CO_2}^{opt.}$ decreases. A larger target density implies a larger initial concentration of TMOS in the solution (see the definition of the target density, Eq.(26).

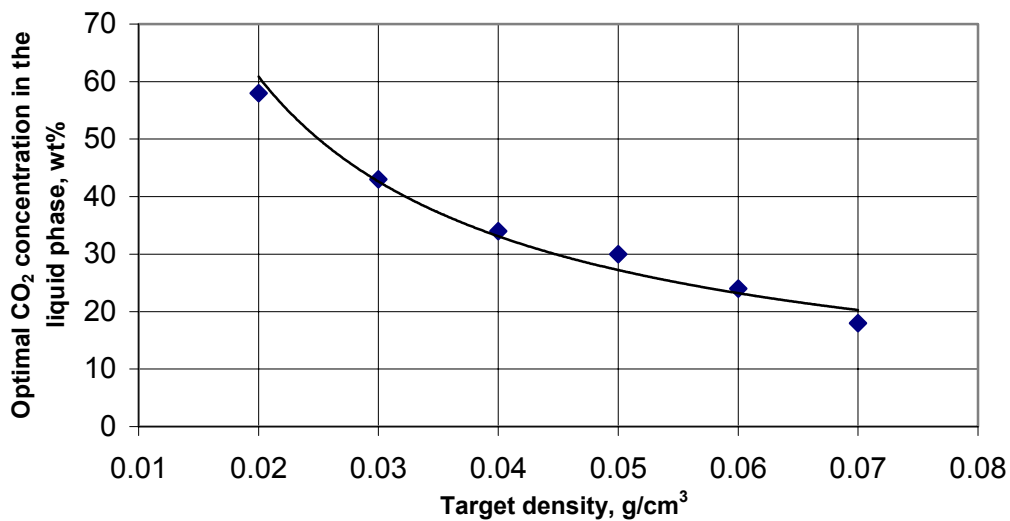$$\rho_{target} = \frac{m_{SiO_2}}{V_{sol}}$$

(26)

Figure 3-15 Dependence of the CO₂ concentration in the liquid phase needed for the gelation on the target density of the aerogel at 25°C.

The correlation between the target density and TMOS concentration is shown in Figure 3-16.

As discussed previously (section 2.5), a larger initial concentration of TMOS leads to an acceleration of the gelation process and to a denser gel. In this case, the solution is simply more concentrated and so more monomers participate in the condensation reaction. This is why less CO_2 is needed to complete the gelation in the case of a higher TMOS concentration.
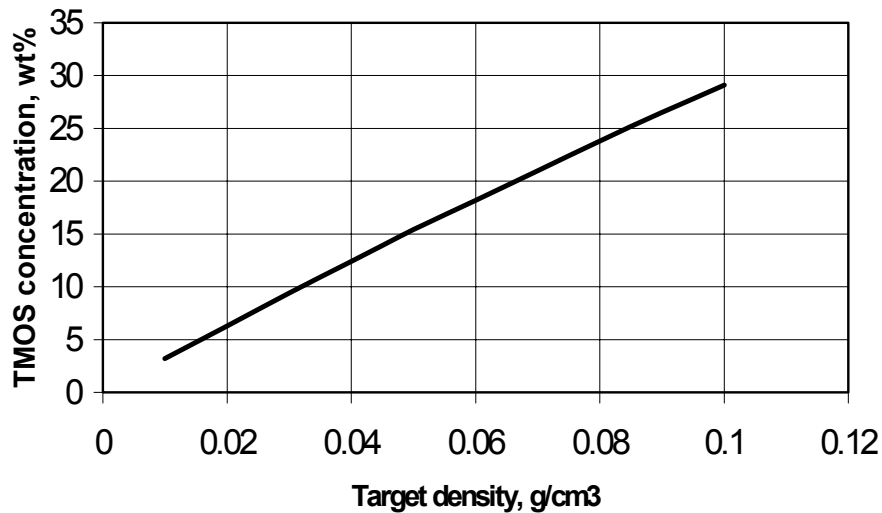
Figure 3-16 Correlation between the target density of the solution and the initial concentration of TMOS

3.2.1.2   Influence of the temperature

It is well known that the gelation time depends on the temperature of the process (see chapter 2). Independent of the component ratio, the gelation time decreases with increasing temperature. In this work, the influence of the temperature on the optimal CO_2 amount needed for the gelation was studied. It can be expected that at a higher temperature, less CO_2 is needed for gelation to be completed. The experiments were carried out for the following solution:

1 mol TMOS : 2.4 mol MeOH : 4 mol H_2O : 10^{-5} mol HCl: $2 \bullet 10^{-3}$ mol NH_4OH. Acetonitrile was used as a solvent in order to reach the corresponding target density.

The results for the solution of a 0.03 g/cm^3 target density are summarized in Table 3-3.

Temperature, °C	25	29	40	70
$C_{CO_2}^{opt.}$ in the liquid phase, wt%	44.7	40.3	37	26.4

Table 3-3 Temperature dependence of the optimal CO_2 concentration needed for gelation.

One may note that $C_{CO_2}^{opt.}$ decreases with increasing temperature. This is because both hydrolysis and condensation take place at a faster rate at a higher temperature, so that less CO_2 is needed for the reaction enhancement. The temperature dependence of the $C_{CO_2}^{opt.}$ was measured for different target densities. The results for different temperatures and target densities are summarized in Figure 3-17. One can see that for the solutions of all target densities, $C_{CO_2}^{opt}$ decreases with increasing temperature. Solid lines represent the trend lines fitted to the experimental data.

The target density region of the solutions studied was chosen following several criteria:

in the case of relative high target densities ($\rho_{target} > 0.1$ g/cm^3) the gelation time achieved by common processes is already low (<1 hour); in this case no additional reaction enhancement is needed. Samples of low densities require longer gelation time, so the method suggested in this work is advantageous. In the case of very low density ($\rho_{target} < 0.01$ g/cm^3) a very large amount of CO_2 would be needed (see Figure 3-15). In this case it is useful to increase the amount of the basic catalyst before CO_2 addition is conducted. The influence of the catalyst concentration on the $C_{CO_2}^{opt}$ will be discussed later.

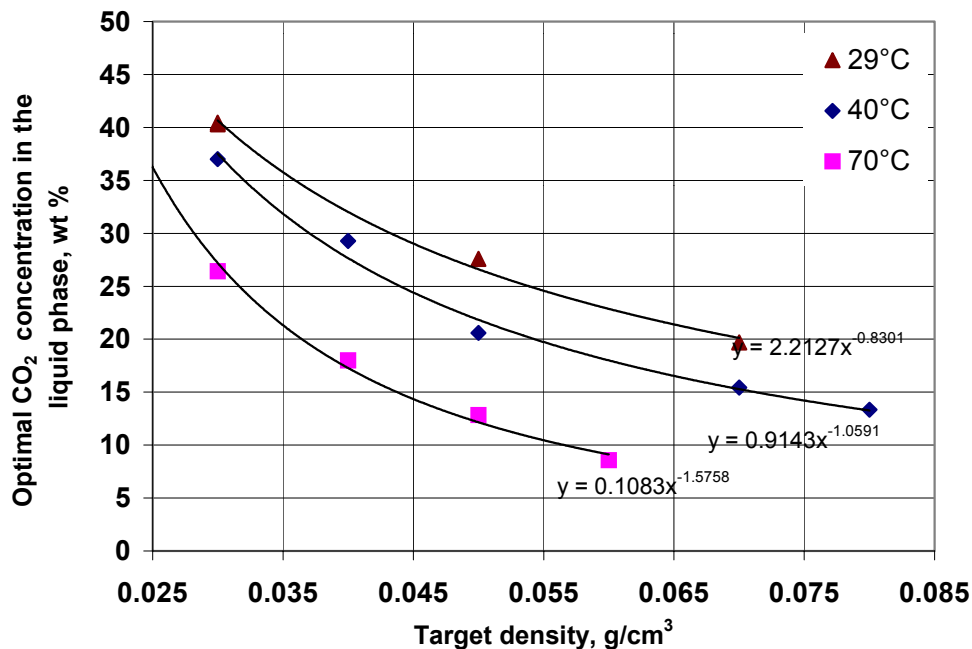**Figure 3-17 Dependence of $C_{CO_2}^{opt}$ in the liquid phase on the target density of the aerogel at**

different temperatures.

3.2.1.3   Combination of CO_2 with other catalysts

Catalysts play a decisive role in the gelation process. As discussed previously (section 2.1.3.3) a number of different catalysts as well as their combinations were used for the aerogel synthesis. Since CO_2 accelerates the gelation process, it may be assumed to act in some way as a catalyst. In order to prove this, different catalysts were used in combination with CO_2 and their influence on the gelation process was studied. At first, all the possible combinations of both catalysts commonly used for the gel synthesis (NH_4OH and HCl) with CO_2 were studied. All experiments were carried out at 25°C for the following component ratio:

1 mol TMOS : 2.4 mol MeOH : 4 mol H_2O : a mol HCl: b mol NH_4OH. Acetonitrile was used as a solvent in order to reach the target density of 0.03 g/cm^3. The corresponding catalyst concentrations as well as the appearance of the final solution are summarized in Table 3-4.

Sample number	Catalyst used (mol catalyst per mol TMOS)		CO_2 mol ratio (mol CO_2 : mol TMOS)	Appearance of the final solution
	HCl (a)	NH$_4$OH (b)		
A1	10^{-5}	$2*10^{-2}$	0	Slow gelation resulted in a transparent gel
A2	10^{-5}	$2*10^{-2}$	16.72	Fast gelation resulted in a transparent gel
A3	0	0	0.1	Precipitation of colloid particles
A4	10^{-5}	0	0.1	Precipitation of colloid particles
A5	0	$2*10^{-2}$	16.72	Gelation resulted in slightly opaque gel

Table 3-4 Dependence of the gelation process with CO_2 addition on the catalysts combination used

- Sample A1 was made by the common procedure using both HCl and NH_4OH in the first and second step respectively. This solution formed a transparent gel after 23 hours.

- Sample A2 was made using the same procedure, but CO_2 was added to the solution. The CO_2 amount used was $C_{CO_2}^{opt}$ determined for these conditions as described previously. This also resulted in a transparent gel but the gelation process was faster (t_{gel} = 30 min) in agreement with our previous experiments described in section 3.2.

- Sample A3 was made in the absence of catalysts in both the first and second step. In the first step TMOS, H_2O and methanol were stirred for 30 min. After this, additional water was added to reach the final component ratio 1 mol TMOS : 4 mol H_2O and the system was diluted with acetonitrile to obtain a target density of 0.03 g/cm^3. The mixture was then filled in the autoclave and heated to 40°C. CO_2 was slowly added to the system. Immediately after the addition of 5 wt% of CO_2 a precipitate appeared in the autoclave. CO_2 addition was stopped, the solution was filtered and a white powder was obtained.

- Sample A4 was prepared similarly to sample A3, but no NH_4OH was added during the second step. The result was a white precipitate in the system.

- Sample A5 was made similarly to sample A4, but no HCl was added during the first step.. In contrast to the previous case, gelation took place within 30 minutes and the resulting gel was slightly opaque.

The gels formed by samples A1, A2 and A5 as well as the powders obtained from samples A3 and A4 were dried at ambient pressure at 60°C. The resulting samples were analyzed by IR spectroscopy. The corresponding spectra are shown below.
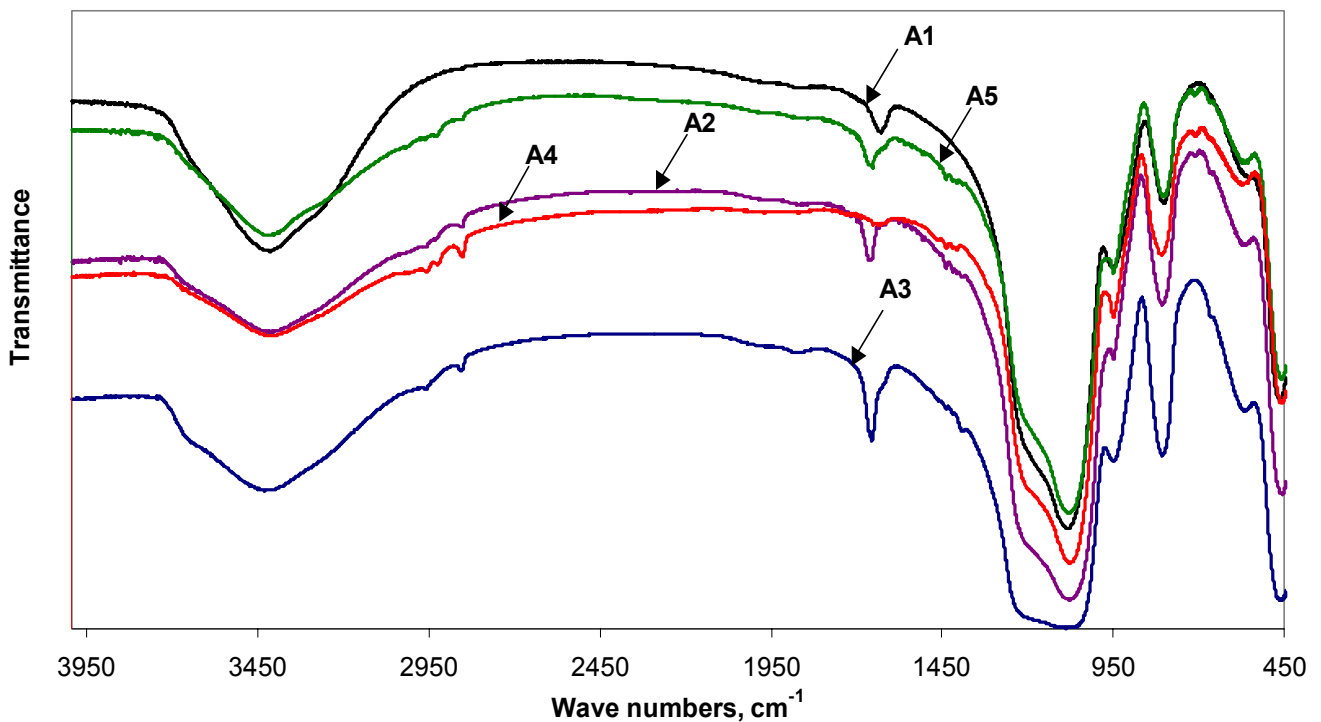

Figure 3-18 IR spectrum of the samples A1-A5

It can be seen that the spectra are very similar. The spectra were compared with the spectrum of silica aerogel and the major peaks were assigned as shown in Table 3-5.

Wave number, cm^{-1}	Chemical Bond, [Yoda 1999], [Hüsing 1997], [Orcel 1986]
3500-3400	Absorbed molecular water
3750	Free Si-OH on the surface of the gel
3665, 3540	Silanol groups linked to molecular water through hydrogen bonds, internal Si-OH
2958	Si-O-CH$_3$ symmetric stretching, C-H stretching
2856	C-H second stretching (methanol and unhydrolized TMOS)
1868, 806	(Si-O-Si); vibration of SiO$_2$ network
1655	H-O-H, absorbed molecular water
1456, 1412	C-H, $\equiv$ Si -O-CH$_3$ (unhydrolized TMOS)
1090	$\equiv$ Si -O, vibration of silica network
806	Si-O-Si vibrational mode
948, 460	Si-O-Si deformation

Table 3-5 IR Absorption bands and its attribution for silica aerogel

By comparison of the corresponding peaks, it can be concluded that all samples consist predominantly of silicon oxide. The characteristic absorptions at 1090 cm^{-1} and 806 cm^{-1} (SiO$_2$) are very strong. Some unreacted TMOS (2856 cm^{-1}) and water (3429, 1655 cm^{-1}) were also identified in the samples A2-A5, although it is difficult to say whether the corresponding peaks represent the free unreacted water or water adsorbed onto the gel surface, as in the case of silica aerogel. It may be due to the uncompleted drying at 60°C. It should be stressed that IR spectra give only qualitative (and not quantitative) information about a sample. Thus information about the concentration of the corresponding compounds cannot be obtained though this technique.

Based on the spectra, it may be concluded that precipitates obtained from the samples A3 and A4 consist mostly of silicon oxide and, thus, should be the result of the same chemical reaction as the gels A1, A2 and A5. This implies that after CO$_2$ addition to samples A3 and A4, hydrolysis and condensation reactions also take place very rapidly, but lead to the formation of colloidal particles and not to a monolithic gel. Thus, here, the effect of the reaction enhancement also takes place but leads to another product.

As we can see from the Table 3-4, CO_2 addition to the sol, in the case of no additional catalysts (sample A3), leads to a rapid precipitation of colloid particles. This proves that CO_2 is not suitable as the only catalyst for gel formation.

The combination of CO_2 and acid catalyst used in the first step (sample A4) shows the same effect. On the contrary, combination of CO_2 with only basic catalyst (NH_4OH) leads to rapid gelation (sample A5). The resulting gel is slightly opaque. As discussed in setion 2.1.3.3,the acid catalyst mostly accelerates the hydrolysis, and the basic one accelerates condensation. Since CO_2 addition without HCl results in gelation we can suppose that CO_2 acts as an acid catalyst to some extent. A transparent gel can, however, only be obtained if both HCl and NH_4OH are used.

3.2.1.4 Influence of concentration of basic and acid catalysts on the optimal CO2 concentration

As long as successful gelation with CO_2 addition is possible only in presence of other catalyst, it can be supposed that the CO_2 amount needed for the gelation might depend on the catalysts concentration.

The influence of the concentration of HCl and NH_4OH on the gelation in presence of CO_2 was studied. The concentration of one catalyst was kept constant while the amount of the second catalyst was varied. All experiments were carried out at 40°C. CO_2 was preheated to the same temperature and added in small portions until gelation took place. The concentration of HCl was changed from 10^{-5} to 10^{-3} mol per mole of TMOS. Higher concentrations were not used, because of the high corrosivity of HCl under these conditions. The results are presented in Figure 3-19 and Figure 3-20 as the dependence of $C_{CO_2}^{opt.}$ on the concentration of the corresponding catalysts. It can be seen that an increase of the HCl concentration (represented as a mol ratio - mol HCl per mol TMOS) by 100 times leads to the decrease of $C_{CO_2}^{opt.}$ by just 2 wt %. It should be noted that this value is not much higher than an experimental error.

We can, therefore, conclude that the acid catalyst used during the first synthetic step on the one hand does not interact with CO_2, but on the other hand is essential for the whole process. Without the acid catalyst during the first step, only colloidal particles can be obtained, as discussed previously. Obviously some minimal concentration of the acid catalysts is required to start the hydrolysis reaction - CO_2 is not able to replace the acid catalyst.

Figure 3-19 Dependence of the CO_2 concnetration in the liquid phase needed for the gelation on the concentration of HCl in the system at 40°C. Component ratio in the sol solution: 1 mol TMOS : 2.4 mol MeOH : 4 mol H_2O : $2*10^{-3}$ mol NH_4OH. Acetonitrile was used as a solvent to reach the target density 0.03 g/cm^3.
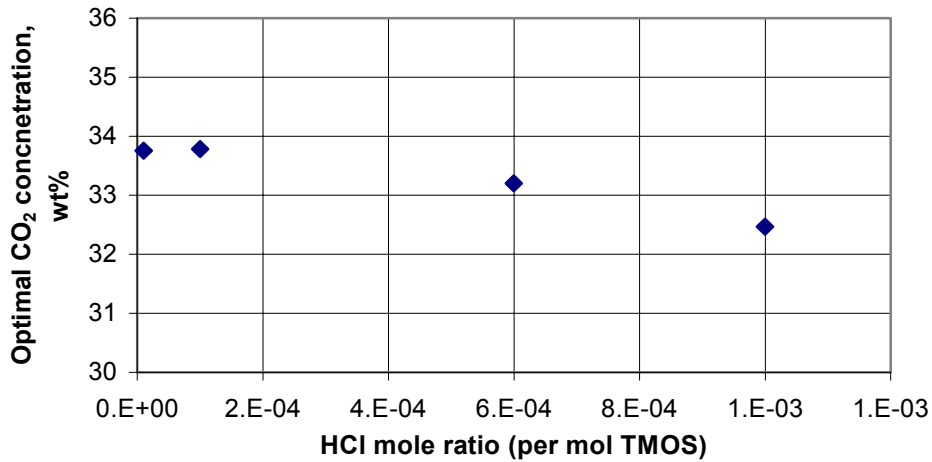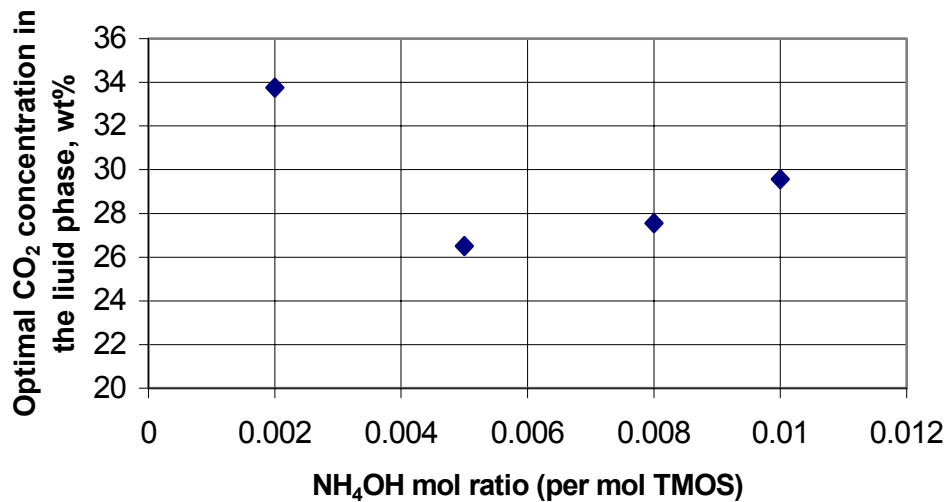

Figure 3-20 Dependence of the CO_2 concnetration in the liuid phase needed for the gelation on the concentration of NH_4OH at 40°C. Component ratio in the sol solution: 1 mol TMOS : 2.4 mol MeOH : 4 mol H_2O : 10^{-5} mol HCl. Acetonitrile was used as a solvent in order to reach the target density 0.03 g/cm^3.

The basic catalyst seems to have a stronger influence on $C_{CO_2}^{opt.}$. As shown in Figure 3-20 an increase in the ammonium hydroxide concentration by 100% leads to the decrease of the optimal CO_2 concentration needed for the gelation by 10%. It is not quite clear why a further increase in the ammonium hydroxide concentration leads to a slight increase in the optimal CO_2 concentration. It is known [Brinker 1990] that in the case of the one-step reaction, the gelation time strongly depends on the concentration of the basic catalyst. The modified two-step procedure, which was used in the present work shows the same effect. The gelation time of the solution with a target density of 0.06 g/cm^3 at different NH_4OH concentrations measured at 25°C are shown in Table 3-6.

NH_4OH concentration (mol per mol TMOS)	0.01	0.05	0.1
Gelation time, hours (25°C)	78.33	2.5	0.55

Table 3-6 Dependence of the gelation time on the ammonia concentration at 25°C; target density 0.06 g/cm^3.

One may note that the higher the ammonium hydroxide concentration, the shorter is the gelation time. It is also known that a base catalyst accelerates the condensation more than the hydrolysis [Tillotson 1992]. The stronger dependence of $C_{CO_2}^{opt.}$ on the NH_4OH concentration, compared to the HCl concentration, might mean that CO_2 has a stronger influence on the condensation, than on the hydrolysis. Assuming that both ammonium hydroxide and CO_2 enhance the condensation, it may be concluded that the reason for the decrease in gelation time with increasing $_{NH4OH}$ concentration is a superposition of both effects.

Nevertheless, it should be noted, that the concentration of the base catalyst can be increased only up to the certain value. If the concentration is too high, the precipitation of colloidal particles can take place.

The effect of the substitution of the ammonium hydroxide for potassium hydroxide (KOH) and sodium hydroxide (NaOH) in the second step was analyzed. The purpose of these experiments was to prove whether the gelation enhancement by CO_2 is influenced by the nature of the base catalyst.

The starting solution was prepared in the same way, as described above. Acetonitrile was used as the solvent to reach a target density of 0.03 g/cm^3. Both NaOH and KOH were used instead of ammonium hydroxide in the second step. The component ratio was as follows: 1 mol TMOS : 2.4 mol MeOH : 4 mol H_2O : 10^{-5} mol HCl: $2 \bullet 10^{-3}$ mol NaOH (or KOH). CO_2 was

added to the solution in small portions at 40°C. The same effect, namely a fast gelation was observed, as in the case of ammonium hydroxide. The solutions formed gels within 20 minutes, whereas the gelation time of the corresponding control samples was much longer. The results are illustrated in the Table 3-7.

| Base catalyst concentration	CO_2 concentration	$t_{gel}^{CO_2}$	t_{gel} (control sample)
1 mol TMOS: 0.002 mol NaOH	33,8 wt%	20 min	20 hours

Table 3-7 Effect of CO_2 addition in the system with NaOH at 40°C.

It may therefore be concluded, that the gelation enhancement by CO_2 does not depend on the nature of the catalyst.

3.2.1.5   Influence of the hydrolysis time

As discussed in section 2.1.3, the gelation time is a function of hydrolysis time [Boonstra 1989]. The concentration of silanols, which can afterwards participate in the condensation reaction, increases with the hydrolysis time and, as a consequence, the gelation time in the basic step decreases. If CO_2 acts as a catalyst for the condensation, its amount should also decrease with increasing hydrolysis time.

The dependence of $C_{CO_2}^{opt.}$ on the hydrolysis time was studied keeping all other parameters fixed. The same initial solution as in previous experiments was used. Acetonitrile was used as a solvent in order to reach a target density equal to 0.03 g/cm^3. In the first step, TMOS was mixed with methanol, water and HCl in the following ratio:

1 mol TMOS : 2.4 mol MeOH : 1.3 mol H_2O : 10^{-5} mol HCl
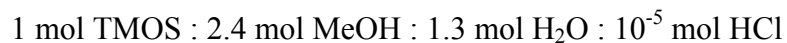
The mixture was stirred for 1 hour and in the second step water, acetonitrile and ammonia were added in order to obtain the following final ratios:

1 mol TMOS : 2.4 mol MeOH : 4 mol H_2O : 10^{-5} mol HCl : $2 \bullet 10^{-3}$ mol NH_4OH.
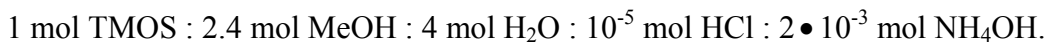
Then CO_2 was added at 40°C in small portions until gelation occurred. The dependence of the CO_2 concentration reached in the system up to this point ($C_{CO_2}^{opt.}$) is represented in Figure 3-21 as a function of the duration of the first step (i.e. as a function of the hydrolysis time). It can be seen that the amount of CO_2 needed for gelation decreases with an increasing hydrolysis time. During the long hydrolysis time some of the hydrolyzed silanols are partly condensed and so the condensation is "well prepared". Typically, a hydrolysis time of 30 minutes was

used for the experiments. Boonstra et al [Boonstra 1988] have shown that this hydrolysis time is optimal for the gel preparation.
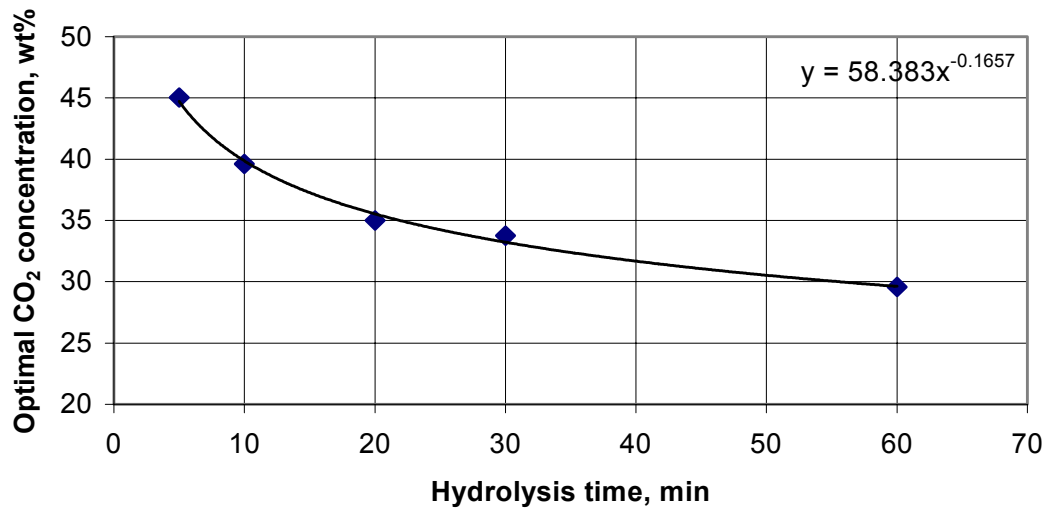
Figure 3-21 Dependence of the CO_2 concentration needed for the gelation from the hydrolysis time at 40°C.

3.2.1.6   Influence of the solvent

As discussed in section 2.3.1, solvents play an important role in hydrolysis and condensation processes. Interactions between the solvent and reaction products (dimers, oligomers etc.) presented in the solution have a strong influence on the process itself and, in particular, on the gelation time. It is supposed that the effect of the gelation acceleration by CO_2 depends on the solvent used for the reaction. It was, therefore, essential to study this effect in different solvents. Seven solvents were selected for this experiment: methanol (MeOH), ethanol (EtOH), acetone, acetonitrile, formamide, dimethylformamide (DMF) and dimethylsulfoxide (DMSO). These solvents belong to two different solvent types: protic polar solvents and aprotic polar solvents as denoted in the following table.

Protic polar solvent		Aprotic polar solvent	
CH_3OH	Methanol	C_2H_6OS	Dimethylsulfoxide
C_2H_5OH	Ethanol	C_3H_7NO	Dimethylformamide
CH_3NO	Formamide	CH_3CN	Acetonitrile
		C_3H_6O	Acetone

Table 3-8 Classification of the solvents used for the synthesis.

Characteristic properties of both solvent types have already been discussed in section 2.3.1. The solubility of CO_2 in these solvents must be taken into account. Consequently the vapour-liquid equilibrium data for each solvent-CO_2 system were collected. These are presented in Figure 3-22 and Figure 3-23.
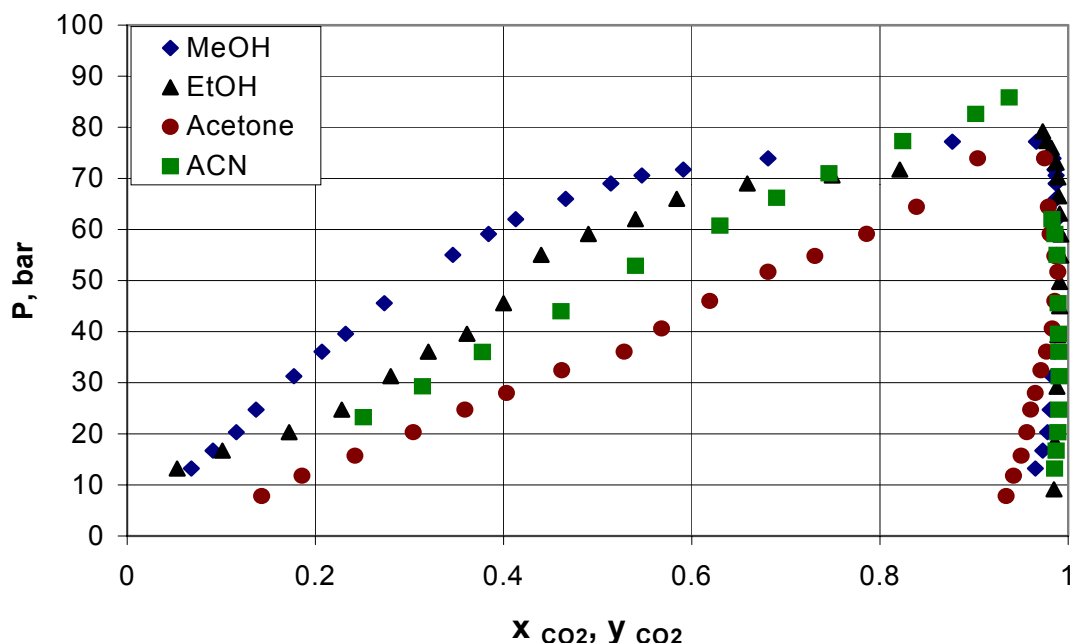

Figure 3-22 P-x-y diagram for the binary systems CO_2 – solvent at 40°C [Chiehming 1998]

In the case of DMF and DMSO, no experimental data regarding the solvent concentration in the vapour phase could be found, but the concentration in the liquid phase is available. The data were fitted with the Peng-Robinson Equation of State and the parameters obtained were used to predict the corresponding concentrations in the vapour phase (Figure 3-23).

It may be seen (Figure 3-22 and Figure 3-23) that for all systems, the concentration of CO_2 in the vapour phase is close to 100 wt%, as already mentioned for the CO_2-acetonitrile system. This fact is important because in the following experiments, as in the case with acetonitrile, it was very difficult to determine the concentration of CO_2 in the liquid phase by direct measurements. This value was estimated using the iteration procedure described in section 3.2. The densities of the solutions, which are necessary for the calculation, were measured at 40°C, using a pycnometer. For each solvent, the values are presented in the Table 3-9. It can be seen, that the densities of the sol solutions are similar to that of the corresponding solvents.

The experiments were carried out at 40°C following the procedure described in section 5.3. Solvents described above were used in order to obtain a target density of 0.03 g/cm^3. In both the first and second step, the same solvent was used. Control samples were stored for gelation

at the same temperature. All experiments were repeated at least twice. The results are summarized in Table 3-10.
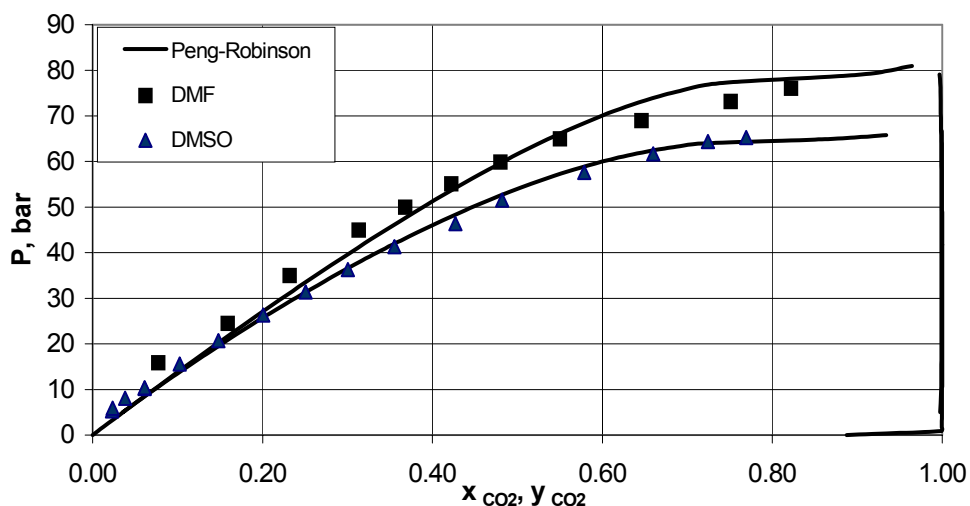
Figure 3-23 P-x-y diagram for the binary systems CO_2 – solvent at 40°C . Experimental data from [Kordikowski 1995]; fitting - Peng-Robinson EOS.

Solvent used for the reaction	Density of the pure solvent, 20°C	Density of the solution just after the second step, 40°C
Methanol	0.791	0.801
Ethanol	0.789	0.789
DMF	0.949	0.939
Acetone	0.790	0.810
Acetonitrile	0.782	0.789
DMSO	1.101	1.06

Table 3-9 Densities of the reacting mixtures at 40°C

It was observed that CO_2 addition to the solution, made with DMF, acetonitrile or acetone as the solvent led to a gel formation. It should be noted that the gelation in acetone and DMF solutions was not as complete as in the case of acetonitrile. Gels obtained in these systems were not as uniform and were more opaque than in the case of acetonitrile. It is suggested that the quality of such gels may be improved by optimization of the reaction conditions, such as catalyst concentration and temperature.

In the case of methanol and ethanol, no gelation was achieved. After a certain concentration of CO_2 was reached in the solution, precipitation of colloidal particles was observed. This effect was similar to the gelation process involving CO_2 but in the absence of other catalysts (section 3.2.1.3).

Solvent	P, bar	Total CO_2 concentration, wt%	C_{co_2} in the liquid phase, wt%	Appearance of the solution after CO_2 addition
Methanol	73.6	64.9	36.09	Precipitation of colloid particles
Ethanol	75.5	46.8		Precipitation of colloid particles
DMF	57.4	47.8	31.54	Gelation
Acetone	57.9	49.7	36.42	Gelation
Acetonitrile	32.1	37.2	28.08	Gelation
DMSO	65.2	38.9	21.82	LLE

Table 3-10 Effect of the CO_2 addition on the gelation process with different solvents

In order to prove the chemical nature of these particles, the precipitate was collected, dried at 60°C and analyzed by IR spectroscopy. The corresponding spectra are presented in Figure 3-24.
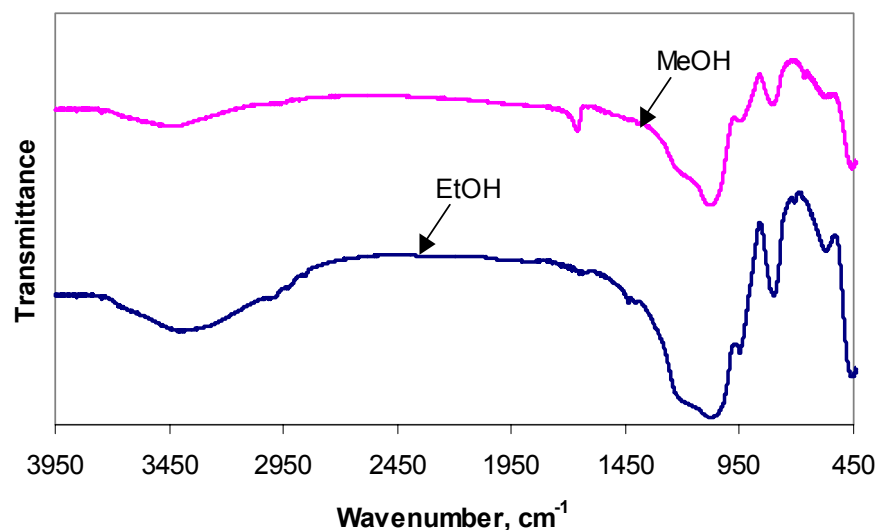
Figure 3-24 IR Spectra of the colloidal particles obtained from EtOH and MeOH solutions after CO₂ addition.

It can be seen that the spectra of the colloidal particles obtained in these experiments are similar to those of silica aerogel, presented in **Figure 3-18**. It may be concluded that in the case of ethanol and methanol as solvent, reaction enhancement also takes place, but leads to the precipitation of the colloidal particles and not to gel formation.

From these results it is clear that gelation enhancement by CO_2 addition takes place preferably in polar aprotic solvents (DMF, acetone, acetonitrile). As discussed in chapter 2, polar aprotic solvents dissolve both organic and inorganic reactants, but are not able to hydrogen bond with them - they are more inert, than the protic solvents.

As discussed in section 2.1.3.1 the gelation time in aprotic solvents is longer than in polar protic solvents. In polar aprotic solvents the condensation rate is higher resulting in highly condensed particles [Artaki1986]. It was of interest to see whether the gelation times for the two-step process used in the present work show the same tendency as reported by [Artaki1986]. Gelation times without CO_2 addition were studied for all solvents used in the experiments with CO_2 enhanced gelation. The results are presented in Table 3-11.

One may note that the gelation time in the case of polar aprotic solvents (acetonitrile, acetone, DMF, DMSO) is considerably longer than that in polar protic solvents (methanol, ethanol). This agrees with the results obtained for the one-step reaction [Artaki 1986].

Solvent	Gelation time, hours
Methanol	1.7
Ethanol	1.8
Formamide	0.3
DMF	24.7
Acetone	54
Acetonitrile	40
DMSO	37

Table 3-11 Gelation times in the systems with different solvents. Component ratio in the sol solution: 1 mol TMOS : 2.4 mol MeOH : 4 mol H_2O : $2X10^{-3}$ mol NH_4OH. Target density = 0.03 g/cm^3.

The gelation time in the case of protic solvents is very short and the additional enhancement of the reaction by CO_2 might make the reaction so fast, that colloidal particles are formed. In the case of aprotic polar solvent, the gelation time without CO_2 addition is longer. CO_2 enhances the reaction also in this case, but the reaction is still slow enough to allow the formation of a uniform cluster (a gel). This suggestion would explain the results presented in Table 3-10, showing that the gelation takes place preferably in the polar aprotic solvents.

3.2.2   Further experiments for the clarification of the gelation enhancement by CO_2.

Although the effect of the gelation enhancement by CO_2 addition was studied under a multitude of experimental conditions, its nature could not be fully understood from these studies. As a result, further experiments were conducted so as to clarify the nature of the discovered effect.

It is known that the addition of strong acids during the second step can decrease the gelation time. This effect is based on the variation of the pH value and the shiftof the isoelectric point of the solution [Huang 1999]. In our case, CO_2 dissolves in the sol solution and reacts partially with water, present in the system, giving rise to carbonic acid. Nevertheless, H_2CO_3 is a weak acid and, in our case, the pH of the solution changes only slightly with CO_2 addition (pH=8 before CO_2 addition, pH=7.5 after CO_2 addition). The pH values were measured in the autoclave directly by means of pH paper. On account of the possibilty that gelation enhancement is caused by carbonic acid, replacement of CO_2 by other acids was performed. In the case where this assumption is true, the addition of another weak acid (instead of CO_2) under the same conditions would also lead to an acceleration of the gelation process. Formic

acid was used as the substitute for CO_2. The starting sol solutions were prepared using the same method, as in the case of CO_2 addition.

Formic acid solutions having different concentrations (0.01 %, 0.1 %, 1 %, 10 %) were added to 80 ml of sol solution in 1 ml portions. After the addition of every portion of the formic acid, the system was stirred vigorously for 4-5 minutes and pH value was monitored. Formic acid was added until a pH value of 3 was reached. No gelation enhancement was observed during this experiments. The final solutions were left to stand and gels formed after a period of 2-3 days. So it was proved that the gelation enhancement can not be due to the simple changing of the pH value because of carbonic acid formation.

It is supposed that the carbonic acid resulting from the CO_2 addition might react with other components, presented in the solution.

One possibility may be that H_2CO_3 reacts with NH_4OH, as depicted in eq. (27).

$$CO_2 + H_2O \leftrightarrow H_2CO_3$$

$$2\ NH_4OH + H_2CO_3 \leftrightarrow (NH_4)HCO_3 + 2H_2O$$

(27)
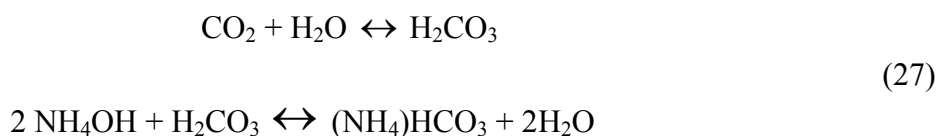
This system is known to be a buffer solution, which can provide a favourable setting for the condensation reaction. In order to model this effect and prove the suggestions, the influence of carbonate buffer solution ($Na_2CO_3 + NaHCO_3$) was studied.

Similar experiments as in the case with formic acid were carried out with the carbonate buffer. Carbonate buffer having the pH value 10.1 was added to the 80 ml of sol solution in 1 ml portions under constant stirring until a pH of 9 was reached. No gelation enhancement was observed as in the case of formic acid. Control samples formed a gel after a time period of 3 days.

The effect of ammonia hydrocarbonate ($NH_4 HCO_3$) itself was also studied. The experiments were carried out similar to the case of formic acid. Aqueous ammonium hydrogencarbonate solutions having different concentrations (0.5 %, 2.5 %, 5%) were added to 20 ml of sol solution in 1ml portions at 20 °C. After the addition of every portion of ammonium hydrogencarbonate, the system was stirred vigorously for 4-5 minutes. No gelation was observed during the experiments. The final solutions were left to stand and gelation occurred after 2-3 days. The results of this experiment are summarized in Table 3-12.

Sample number	NH$_4$HCO$_3$ concentration of the initial solution, wt%	Final NH$_4$HCO$_3$ concentration in sol, wt%	t$_{gel}$	Appearance of the final solution
B1	5	0.43	-	Precipitation of colloid particles
B2	2.5	0.123	-	Precipitation of colloid particles
B3	0.5	0.0043	4 days	"Slow" gelation resulted in a transparent gel

Table 3-12 Influence of ammonium hydrogencarbonate on the gelation

When a relatively large concentration of ammonium hydrogencarbonate was used (B1, B2), precipitation of colloidal particles took place. This effect was also observed with other base catalysts (section 3.2.1.4). When certain catalyst concentration is exceeded, such a precipitation takes place. This is why it is impossible to increase the catalyst concentration more than up to a certain level, if a gel formation is required. In the case of a lower ammonium hydrogencarbonate concentration (B3), a normal slow gelation took place, as in the case of a common two-step procedure. No gelation enhancement was observed.

Based on these experiments, one may conclude that the enhancement of the reaction by CO_2 is not a simple effect of the change of pH or of the nature of the carbonate. Both carbonate buffer and ammonium hydrogencarbonate solution are unable to act as substitutes of CO_2 with the same effect of the gelation enhancement.

The possibility that the pressure increase resulting from CO_2 addition may also influence the reaction and lead to faster gelation, was also considered. It is known that reactions in the liquid phase are not much influenced by the pressure; yet, the addition of other gases (nitrogen and trifluoromethane) instead of CO_2 was studied under at the same conditions. Both nitrogen and trifluoromethane are in the supercritical state under the conditions used. R23 was chosen because its critical data are close to those of CO_2.

Substance	T^{cr}, K	P^{cr}, bar
N$_2$	126	34
R 23 (CHF$_3$)	299	48
CO$_2$	304.2	73

Table 3-13 Critical properties of the substances used.

The gases were added to the sol solution in small portions at 40°C. In both cases the precipitation of colloid particles took place just after the first portions of gases were added. No enhancement of the gelation was detected. We can therefore exclude the possibility of the pressure as the factor that leads to an acceleration of the gelation process

3.2.3   Gelation enhancement by CO_2 : suggestion for the nature of the process

The nature of the gelation enhancement by CO_2 has not been fully resolved by the conducted work. Further investigation is needed for the understanding of this effect. However, a summary of the results obtained is presented together with a few suggestions for the nature of this process.

It has been found that the addition of supercritical CO_2 to a sol solution after the second step enhances the gel formation. The enhancement of the reaction, determined as the ratio of the gelation times ($t_{gel} / t_{gel}^{CO_2}$) depends on the target density of the solution and varies between 5 and 100. The CO_2 concentration usually reached in the liquid phase at the gel point is around 30 wt%. It was demonstrated that an increase in the temperature, concentration of acid or base catalyst and hydrolysis time leads to the decrease of the optimal CO_2 concentration needed for the gelation. It was also shown that the reaction enhancement by CO_2 takes place only if CO_2 is combined with both catalysts used in the common two-step process. If one or both catalysts are not used, CO_2 addition leads to the rapid precipitation of colloidal particles.

This concluded that the reaction enhancement by CO_2 addition always takes place, but in some cases it results not in gelation, but in particle formation.

The same effect was observed when other solvents such as acetonitrile were used for the reaction. It was found, that the fast gel formation enhanced by CO_2 preferably takes place in polar aprotic solvents (acetonitrile, dimethylformamide), whereas polar protic solvents (methanol, ethanol) promote particle formation. At the same time, this effect is not sensitive to the nature of catalyst. The reaction enhancement was also observed in cases where other catalysts instead of hydrochloric acid and ammonium hydroxide were used for the process.

The replacement of CO_2 with other substances, which could appear in the mixture due to the chemical reactions (NH_4CO_3) did not result in the reaction enhancement. The addition of other gases, namely nitrogen and trifluoromethane does not lead to the gelation, but to the precipitation of SiO_2 particles. This indicates that the nature of CO_2 plays an important role in the gelation process.

Since CO_2 acts successfully only in combination with the acid and base catalysts, we can conclude that CO_2 acts not (or not only) as a catalyst itself, but provides some optimal conditions for the condensation reaction, being accelerated by normal base catalysts (NH_4OH or $NaOH$). Also the strong dependence of this effect on the solvent nature allows one to conclude that some interaction between CO_2 and the solvent might be taking place.

CO_2 may also take part in the solvation process. At the beginning of the reaction, acetonitrile solvates the partly hydrolyzed TMOS and thus inhibits the condensation to some extent. CO_2 may build an ionic complex with acetonitrile and so compensate the solvation effect. Although this suggestion could not be proved directly, it is indirectly supported by some other measurements. Ferrieri et al [Ferrieri 1999] studied several reactions in supercritical CO_2 using acetonitrile as a co-solvent. They have shown that acetonitrile forms clusters around the dilute solutes, so that their local concentration increases leading to a faster reaction.

This suggestion might be proved by the spectroscopic measurements.

3.3. Aerogels produced by the two-step method modified by CO_2 addition

3.3.1   Optimization of the process parameters

A number of silica aerogels were produced by the two-step method modified by CO_2 addition. The drying procedure has already been described in chapter 2. The process parameters were varied in order to determine their optimal values, to allow for the production of transparent monolithic aerogels.

- The aging time was varied between 0 and 72 hours. It was observed, that a relatively short aging period (0-5 hours) results in weak aerogels, exhibiting fractures within the whole volume. It is well known that a certain aging period is required for the stabilization and strengthening of the gel structure. Of importance to note, however, is that an extended aging process beyond that of 48 hours does not further improve the quality of the final product. The aging time also greatly influenced the optical properties of the aerogels - opaque, white aerogels were obtained after a short aging period. These results are in good agreement with those discussed in section 2.7. The optimal aging time was found to be 15 hours.

- The extraction temperature was varied from 4°C to 70 °C. it was found that low extraction temperatures (4-25°C) result in opaque aerogels and even lead to particle formation within the gel body. The extraction temperatures > 35°C lead to transparent aerogels. Because

CO_2 becomes a supercritical fluid at 31°C, it follows that supercritical CO_2 is a better extraction medium for this process than liquid CO_2. Further increase of the extraction temperature (up to 70°C) did not further influence the properties of the aerogels. The most practical approach is to run the extraction at the same temperature as the gelation and aging processes. This is because a temperature change may result in the appearance of small cracks within the gel body, which lead to shrinkage during the extraction process. It has been found that 40°C is the optimal temperture for the gelation, aging and extraction procedures.

- The extraction time depends strongly on the size of the gel, being controlled by the diffusion of the CO_2 through the pores of the aerogel. The binary diffusion coefficients have been measured for several CO_2-organic solvent mixtures [Novak 1997] and can be used for the modeling of the drying procedure. Several models have been applied to this purpose [Orlovic 2001]. It was shown that the extraction time needed to complete the solvent exchange depends mostly on the thickness of the gel sample. When the gelation is carried out directly in the autoclave, as was the case in the present work, the gel has the same form as the autoclave, making it difficult to vary the thickness of the gel. It was found that for samples having a volume of 50 cm^3, 3-4 hours extraction time is needed, whereas a 120 cm^3 sample requires at least 24 hours for complete solvent exchange. Thus, the size and shape of the apparatus should be optimized in order to allow for minimum extraction time.

- The flow rate during the extraction process also plays an important role in the drying procedure. Flow rates that are too high may lead to the non-homogeneity of the aerogel. Slow flow rates, however, lead to long extraction times. It has been found that a flow rate of 100 NL/h is optimum for the extraction process.

3.3.2   Physical properties of the aerogels obtained by CO_2 addition

Using the parameter set described above, a number of gels obtained by CO_2 addition were dried to obtain the corresponding aerogels. In each case, the control sample formed a gel without CO_2 addition. This was also dried and its properties were compared to the corresponding sample. It was found that the CO_2 amount used for the gelation process ($C_{CO_2}^{opt.}$) is very important. This amount should be determined experimentally for every specific solution, as expressed in section 3.2.1. As previously mentioned, if this amount is exceeded, the transparency of the final aerogel is very low. Such a sample is shown below. One can see that the aerogel produced in the presence of excess amounts of CO_2 (Figure 3-25) is white and

not transparent. On the contrary the sample produced in the presence of an optimal CO_2 concentration is completely transparent. This confirms that the $C_{CO_2}^{opt.}$ should not be exceeded during CO_2 addition. If $C_{CO_2}^{opt.}$ is unknown for the conditions used, CO_2 should be added in small portions until gelation takes place.

Figure 3-25 Aerogel sample: CO₂ concentration exceeds $C_{CO_2}^{opt.}$ by 50%

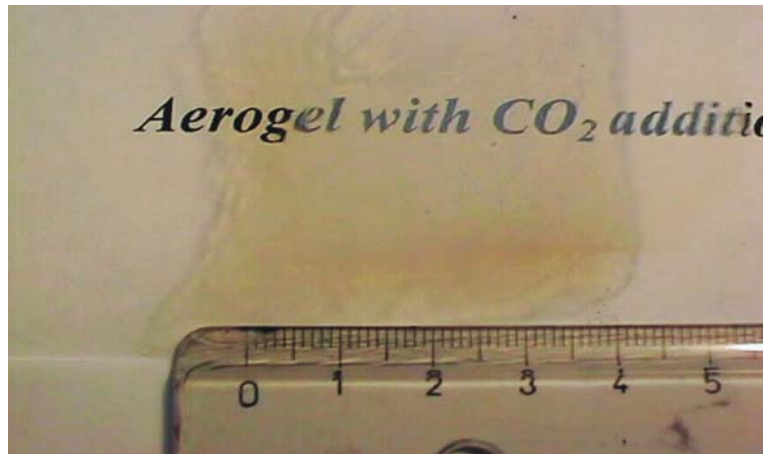**Figure 3-26 Aerogel sample: CO₂ concentration used is equal to $C_{CO_2}^{opt.}$**

For all aerogels subsequently discussed, the CO_2 amounts used for gelation were equal to the $C_{CO_2}^{opt.}$ values determined experimentally. The corresponding values have been presented in sections 3.2.1.1 - 3.2.1.5.

The physical properties of the aerogels obtained by the method proposed in this work are summarized in Table 3-14 where they are also compared to those of the aerogels obtained by the common one- and two-step procedure.

Synthesis method	Bulk density, g/cm^3	Average pore diameter, nm	BET surface area, m^2/g	Transparency
Common one – or two step	$0.003 < \rho < 0.35$	10 - 20	600-1000	Transparent
CO$_2$ enhanced gelation	$0.02 < \rho < 0.1$	8 - 25	500-700	Transparent to slightly opaque

Table 3-14 Properties of silica aerogels produced by CO$_2$ addition and by common one- or two-step methods.

It is clear that the properties of the aerogels obtained in this work are comparable with those aerogels obtained by the common one-step or two-step methods. Through the CO$_2$ addition method, the resulting aerogels have a density of 0.02-0.1 g/cm^3 and a BET surface area of 500-700 m^2/g. Aerogels having lower densities can be also synthesized by the method with CO$_2$ addition, but such samples are very unstable, so a longer aging time is required. It was not the purpose of this work to synthesize aerogels with ultra-low densities, so the optimal parameters for such samples were not investigated.

All aerogels produced by the CO$_2$ method exhibited a high degree of transparency and a pore diameter of 8-25 nm, which is close to that of the aerogels produced by the common methods without CO$_2$ addition. In order to compare both methods, the properties of two aerogel samples having the target density of 0.03 g/cm^3 obtained from the same start solution are compared. Sample C1 was obtained from the gel, synthesized with CO$_2$ addition while sample C2 was prepared without CO$_2$ addition. Their physical properties are compared in Table 3-15. One can see that the properties of both samples are somewhat similar. The aerogel obtained using the CO$_2$ addition has a smaller pore diameter and slightly lower surface area than the sample prepared by the conventional method. The difference is very small, so it may also be attributed to experimental uncertainty.

Sample number	Density, g/cm^3	Average pore diameter, nm	BET surface area
C1	0.0306	18.6	687 m^2/g
C2	0.031	21.2	700 m^2/g

Table 3-15 Comparison of the physical properties of aerogels obtained by different methods

The nitrogen adsorption-desorption isotherm for sample C1 is shown in Figure 3-27. The isotherm shows a hysteresis, typical for mesoporous substances. This shape of the isotherm was typical for all samples studied.
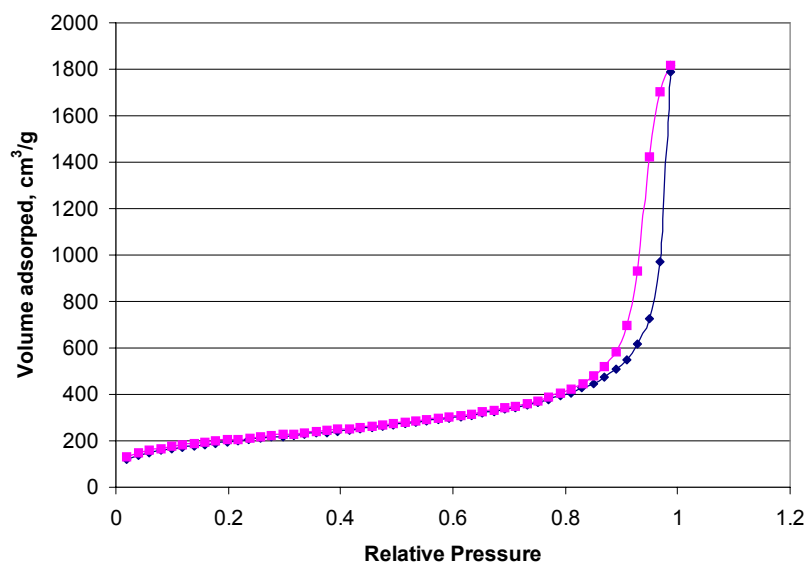

Figure 3-27 Nitrogen adsorption - desorption isotherm for silica aerogel.

Transmission and scanning electron microscopy were used in order to obtain information about the aerogel microstructure. A SEM image of the sample obtained with CO_2 addition is shown in Figure 3-28 (courtesy of the Zentrale Einrichtung für Elektronische Mikroskopie, TU Berlin).

It is evident that the aerogel has a considerably fine morphology. An average pore diameter could be also estimated from the SEM pictures and was in good agreement with that obtained by BET measurements.

Both aerogel samples C1 and C2 were also analyzed by IR spectroscopy. The corresponding spectra are shown in Figure 3-29.
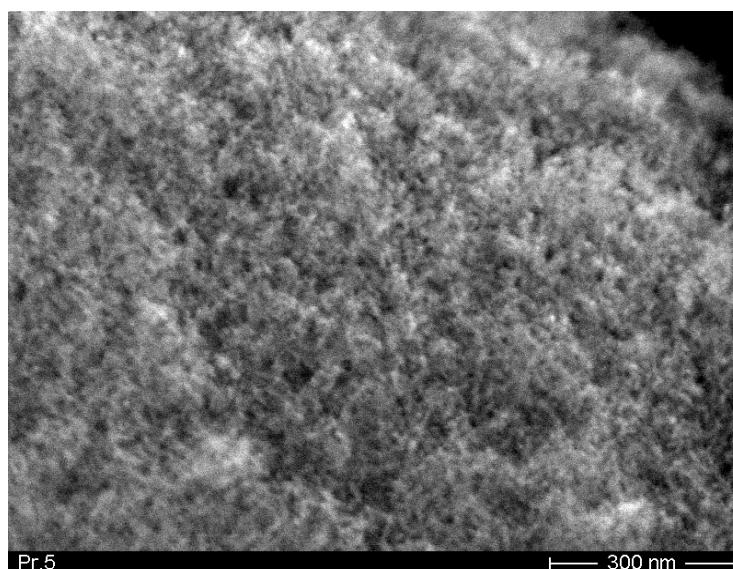
Figure 3-28 SEM picture of silica aerogel sample (ρ = 0.03 g/cm^3)
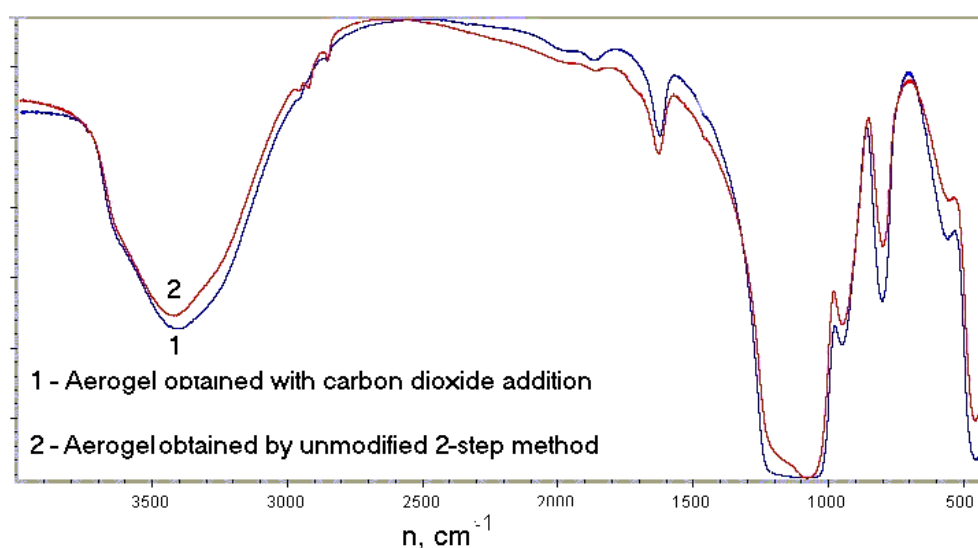
Figure 3-29 IR spectra of two different aerogel samples

The IR spectra of the two samples are very similar. The specific peaks have already been presented in Table 3-5. Both aerogels contain a certain amount of molecular water. Also the surface contains unreacted OH groups. In general, aerogels obtained by low temperature supercritical drying are hydrophillic (section 3.4.2). If such aerogels come into contact with liquid water, they become fully wetted and, as a result, their structure is immediately destroyed.

3.3.2.1 Storage behaviour of the aerogels

Although the hydrophilic nature of such aerogels cannot be influenced by the temperature, the amount of the adsorbed water and OH groups on its surface can be reduced by thermal treatment. Themal treatment does not change the hydrophilic nature of the aerogel, but makes it less sensible to atmospheric moisture. This is especially important, if aerogels need to be stored for later application. Because the aerogels synthesized in this work were to be later applied as drug carriers, it was important to investigate their storage behaviour.

The water adsorption during storage of the silica aerogels prepared by the CO_2 method and the influence of temperature treatment was studied. Different experimental conditions were used. One part of the aerogel was stored at normal atmospheric conditions in a vessel open to atmosphere. The second part was stored in a tightly closed vessel. A little amount of water was poured onto the bottom of the vessel to allow for a high humidity, yet the aerogel was not allowed to come into contact with the liquid water. Both samples were regularly weighed and the weight increment was monitored. The results of both experiments are presented in Figure 3-30.
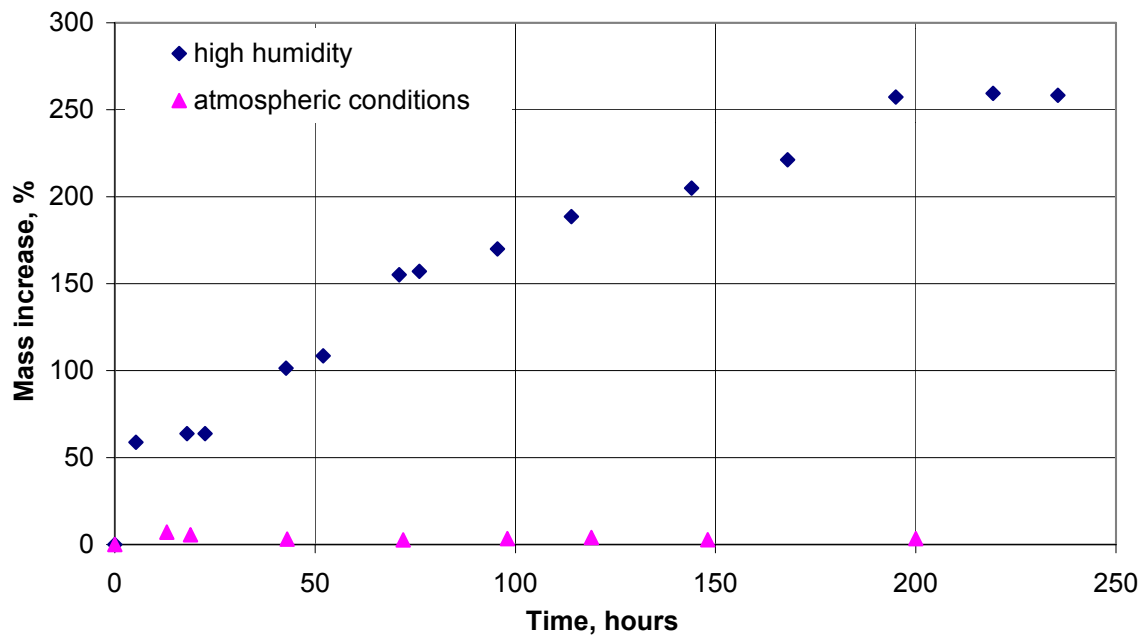
Figure 3-30 Water adsorption by silica aerogel at 20°C.

Figure 3-30 shows that the aerogel under normal atmospheric conditions does not adsorb much water - the weight increase does not exceed 5 %. When stored in a very humid atmosphere, however, the aerogel adsorb a considerable amount of water (up to 250 % of its initial weight). Also, under very humid atmospheric conditions, the appearance of the aerogel greatly alters. The volume of the sample decreases, because of shrinkage due to water

condensation in the pores. The transparency of the aerogel is also influenced by water adsorption – transparency decreases gradually with increasing water content. Figure 3-31 shows how the aerogel's absorbance in UV-VIS region changes when stored in a humid atmosphere for a period of 5 days. Both spectra exhibit the typical spectrum of a silica aerogel as shown in section 2.2.3. At every wavelength, however, the transmitance of the aerogel sample containing adsorbed water is much lower than that of a pure silica aerogel.
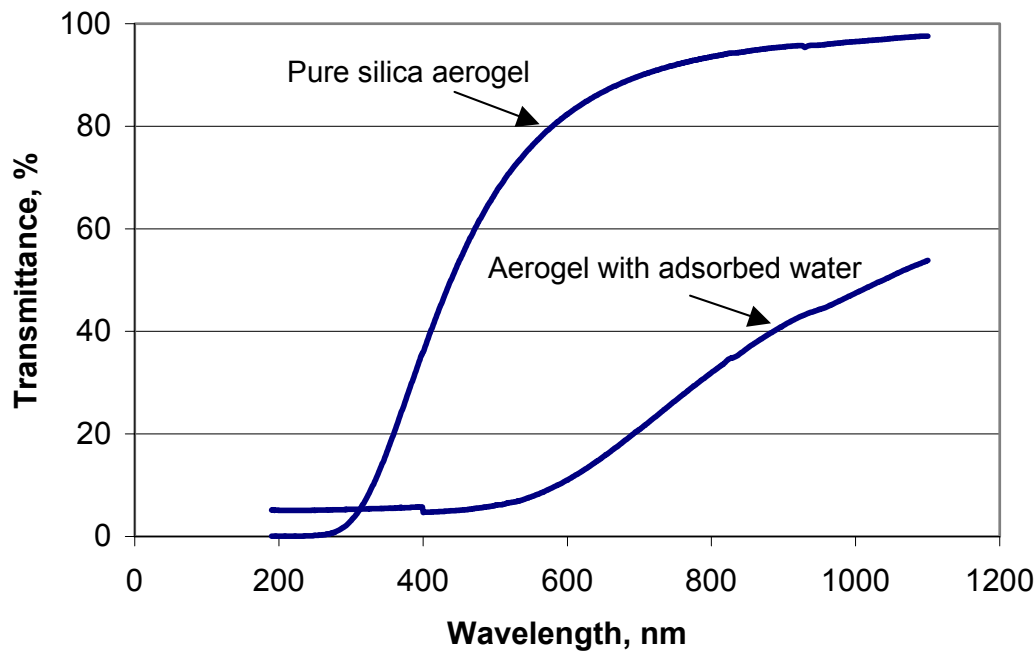

Figure 3-31 UV-VIS spectra of 2 aerogel samples : influence of the adsorbed water

Photographs of both samples are shown in Figure 3-32. One may note that note that the volume of the aerogel stored under humid conditions is decreased due to shrinkage. It is also clear that the sample stored in a humid atmosphere has a white color and is not transparent. Thus, if the corresponding application requires a high transparency in the visual region (e.g. window insulation) hydrophilic aerogels cannot be employed. For aerogels to be applied in a very humid atmosphere, they must be hydrophobic. Hydrophilic aerogels are transformed into hydrophobic ones by reaction with methanol at high temperature [Lee 1995]. Since in the conducted work the hydrophilic nature of the aerogel was desirable for the further application, no additional post-treatment was conducted.

The strong water adsorbtion of hydrophilic aerogels enables the use of this type of aerogel as a drying agent. This application has already been addressed in chapter 4.

Figure 3-32 Water adsorption in the aerogel. Initial aerogel (left) and the same sample after 5 days in a humid atmosphere (right).

3.4. Evaluation of the aerogel synthesis suggested in the present work

It has been demonstrated that the gelation enhancement by CO_2 addition results in a fast gelation, but does not greatly influence the aerogel properties. Both surface area and pore size exhibit similar values to the corresponding samples prepared without CO_2 addition.

The same is true for the transparency and hydrophilic nature of the aerogels. CO_2 can, therefore, be regarded as an alternative catalyst for the gelation process. The process suggested in the present work allows the synthesis of an aerogel of the same high quality, as produced by common methods.

The most important advantage of the method proposed in this work is a very short gelation time even for the samples with extremely low densities (Table 3-1). In the common processes the gelation time can be reduced by increasing the temperature or by using a higher concentration of the basic catalyst [Brinker 1992]. Both strategies have some disadvantages, however. An increase in the temperature is achieved through the use of additional energy and this leads to additional costs. Also, the gelation time can be only diminished up to the certain value, because a high temperature results in a significant solvent evaporation.

On the other hand, extremely high catalyst concentrations negatively influence the structure of the silica gel. Furthermore, a high catalyst concentration sometimes leads to precipitation of colloidal particles and therefore hinders the gelation process. Moreover, during

supercritical drying, catalysts should be extracted from the gel, so higher catalyst concentrations result in a longer extraction time.

The process suggested in this work allows a reduction in the gelation time at a moderate temperature (40°C) and without the use of the additional chemicals (CO_2 cannot be regarded as an additional chemical, because it is used anyway in the extraction process).

Further advantage of this method is that the gelation takes place directly in the autoclave. The final pressure (after aging) is around 30-40 bar, so no additional pre-pressurizing is required for the drying procedure. As a result, the additional stress parameter induced by the sudden pressure increase in the autoclave is eliminated.

The process proposed in the present work also allows for a lower extraction time than that in the conventional method, because the gel phase already contains around 30% CO_2 at the beginning of the extraction process.

In summary, one may conclude that the method proposed in the present work can be successfully applied for aerogel production, especially in the case of low density aerogels.

4. Silica aerogels as a drug release system: Experimental results

As discussed in section 2.2, the combination of the many unusual solid material properties of aerogels enables their application in various industrial fields. Silica aerogels also have the advantage of being environmentally friendly and non-toxic.

Since aerogels have an extremely large surface area, one may expect that its use as a carrier can improve the dissolution and adsorption of drugs (section 2.3.6).

Two different mechanisms of chemical release from aerogels are possible:

- Hydrophilic aerogels collapse in aqueous media and thus promote dissolution of the target compound in water. The pharmaceuticals are adsorbed on the aerogels surface (eventually as a monolayer) and thus fast release is expected.

- Hydrophobic aerogels are more stable and chemical release is controlled by the diffusion of the substance from the aerogel pores. In this case slow release is expected.

By selection of a suitable hydrophilic or hydrophobic aerogel, the pharmaceutical loaded onto the aerogel can be released in an accelerated or delayed form.

The type of loading also plays an important role. As discussed in section 2.2.4.2, liquids wet the hydrophilic aerogel structure and partly destroy it. If adsorption from the liquid solution (as suggested by Schwertfeger et al. [Schwertfeger 2001]) is to be used as the mechanism of loading, the drug which would then be released would, to some extent, have lost the characteristic properties of the aerogel. As a result, this loading mechanism does not seem to be optimal, especially in the case of hydrophilic silica aerogels.

During the present work, it was of interest to find a procedure that allowed for loading of active substances onto hydrophilic aerogels without changing the aerogel structure. It was also essential to investigate the release of the corresponding pharmaceuticals from the aerogels so as to prove whether the drug-aerogel formulation is suitable as a drug delivery system.

Special attention was paid to those substances, whose immediate release is desired. In this case, hydrophilic aerogels seemed to be well-suited as carriers, due to their immediate collapse in water.

As mentioned in section 2.3.5, there are two general processes to load aerogels with chemicals:

a)   Through the chemical reaction during the sol-gel process;

b)   By the post-treatment of dried aerogels.

In principle, both processes can be used for the loading of aerogel with an active substance.

If process (a) is used, an active substance should be added to the solution during sol-gel process. Thereafter the gel containing the active substance should be dried by HTSCD or LTSCD (section 2.1.5). In the case of HTSCD, the corresponding substance is exposed to high temperature and high pressure. This may cause undesirable chemical reactions, leading to changes in the chemical structure of the active agent.

In the case of LTSCD, the temperature is relatively low (30-40°C). However, many pharmaceuticals are, to some considerable extent, soluble in CO_2. In this case, it is highly possible that the active agent will be extracted from the gel by supercritical CO_2. This process can therefore, only be used in cases where the active substances have a considerably low solubility in CO_2 under the stated conditions.

Process (b) can be realized in a multitude of ways. Generally, an adsorption process (from either liquid and vapour phase) is used (section 2.3.5). Adsorption from the liquid phase is widely used in the pharmaceutical industry [Stricker 1998]. Some problems may however, arise from the use of organic solvents during this process. Residual traces of solvent may be present in the final product and these may influence the drug's therapeutic properties [Magnan 1996]. An attempt to eliminate the solvent by evaporation, however, may cause degradation of thermosensitive drugs. Additionally, contact with a liquid may destroy the structure of the hydrophilic aerogel to a considerable extent.

In the present work adsorption from the supercritical gas phase was proposed.

Two different processes of adsorption from thevapor phase exist:

- Exposure of an aerogel to the vapour of an active agent. In this case, the vapour pressure of this substance must be high enough to allow for a reasonable extent of loading.

- Dissolution of the active substance in the supercritical gas phase followed by adsorption of this compound onto the aerogel from the resulting solution. In this case the target compound should be soluble in the corresponding gas.

Supercritical CO_2 was selected as the solvent for this process. The target substance was dissolved in supercritical CO_2 and was left to come into contact with the aerogel for a period long enough to reach equilibrium. The open pore structure of the aerogel allowed diffusion of the chemicals through the aerogel body allowing them to become adsorbed on the aerogel surfaces. Supercritical CO_2 was chosen for this process for several reasons:

- CO_2 is non-toxic.

- Elimination of CO_2 from the medium can be easily achieved by lowering the pressure.

- Supercritical CO_2 is one of the most well studied media among the supercritical fluids. The solubilities of many organic substances including pharmaceuticals in this fluid have been reported [Bartle 1991], [Vetere 1998], [Vandana 1997].

- Supercritical CO_2 has already been used to load porous support materials, other than aerogels, with pharmaceuticals [Magnan 1996], [Domingo 2001].

- CO_2 is generally used for the production of silica aerogels as described in chapter 0.

4.1. Methods and apparatus

4.1.1   Loading of silica aerogels with chemicals

For the loading of silica aerogels with organic substances, the autoclave used in the aerogel production was employed. Aerogels having a density of 0.03 g/m^3 and a BET surface area of 450-500 m^2/g were used for these experiments, unless otherwise specified.

Firstly, the solubility of every substance in supercritical CO_2 was determined. To achieve this, a specific amount of the substance was filled into a metal cage, weighed and placed onto the bottom of the autoclave. The autoclave was closed and heated to a fixed temperature (20-70°C). Then CO_2 , preheated to the same temperature, was pumped into the autoclave until a target pressure (140-180 bar) was reached. The system was left to stir for 10 hours to 3 days. The temperature could be kept constant with an accuracy of ± 1K and the pressure varied within 5 bar. The optimal dissolution time was determined experimentally for every substance. After equilibrium was reached, CO_2 was vented out at a constant flow rate (~100 N l/h) and then the autoclave was cooled to room temperature. The metal cage and its contents was weighed again and the amount of the dissolved substance determined. The amount of CO_2 in the autoclave was calculated from the known volume and CO_2 density. The values of CO_2 density were taken from NIST data base [NIST]. The solubility of the target substance was calculated and compared with the data stated in literature (when possible).

Then the aerogel samples were loaded with the target substance. A weighed amount of a target compound and two aerogel samples were placed into the autoclave. Thin pieces of aerogels (0.05 – 0.1 g) were used. The aerogel samples were wrapped in filter paper in order to prevent direct contact of both substances in the solid state. The autoclave was heated to a fixed temperature (40-70°C), and CO_2 (preheated to the same temperature) was then added. After the target pressure (140 – 180 bar) was reached, the system was left under these conditions under continuous stirring for at least 10 hours. In some cases, the dissolution

process was very fast and could be visually observed. (For example naphthalene was totally solved in CO_2 after 30-40 minutes). Then CO_2 was vented out at a constant flow rate (~100 NL/h).

In the case of naphthalene, the bulk solution (CO_2 + target compound) was washed out with nitrogen under constant pressure (~140 bar) during 1 hour (flow rate ~ 100 Nl/h). This was necessary, because the direct venting of CO_2 resulted in the crystallization of naphthalene inside the aerogel sample. For the other investigated substances, this procedure was not necessary, because no crystallization took place.

After ambient pressure was reached, the aerogel samples were weighed. The weight increase of the aerogel samples indicated the adsorption of the target compound in the aerogel and its concentration could be roughly estimated.

To determine the concentration of the target compound in the aerogel, the loaded aerogel sample was ground into a powder and dispersed into a suitable solvent. Solvents which provided a good solubility of the target substance at room temperature were seected. The aerogel itself was wetted with the organic solvent and the target compound could dissolve completely. The solution was stirred for at least 30 min to ensure that dissolution was completed. The concentration of the target compound in this solution was determined using gas chromatography or UV spectrometry. In some cases, the concentration was too high for both analytical methods; therefore an additional dissolution step was perofrmed. Based on these measurements, the amount of the target compound in the loaded aerogel was calculated. The corresponding solvents and the method of analysis used for every target compound investigated are summarized in the Table 4-1.

Compound name	Solvent used	Analysis method used
Naphthalene	Toluene	GC
Ketoprofen	Acetonitrile	HPLC, UV–VIS Spectrometer
Griseofulvin	Acetonitrile	UV-VIS Spectrometer
Miconasol	Acetonitrile	UV-VIS Spectrometer

Table 4-1 Methods of the determination of the target compound concentration

4.1.2   Methods of analysis

4.1.2.1   GC analysis

Gas chromatography was used for the analysis of the naphthalene-toluene solution. The experimental parameters were as follows:

GC: HP 5890

Column: HP-5 (5% PH ME siloxane) 30 m × 0.25 mm × 0.25 μm

Injection parameter: 1.0 μl Hamilton 7001

Injector temperature: 100°C

FID Detector temperature   320°C

The calibration curves and the corresponding measurements are summarized in the Appendix.

4.1.2.2   HPLC analysis

Conditions used for the *ketoprofen*-acetonitrile system**:**

Column: Discovery RP-Amide C1615 cm × 4.6 mm, 5 μm particles

                              Mobile Phase: Acetonitrile: 25 mM KH_2PO_4, pH 3.0 (40:60)

Flow rate: 1ml/min

Column Temperature:40°C

Detector: UV, 270 nm

Injection parameter: 10 μl, 1 μg/ml.

4.1.2.3   UV spectroscopy

UV spectrometer (Specord 200 (2 beams), Analytic Jena) was used to determine the concentration of the pharmaceuticals for both the adsorption and drug release measurements. A quartz cuvette with a path length of 10 mm was used for the measurements. The beam was adjusted against an empty cuvette. The absorbance was measured at the maximum value for all substances. The corresponding wavelengths are listed in Table 4-2.

Substance	*Ketoprofen*	*Griseofulvin*	*Miconazol*
Wave length in 0.1 N HCL, nm	258	293	280
Wave length in acetonitril, nm	252	293	280

Table 4-2 Wavelength used for the UV measurements

4.1.3   Drug release measurements

A special apparatus was constructed for the drug release measurements. The schematic diagram of this apparatus is shown in Figure 4-1. A detailed drawing can be found in the Appendix.

The drug release measurements were carried out following the recommendations of the United States Pharmacopeia (USP XXI). Following these recommendations, the assembly consists of the following: a covered vessel made of glass; a motor; a metallic drive shaft and a stirrer. The vessel is partially immersed in a water bath. The water bath permits a constant temperature (37 ± 0.3°C) to be maintained inside the vessel during the experiment. The apparatus permits the observation of the specimen and the stirring element during the experiment. The vessel is cylindrical and has a hemispherical bottom. Its sides are flanged at the top and a fitted cover is used to retard evaporation. A shaft rotation speed is maintained at the specified rate.
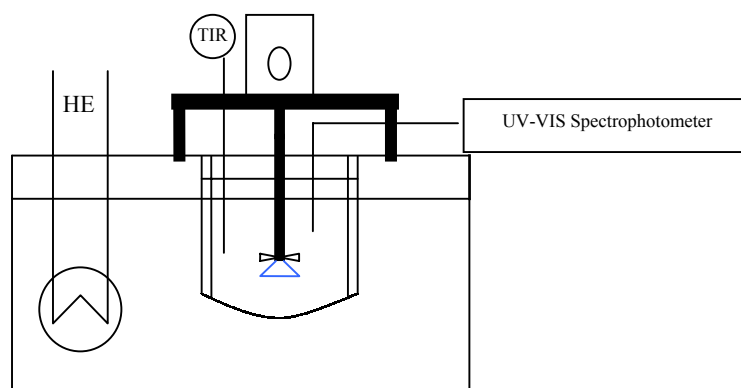

Figure 4-1 Scheme of the release apparatus constructed at TUB, HE is a heating element, TIR - PT 100 thermometer.

Indeed, the constructed apparatus exhibits a few differences to that recommended by the USP. The apparatus was designed to allow for ideal mixing in the vessel. Because of the low viscosity of the medium used (aqueous solutions), a pitched blade turbine with 6 blades, which provides maximal mixing in the axial direction was selected. Also, 4 baffles were inserted. The stirrer rotated at a speed of 1440 min^{-1}. The flow profiles provided by this type of stirring system are shown in the Figure 4-2.

These flow profiles were measured using coloured ink. It was clear that the stirring profiles changes with rotation number. This fact was taken into account during the release experiments.
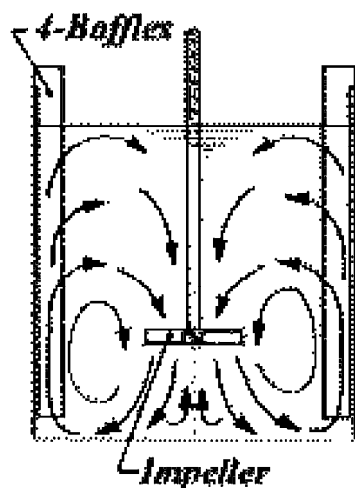
Figure 4-2 Flow profile in the drug release apparatus.

The release of all drugs was studied under 2 different rotation number conditions: 1438 min^{-1} and 100 min^{-1}, the latter corresponding to the recommendation of USP. All measurements were carried out at 37°C in 0.1 N HCl. At the start of the experiment the substance (monolithic aerogel loaded with the corresponding compound or aerogel powder) was introduced into the vessel, the vessel was filled with 900 ml 0.1 N HCl and the motor was switched on. The time was measured form this point on. The amount of the target substance was calculated in order to obtain 10% of its saturation concentration (sink conditions).

A 2 ml sample of the resulting solution was taken every 2-5 minutes. Every sample was filtered using a nylon filter with a pore diameter of 0.45 μm in order to ensure that no aerogel particles remained in the sample vessel. The samples were stored in a water bath at 37 °C and after the release was completed, the concentration of the target compound in every sample was estimated by means of UV absorption. Due to the low concentration of the solution, the absorption did not exceed the maximum value (3 absorption units) and so, no additional dissolution was required. The concentration in the vessel at that time when the sample was taken, was calculated using the corresponding calibration curves. It was taken into account, that the total volume of the solution decreased continuously due to the repetitive removal of sample volumes. The release curves were presented as the relation between time and the concentration of the target compound in the vessel.

4.2. Manufacture of aerogel - drug formulations

4.2.1 Experiments with a test substance

Loading of silica aerogels with chemicals by the adsorption from supercritical CO_2 solution was first conducted using a test substance in order to optimize the process parameters.

The experimental procedure is described in detailed in section 4.1.1. Naphthalene was chosen as the test substance because its solubility in CO_2 has been well studied and is found to be rather high [Bartle 1991], [McHugh 1980]. Adsorption isotherms were measured at 40°C and 70°C. The theoretical maximal naphthalene concentration which can be used for the loading is limited by the solubility of naphthalene in CO_2. The solubility data [McHugh 1980] is given in Table 4-3.

P, bar	100	120	153	200
$X_{naphthalene}$	0.0069	0.01438	0.01969	0.02438
$C_{naphthalene}$, wt%	0.23795	0.4983	0.6848	0.8506

Table 4-3 Solubility of naphthalene in CO_2 at 40 °C

Although in all experiments the concentration of naphthalene was below the saturation point, it was difficult to handle solutions having a naphthalene concentration, $C_{naphthalene} > 0.5$ wt%. This was because, in these cases, crystallization of naphthalene in the autoclave took place during the pressure release. Cystallization of naphthalene inside the aerogel was also observed A photograph taken against a black background to allow for recognition of the naphthalene crystals in the transparent aerogel sample is shown in Figure 4-3.

Although this phenomenon is disadvantageous for the adsorption measurements, it represents an interesting possibility to carry out the crystallization of chemicals inside an aerogel. If the crystallization takes place in the pores of the aerogel, nanocrystals may be obtained. By change of the process conditions (flow rate and pressure) different crystal shapes may result. Because this effect is undesirable for the adsorption measurement, the experiments were carried out only for those concentrations, where crystallization did not occur i.e. $C_{naphthalene}$ was not allowed to exceed 0.5 wt%. In these cases the aerogel samples remained transparent after loading. No naphthalene crystals could be detected by visual inspection, optical means or electron microscopy.
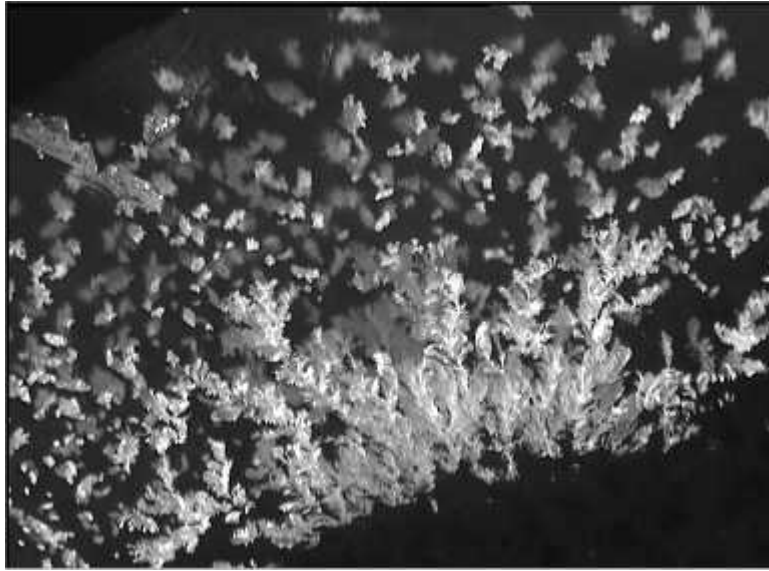
Figure 4-3 Picture of the aerogel sample having naphthalene crystals inside.

The adsorption isotherms are presented in Figure 4-4. It can be seen that the load of the aerogel with naphthalene increases with an increasing concentration of naphthalene in CO_2. It is expected that saturation will be achieved and the loading would reach a constant value at a specific naphthalene concentration. This concentration, however, could not be used because of crystallization, as described above.

The adsorption isotherm at 70°C was fitted using the Langmuir equation for the monolayer adsorption:

$$q_a = \frac{q_m bC}{1 + bC} \qquad (28)$$

where q_a is a weight adsorbed per unit weight of adsorbent, q_m is a maximum load, C is a concentration of the absorbate in the bulk phase and b is a constant.

The following parameters could be determined by fitting of the experimental data: $q_m = 0.079$, $b = 196$.

It can be seen that the loading of silica aerogel with naphthalene which can be achieved by the proposed method is not very high (4%). It is known that the benzene ring system acts as an electron donor interacting with silanol groups. Thus the hydrophobic nature of naphthalene does not provide high adsorption values on the hydrophilic aerogel surface.
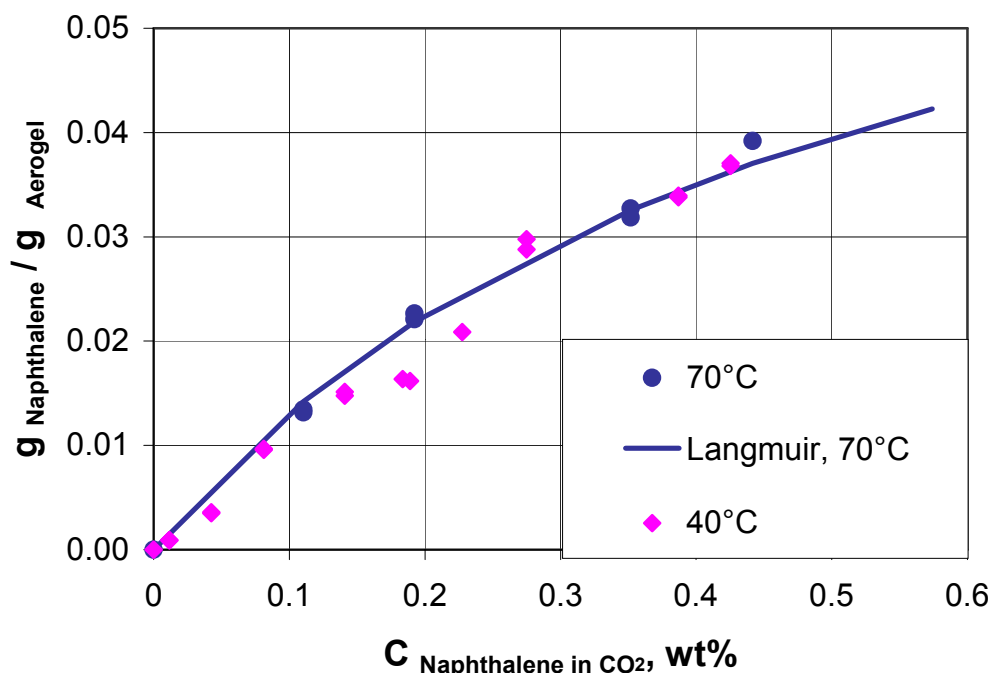
Figure 4-4 Adsorption of naphthalene on silica aerogel at 40°C and 70°C

It should also be mentioned that adsorption of CO_2 molecules takes place simultaneously with the adsorption of naphthalene. Thus, competition of both processes might take place. The CO_2 adsorption was not specifically studied, but it is known that the CO_2 density under the experimental conditions is relatively high, so that the contribution of the CO_2 adsorption is not negligible. However, during the pressure release, desorption of CO_2 takes place and at ambient pressure only traces of CO_2 remain in the aerogel.

## 4.2.2   Loading of aerogels with active substances

Experiments with naphthalene show that the process proposed in this work is suitable for the loading of silica aerogels with chemicals. After determination of the process parameters with the model substance, the experiments with other active substances were carried out.

The following criteria were used to select these substances:

- The active agent should be soluble in CO_2

- It should be stable at the process conditions used

- Immediate release should be desirable for this active agent, because we expect a faster release of the active agent from the aerogel

Three active substances, which fulfill these requirements were chosen for the experiments: *ketoprofen*, *griseofulvin* and *miconazol*.

4.2.2.1 *Ketoprofen* ((RS)-2-(3-benzoylphenyl) propionic acid)
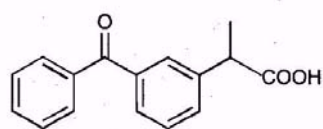
CAS number: 22071-15-4

M_w = 254.29 g/mol

Melting point = 94 °C

Figure 4-5 Structural formula of *ketoprofen*

Ketoprofen is widely used as non-steroidal, anti-inflammatory drug for the relief of acute and chronic rheumatoid arthritis and osteoarthritis, as well as for other connective tissue disorders and pains. Both the immediate release form and sustained release form exists depending on the specific application. Solubility of *ketoprofen* in CO_2 has been reported [Macnaughton 1996].

Experiments have been carried out at 140 bar and 70°C. The experimental procedure is described in detail in section 4.1.1. During the impregnation of *ketoprofen* into the aerogel, no crystallization occurred in the pores of the aerogel as proved by simple inspection and by electron microscopy. The adsorption isotherm of *ketoprofen* is presented in Figure 4-6.
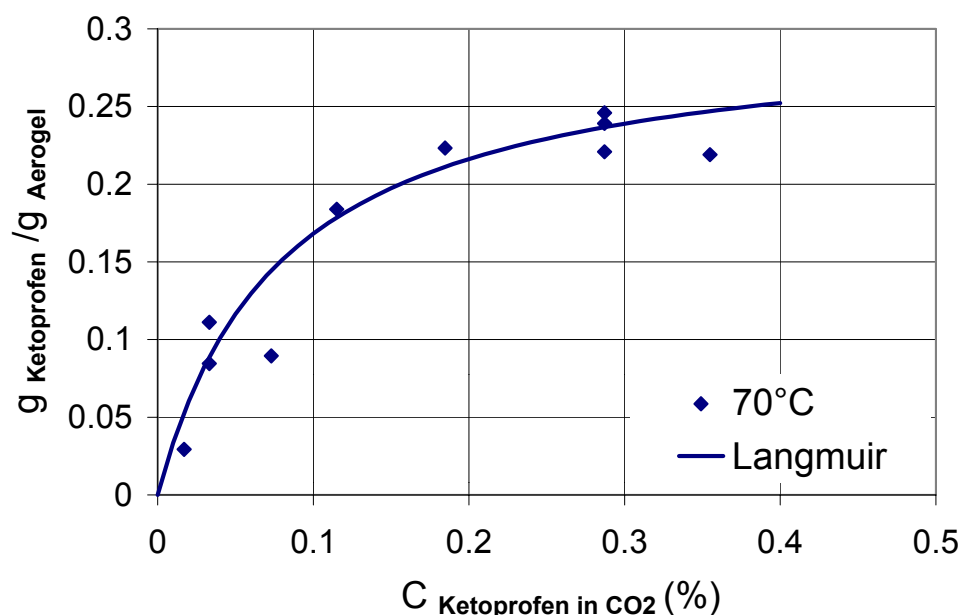

Figure 4-6 Adsorption of *ketoprofen* on silica aerogel 70°C

The adsorption isotherm was fitted using the Langmuir equation. The following parameters were determined by fitting of the experimental data: q_m = 0.303, b = 1249

The results obtained in the experiments confirm that the aerogel can adsorb a relatively large amount of *ketoprofen* (up to 0.25 gram *ketoprofen* per gram aerogel). The better adsorption of *ketoprofen* compared to that of naphthalene might be explained by the hydrogen bonding between the OH groups of *ketoprofen* and silanol groups of silica aerogel.

In all the experiments an aerogel having a density of 0.03 g/cm^3 was used for it was supposed that the adsorption is dependent on the density of the aerogels. To prove this relation, the influence of the aerogel's density on the adsorption of *ketoprofen* was studied. The concentration of *ketoprofen* was kept constant ($C_{ketoprofen}$ = 0.03 wt %) and its adsorption 40 C and 140 bar was studied for aerogels having different densities. The results are presented in Figure 4-7.
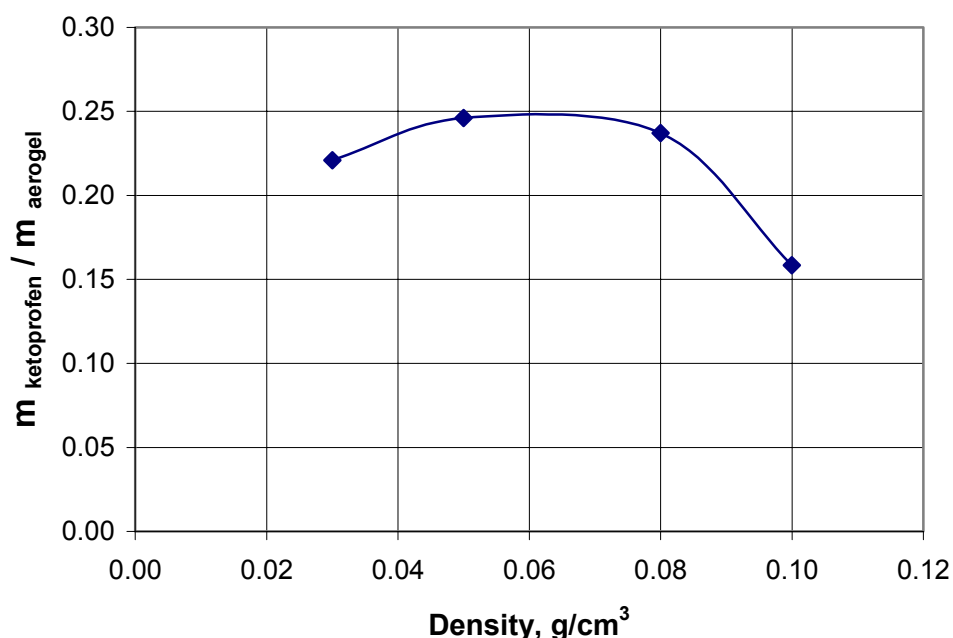

Figure 4-7 Influence of the aerogel density on the adsorption of *ketoprofen*. (40°C, 140 bar).

It can be seen that the same loading of 25% (0.25 gram *ketoprofen* per gram aerogel) can be reached if the aerogel has a density between 0.03 and 0.08 g/cm^3. The decrease in loading at a higher density (ρ = 0.1 g/cm^3) can be explained by the decrease in the aerogel surface area.

Ketoprofen dosage in the pharmaceutical formulation used at present is rather low. Common *ketoprofen* pellets (e.g. Actron pellets from Bayer company, license 1-20705) contain 12.5 mg *ketoprofen* per pellet. In the case of 25 % loading, 0.05 gram aerogel is required to obtain this dosage. If an aerogel having a density of 0.08 g/cm^3 is used, the volume of the aerogel would be 0.63 cm^3. This is quite realistic for capsules (which are filled with pulverized aerogel loaded with *ketoprofen)* or pellets (where the aerogel/*ketoprofen* powder is pressed).

4.2.2.2 *Griseofulvin* (7-Chloro-2',4,6-trimethoxy-6'b-methylspiro[benzofuran-2(3H), 1'-(2)-cyclohexene]-3,4'-dione)
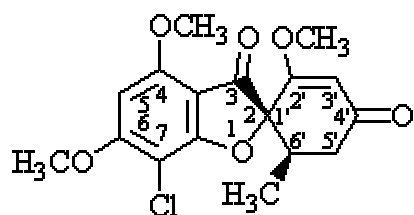
CAS number: 126-07-8

M_w = 352.8 g/mol

Melting point = 222 °C

Figure 4-8 Structural formula of *griseofulvin*

The solubilities of *griseofulvin* in different solvents are summarized in Table 4-4.

Solvent	Methanol	Ethanol	Acetone	DMF	Water
Solubility, mg/ml	2500	1500	33	150	40.1

Table 4-4 Solubility of *griseofulvin* in different solvents at 25°C [Ullmann 1998]

The solubility of *griseofulvin* in CO_2 is not available, and had to be determined experimentally according to the procedure described in section 4.1.1. The solubility of *griseofulvin* in supercritical CO_2 at 40°C and 180 bar was found to be 0.03 wt%.

The adsorption of *griseofulvin* on silica aerogels was studied under the same conditions. The experimental results are presented in Figure 4-9.

The maximum loading that could be reached with *griseofulvin* is 8 %. This value is much lower as that of *ketoprofen*. An explanation for this fact proves rather difficult. It can only be supposed that there are no groups in *griseofulvin*, which can interact with silanol or other groups in the silica aerogel. It is also possible, that an extremely low solubility of *griseofulvin* in CO_2 under the experimental conditions is responsible. The loading may probably be increased by an increase of the solubility of *griseofulvin* in CO_2. There are several methods, that allow for this. A higher pressure can be used during the experiment that would result in a higher CO_2 density and thus, a better solubility. Also entrainers, such as ethanol or acetone can be employed. It is known that even very little amounts of entrainer (2-5 wt%) can improve the solubility of t organic compounds in CO_2 by several orders of magnitude.
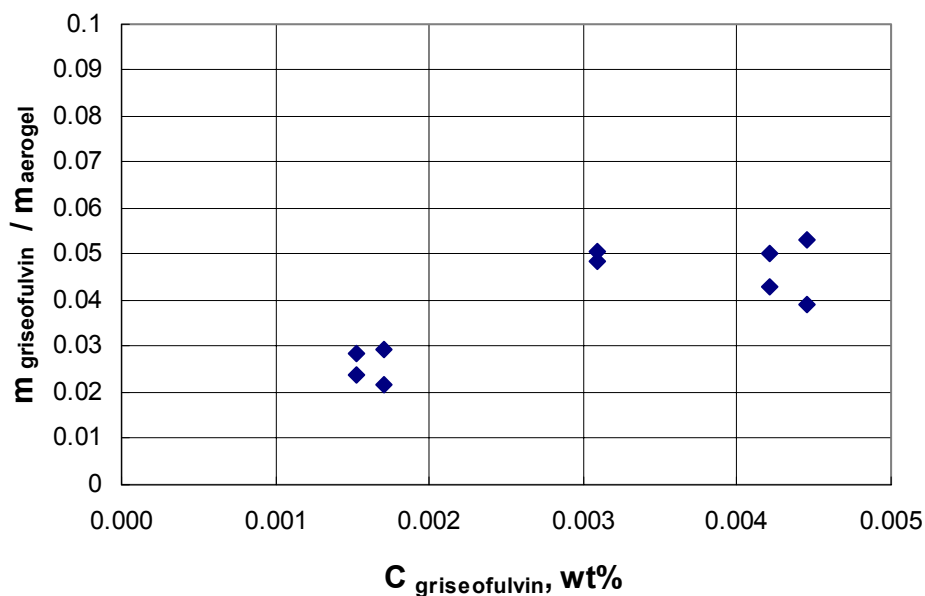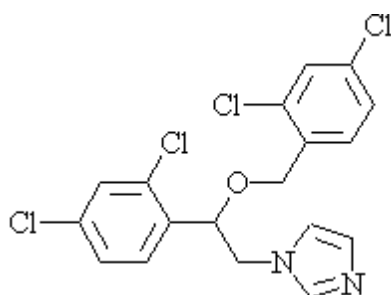
Figure 4-9 Adsorption of *griseofulvin* on silica aerogel at 40°C

4.2.2.3   *Miconazol* (1-[2-(2,4-dichlorophenyl)-2-[(2,4-dichlorophenyl)methoxy]ethyl]

‑1H-imidazole

CAS number: 22916-47-8

M_w = 479.15 g/mol

Melting point = 184.5 °C

The solubility of *miconazol*e in water and hydrochloric acid are presented in Table 4-5. The solubility in organic solvents is unknown, although it was reported, that *miconazol*e is slightly soluble in acetone and 2-propanole [Ullmann 1998].

Solvent	Water	0.1 N HCl
Solubility, mg/ml	0.3	0.0505

Table 4-5 Solubility of *miconazol*e at 25°C [Ullmann 1998]

Solubility of *miconazol*e in supercritical CO_2 was not available, so had to be determined experimentally, according to the procedure described in section 4.1.1.

It was found that at 40°C and 180 bar, the solubility of *miconazol*e is close to 0.2 wt%. The concentration range below saturation was used for the adsorption experiments. All

experiments were carried out at 40°C and 175 bar, as in the case of *griseofulvin*. The experimental results are presented in Figure 4-10.
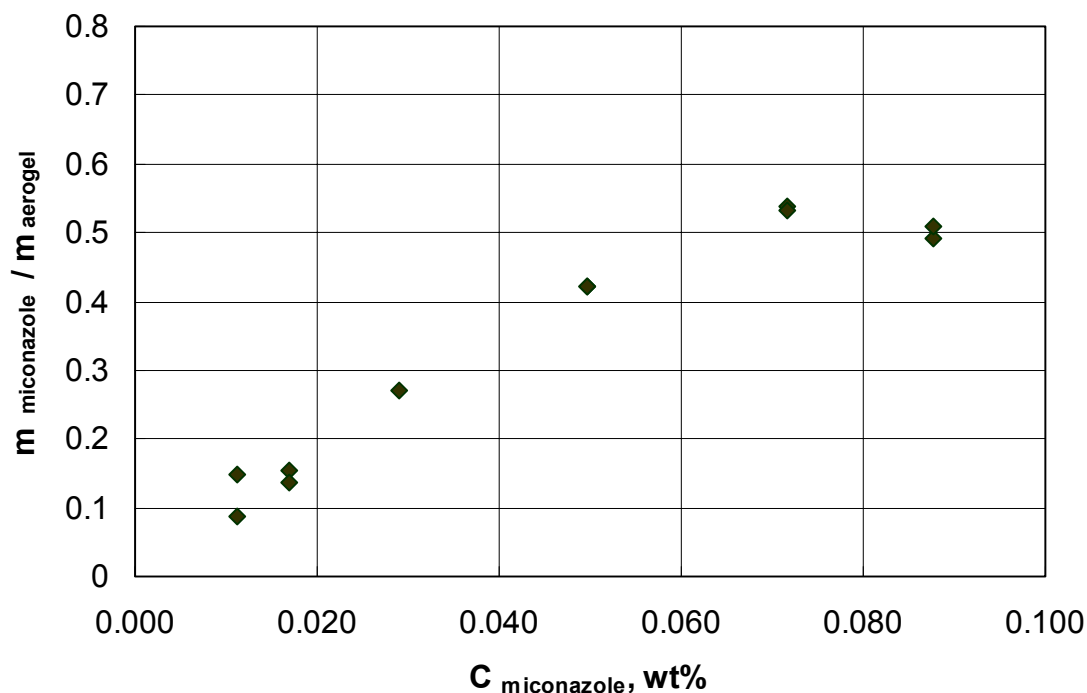

Figure 4-10 Adsorption isotherm of *miconazol*e on silica aerogel at 40°C, 175 bar.

It can be seen that the loading of an aerogel with *miconazol*e is pretty high (up to 50%). The solubility of *miconazol*e in CO_2 is also much better than that of *griseofulvin*. Because of this the aerogel is propsed as a carrier material for *miconazol*e. As already mentioned (section 2.3) aerogels can improve the rheological properties of powders. In this case the aerogel loaded with *miconazol*e can be used simultaneously as a carrier material and as a free flow agent.

4.2.3   Influence of the loading procedure on the chemical structure of drugs

Taking into consideration that the pharmaceuticals were dissolved in supercritical CO_2 at high pressure and then adsorbed on silica aerogel, it was essential to prove whether the chemical nature of a drug is changed during this process. UV spectra of all drugs used in this work were taken before and after the loading procedure and compared. For the measurment of absorption in UV-VIS region, the aerogel-drug formulations were dispersed in 0.1 N hydrochloric acid (standard dissolution medium). The position of the characteristic band was compared with those available in the literature. This method is one of the identification tests, recommended in German Pharmacopea [DAB 1997]. Corresponding results are shown in Table 4-6.

Substance	Maximal absorption, nm		
	Literature [DAB 7]	Pure drug dissolved in 0.1 N HCl	Formulation aerogel-drug dispersed in 0.1 N HCl
Ketoprofen	260	259	259
Griseofulvin	292	292.5	293
Miconazol	280	280	280

Table 4-6 Specific UV absorption bands of different drug formulations

It can be seen that the characteristic peaks were detected at the same positions in both pure drug solutions and aerogel-drug formulations. Deviations of $\pm$ 1nm are supposed to be a result of instrumental error.

It can therefore be concluded that the loading procedure proposed in this work does not influence the chemical nature of the drugs investigated in the conducted experiments.

Another parameter of interest was the aggregation state of the drug in the aerogel. As already mentioned, no crystalline structures have been found in the aerogel-drug formulations. In section 2.2 it was mentioned that pure silica aerogels exhibit an amorphous structure. It is supposed that the drug molecules adsorbed on the surface of the silica aerogel in a monomolecular layer fashion. This fact also favours the rapid release of the pharmaceuticals adsorbed onto the aerogel. In the case of crystalline drugs, even in the case of very small particle sizes, the crystalline structure would be destroyed before the drug can be really dissolved. In the case of aerogel-drug formulations this step is eliminated.

4.3. Release of drugs from aerogel-drug formulations

The release rate of a drug is the most important characteristic of the aerogel-drug formulation. The conducted work demonstrated that three particular pharmaceuticals can be adsorbed on a silica aerogel. The reverse process -desorption – also had to be studied. The release kinetics of all three aerogel-drug formulations obtained by adsorption from supercritical CO_2 were investigated.

The experiments were carried out according to the procedure described in section 4.1.3. A solution of hydrochloric acid was chosen as the dissolution media following the recommendations of the German Pharmacopea [DAB 9]. The final concentration reached in the solution was equal to 10 % of the solubility of the corresponding drug in 0.1 N HCl at

37°C. Pure drug powders, used for the loading were used as a standard. In every case the dissolution profile of the drug-aerogel formulation was compared with that of the pure drug.

4.3.1   Release of *ketoprofen*

In the case of *ketoprofen* both immediate release and sustained release are desirable, depending on every specific therapeutic effect.

Release of *ketoprofen* from the *ketoprofen*–aerogel formulation was determined experimentally and is shown below in comparison with that of crystalline *ketoprofen*. The experimental results were fitted with the first order model (30).
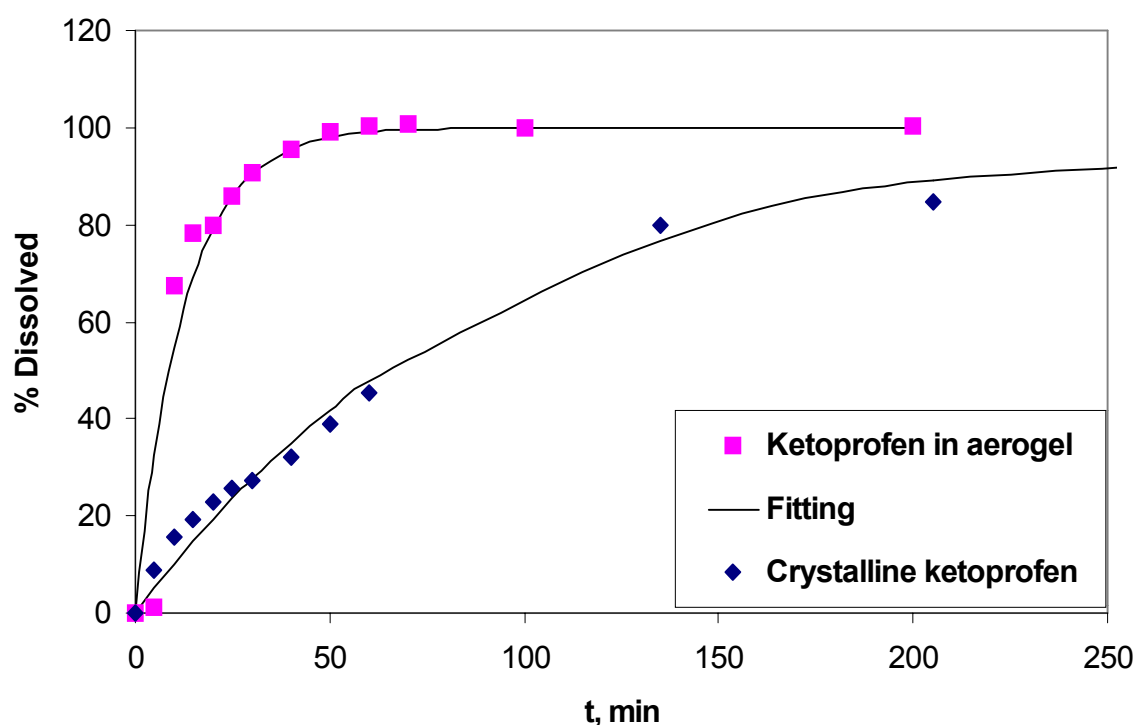

Figure 4-11 Dissolution profiles of crystalline *ketoprofen* and aerogel-*ketoprofen* formulation, 37°C, 100 min⁻¹.

It can be seen that the dissolution of *ketoprofen* from the aerogel-*ketoprofen* formulation, prepared by the adsorption from supercritical CO_2 solution is much faster than the dissolution of crystalline *ketoprofen*. Around 80 % of *ketoprofen* is dissolved after 25 min in the case of the aerogel-drug formulation whereas in the case of crystalline drug, 80 % is dissolved only after 200 min. This effect was expected and can be explained by both the increase of the specific surface area of the *ketoprofen* adsorbed on the aerogel and its non-crystalline structure in this formulation.

Several approaches to describe the release profile exist [Stricker 1998]. The choice of the fitting model depends on the kind of dissolution. For instance, the release of a drug from an insoluble matrix is well described by the Higuchi model [Higuchi 1961], [Gohel 2000]:

$$C_{drug}(t) = k\sqrt{t} \qquad\qquad (29)$$

where C_{drug} is a percent of drug released at the time t; t is a dissolution time.

For the description of the fast release a so-called "first order release model" [Shah 1987] can be used:

$$C_{drug}(t) = 100\,(1 - e^{-kt}) \qquad\qquad (30)$$

Equation (30) was used for fitting of the *ketoprofen* dissolution profiles (Figure 4-11). Both dissolution of crystalline *ketoprofen* and aerogel-*ketoprofen* formulation could be well fitted using this approach.

It is known that the release profiles depend strongly on the stirring rate of the system [Yu 2002]. The rotation number of 100 min^{-1} is recommended by USP and DAB, but it does not provide an ideal mixing in the vessel. The dissolution profiles of *ketoprofen* using a higher rotation number was studied. As mentioned above, the rotation number of 1440 min^{-1} should provide an ideal mixing in the solution. Dissolution curves of the crystalline *ketoprofen* and *ketoprofen*-aerogel formulations were measured under these conditions. The results are shown below.

One can see that the dissolution at a stirring rate 1440 min^{-1} takes place significantly faster than that at a rate of 100 min^{-1}. The same effect was found for *metoprolol tartrate* [Yu 2002] However, even in the case of the slower mixing rate, the release of *ketoprofen* from the aerogel-*ketoprofen* formulation is still faster than that of crystalline *ketoprofen*.

Because the lower mixing rate simulates the dissolution of the drug in the body to a better extent than the higher mixing rate, the lower rotation number was selected throughout the experiments.
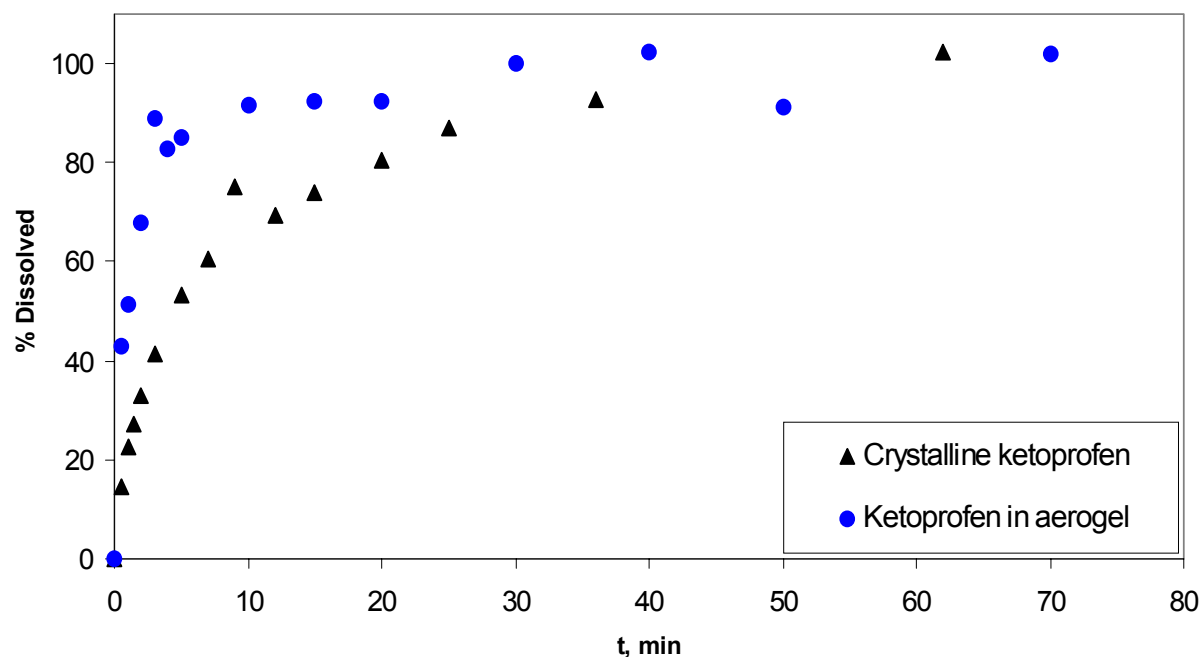
Figure. 4-12 Dissolution profiles of crystalline *ketoprofen* and aerogel-*ketoprofen* formulations; 37°C; 1440 r/min

4.3.2 Release of griseofulvin

Release of *griseofulvin* from the aerogel-*griseofulvin* formulation is presented in Figure 4-13 in comparison with that of the crystalline drug.

Similar to *ketoprofen*, the dissolution of griseofulvin from the aerogel-griseofulvin formulation is faster than that of the crystalline drug. Also, the loading of the aerogel with *griseofulvin* is not very high (see Figure 4-9). As much as 80 % of drug can be released in 30 min, which is 4 times faster than the release of crystalline *griseofulvin* and twice as fast as that of the micronized formulations [Food and Drug Administration, HHS]. If the loading of an aerogel with *griseofulvin* could be improved (for example by use of an entrainer during the dissolution in supercritical CO_2), aerogel-*griseofulvin* formulations with higher *griseofulvin* concentration could be used instead of a common micronized drug.

The experimental results were fitted with the first order model (30).

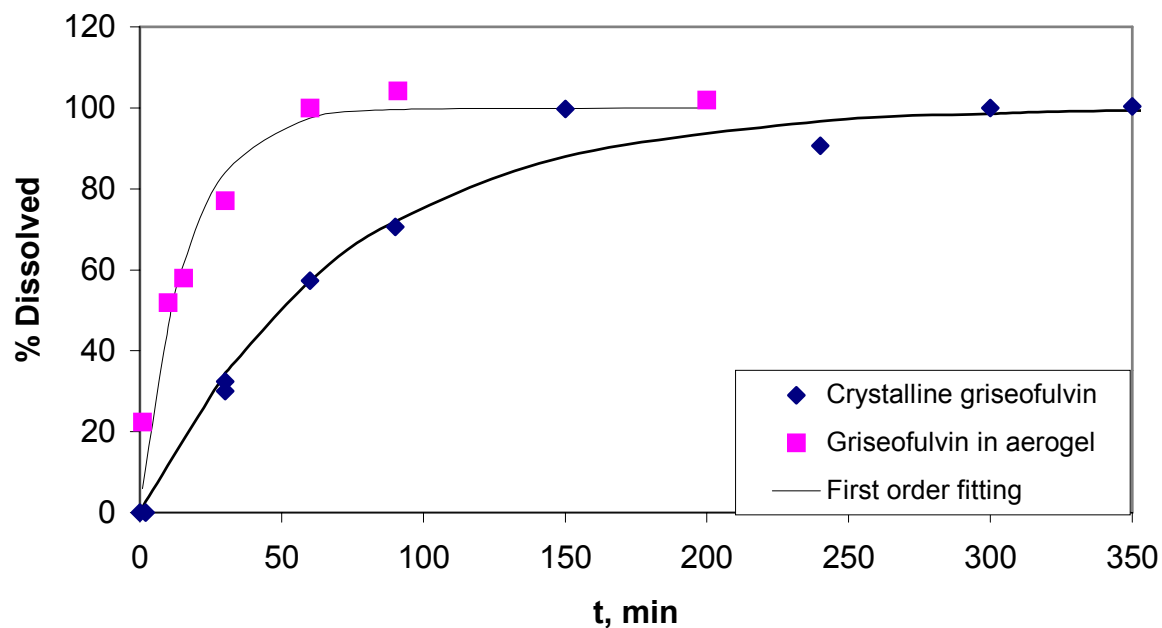**Figure 4-13 Dissolution profiles of crystalline *griseofulvin* and aerogel-*griseofulvin* formulation**

4.3.3   Release of *miconazol*

The release profiles of *miconazol* were studied experimentally. The results are shown below. The experimental results were fitted with the first order model (30).
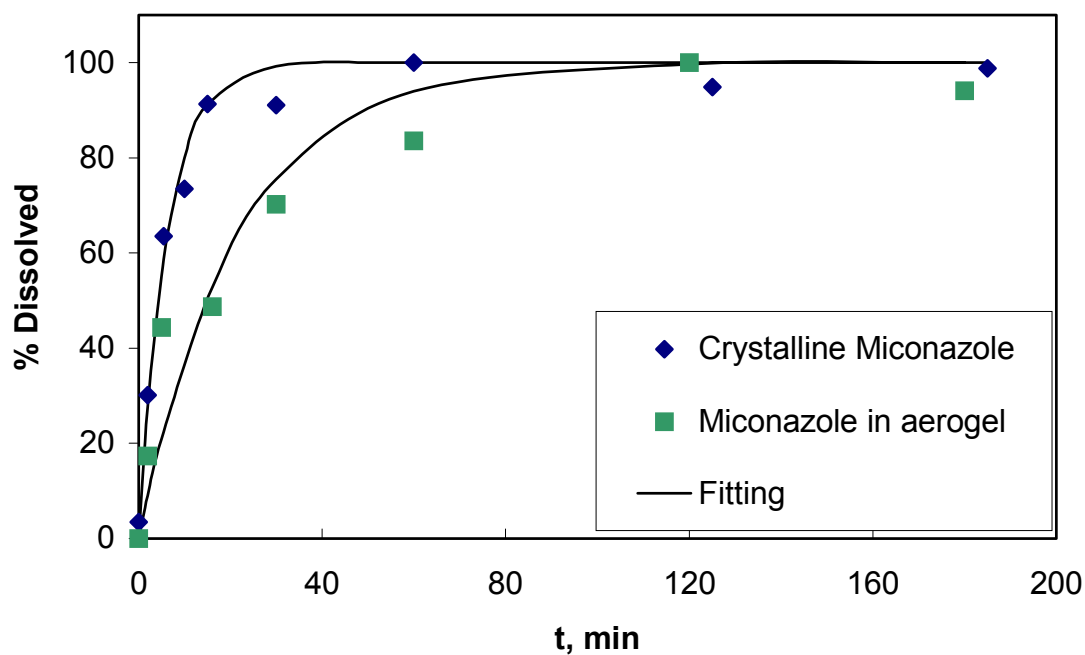

Figure 4-14 Release profile of crystalline *miconazol* and aerogel-*miconazol* formulation.

It can be seen that in the case of *miconazol* the release from the aerogel-*miconazol* formulation is even slower than that of crystalline *miconazol*. It is difficult to explain this result. The fact that release of crystalline *miconazol* itself is pretty fast (80 % of *miconazol* are released in just 20 min), implies that the proposed procedure is not efficient in the case of *miconazol*. The crystalline form of this drug which is commonly used shows a release, which is fast enough for therapeutic purposes. This proves that the procedure, proposed in this work, must be independently tested for every drug in order to prove its efficiency in each individual case.

In our case the release of two drugs (*ketoprofen* and *griseofulvin*) from a study of three drugs was improved by using aerogel-drug formulations.

4.4. Evaluation of the loading method and aerogel-drug formulations

Using three different drugs it was shown that aerogels may be used as a carrier material for pharmaceutical applications. It was also demonstrated that the process based on adsorption from the supercritical CO_2 solution allows for a high loading of the aerogel with the corresponding drugs. The corresponding drug does not exhibit a crystalline structure in this formulation.

Loading is controlled by the process conditions and can be described by means of the Langmuir equation.

In the case of *ketoprofen*, the loading is high enough so that the desirable dosage of the drug can be achieved by using a reasonable amount of aerogel. In the case of *griseofulvin*, the loading is not very high, but probably can be improved by an increase of the *griseofulvin* solubility in CO_2 by changing the process parameters or by using an entrainer.

It was shown that the chemical structure of the investigated drugs is not influenced by the loading method proposed in this work. In cases where no organic solvent is used during loading, drying of the aerogel-drug formulation is not required. It is proposed that the aerogel-drug formulations produced by this method can be used in pharmaceutical applications. Loaded aerogel can be used in the powdered or monolithic form.

It was found that the release of *ketoprofen* and *griseofulvin* from the aerogel-drug formulation is faster than that of the crystalline drugs and commonly used formulations. This effect can be explained by the increase of both the specific surface area of the *ketoprofen* adsorbed on the aerogel and its non-crystalline structure in this formulation. In the case of *miconazol* no acceleration release could be achieved by using the aerogel-drug formulation.

It may be concluded that the aerogel-drug formulations can be effectively used for those drugs, whose immediate release is desirable, but the procedure should be tested for every individual drug.

5. Conclusions

The present work was mainly concerned with the synthesis of silica aerogels and the conditions required to enhance the gelation process. The common two-step procedure was modified by the addition of supercritical carbon dioxide (CO_2) during the second step. CO_2 is commonly used in aerogel production for the solvent extraction, but its influence on the gelation process itself has not yet been reported.

It has been found that the addition of supercritical CO_2 to the sol solution after the second step enhances gel formation. The enhancement factor depends on the aerogel target density and varies between 5 and 100. The CO_2 concentration in the liquid phase generally reaches 30 wt% at the gel point.

It was evident that the amount of CO_2 required to realize such a rapid gelation process strongly depends on the experimental conditions. An increase in the temperature, concentration of acid or base catalyst and hydrolysis time lead to a decrease in the CO_2 concentration needed for gelation. It was also shown that the reaction enhancement takes place only if CO_2 is combined with both catalysts used in the common two-step process; if one or both catalysts are not used, CO_2 addition leads to the rapid precipitation of colloidal particles.

Studies showed that the fast gel formation takes place preferably in polar aprotic solvents (acetonitrile, dimethylformamide), whereas CO_2 addition to the systems with polar protic solvents (methanol, ethanol) promotes particle formation.

It was demonstrated that CO_2 can be used successfully only in combination with other catalysts, used during the first and second steps. This allows one to conclude that CO_2 acts not (or not only) as a catalyst itself, but gives rise to some form of optimal conditions for the condensation reaction, being accelerated by normal base catalysts (specifically NH_4OH). Furthermore, the dependence of this effect on the solvent nature suggests that some interaction between CO_2 and the solvent might be taking place i.e. CO_2 may be participating in the solvation process. At the beginning of the reaction, acetonitrile solvates the partly hydrolyzed TMOS and thus, to some extent, inhibits t condensation. CO_2 may build an ionic complex with acetonitrile and compensating the solvation effect to some extent.

The nature of the gelation enhancement by CO_2 has not been fully explained through this work. Further investigations are required to fully understand this phenomenon.

A number of silica aerogels were synthesized by the modified two-step method described here. It was demonstrated that the gelation enhancement by CO_2 addition does not greatly influence the aerogel properties, the aerogel surface area, pore size and light absorbance have the same values as the corresponding samples prepared without CO_2 addition. Thus, CO_2 can be regarded as an alternative catalyst for the gelation process. The process suggested in the present work allows for relatively short gelation times. Also, the extraction time is reduced to some extent, because the gel phase contains around 30% CO_2 at the beginning of extraction. Summarizing all these facts one may conclude that the method proposed in the present work may be successfully employed in the production of aerogels, especially in the case of low density aerogels.

Silica aerogels produced by this method were tested as potential carrier materials for pharmaceuticals. An alternative method of loading of the aerogel with the corresponding compound was studied. This method is based on the adsorption of the organic compound onto the aerogel from their solutions in supercritical CO_2.

It was demonstrated that, in the case of the 3 investigated drugs this process allows for a high loading of the aerogel. The chemical structure of the investigated drugs is not influenced by the loading method. The aerogel-drug formulations produced by this method are therefore suggested as potential drug delivery systems in pharmaceutical applications.

The release profiles of such formulations were measured using a standard method, recommended in German pharmacopea. It was found that the release of 2 drugs (*ketoprofen* and *griseofulvin)* from the aerogel-drug formulation is faster than that of the crystalline drugs and commonly used formulations. This effect can be explained by both the increase in the specific surface area of the drug adsorbed on the aerogel and its non-crystalline structure in this formulation. In the case of the other investigated drug (*miconazol*), no release acceleration was observed using the aerogel-drug formulation. This indicates that the release characteristics of aerogel-drug formulations must be tested for every individual drug.

As a result of these facts, one may conclude that the aerogel-drug formulations may be effectively used as drug delivery systems for drugs whose immediate release is desirable. Such formulations are especially favoured for those pharmaceuticals that have a long dissolution time beacuase the release of such compounds can be significantly improved by adsorption on silica aerogels. This method can be used as an alternative to the micronization procedure,   used   for   these   purposes   at   present   time.

6. Literature

Ackerman 2001
      W.C. Ackerman, M. Vlachos, S. Rouanet, J. Freundt, J.Non-Cryst.Solids 285, 2001, 264

Aelion 1950
      R. Aelion, A. Loebel, F. Eirich, JACS 72, 1950, 5705

Ahmed 1995
      M.S. Ahmed, Y.A. Attia, J. Non-Cryst. Solids 186, 1995, 402

Ahmed 1998
      M.S. Ahmed, Y.A. Attia, Applied Thermal Engineering 18, 1998, 787

Alkemper 1998
      J. Alkemper, S. Sous, C. Stöcker, L. Ratke J.Cryst.Growth 191, 1998, 252

Andrianov 1965
      K.A. Andrianov, Metal Organic Polymers, J.Wiley, N.Y. 1965

Arai 1991
      H. Arai, M. Machida, Catal.Today 10, 1991, 1

Arlt 2000
      W.Arlt, I.Smirnova DE 10048654 A1, issued on 26.09.2000

Artaki 1986
      I. Artaki, T. Zeda J. Jonas, J.Non-Cryst.Solids 81, 1986, 381

Atkinson 1962
      R.M. Atkinson, C. Bedford, K.J. Child, E.G. Tomich, Nature 193, 1962, 4815

Ayers 2001
      M. Ayers, A. Hunt J.Non-Cryst.Solids 285, 2001, 123

Baiker 1998
      A. Baiker, J.D. Grunwaldt, C.A. Müller, L. Schmid, Chimia 52, 1998, 517

Bandara 1996
      J. Bandara, J. Kiwi, C. Pulgarin, G.M. Pajonk, J.Mol.Catal. A 111, 1996, 333

Bartle 1991
      K.D. Bartle, A.A. Clifford, S.A. Jafar, and G.F. Shilstone, J. Phys. Chem. 20, 1991, 713

Basso 2000
      A. Basso, L. Martin, C. Ebert, L. Gardossi, A. Tomat,M. Casarci, O.Li Rosi Tetrahedron
      Letters 41, 2000, 8627

Bechtold 1968
      M.F. Bechtold, R.D. Vest, L. Plambeck, J.Am.Chem.Soc. 90, 1968, 4590

Bendale 1994
> P.G. Bendale, R.M. Enick, Fluid Phase Equilibria 94, 1994, 227

Bernards 1991
> T.M. Bernards, M.J.Janssen, M.J. van Bommel et al., J.Non-Cryst.Solids 134, 1991, 1

Bianchard 1982
> F. Bianchard, J.P. Reymond, B. Pommier, S.J. Teichner, J.Mol.Catal. 17, 1982, 171

Boonstra 1988
> A.H. Boonstra et al., J.Non-Cryst.Solids 105, 1988, 207

Boonstra 1989
> A.H. Boonstra, J.Non-Cryst.Solids 109, 1989, 153

Boonstra 1991
> A.H. Boonstra et al. J.Non-Cryst.Solids 134, 1991, 1

Borsella 2001
> E. Borsella et al., Mat.Sci. & Eng. B 79, 2001, 55

Brinker 1982
> C.J. Brinker, K.D. Keefer, D.W. Schaefer, C.S. Achley, J.Non-Cryst.Solids 48, 1982, 47

Brinker 1984
> C.J. Brinker, K.D. Keefer, D.W. Schaefer, R.A. Assink, B.D. Kay, C.S. Ashley, J.Non-Cryst.Solids 63, 1984, 45

Brinker 1990
> C.J. Brinker, G.W. Sherer, "The physics and chemistry of sol-gel processing", Acad. Press, New York, 1990.

Buisson 2001
> P. Buisson, C. Hernandez, M. Pierre, A.C. Pierre, .J Non-Cryst.Solids 285, 2001, 295

Burger 1998
> T. Burger, J. Fricke, Phys. Chem. 102, 1998, 1523

Buzykaev 1999
> A.R. Buzykaev, A.F. Danilyuk, S.F. Ganzhur, E.A. Kravchenko, A.P. Onuchin, Nuclear Instruments & Methods in Physics Research A, 433, 1999, 396

Byun 1996
> H.S. Byun, B.M Hasch, M.A. McHugh, Fluid Phase Equilibria 115, 1996, 179

Cao 1994
> W. Cao, A.J. Hunt, J.Non-Cryst.Solids 176, 1994, 18

Cao 1999
> W.Cao, A.Hunt US Patent 5,855,953 issued 05.01.1999

Casas 2001
> L. Casas, A. Roig, E. Rodriguez, E. Molins, J. Tejada, J. Sort, J. Non-Cryst.Solids 285, 2001, 37

Chen 1986
    K.C.Chen, T.Tsuchiya, J.D.Mackenzie, J. Non-Cryst.Solids 81,1986, 227

Chiehming 1998
    C. Chiehming, C.Kou-Lung, D. Chang-Yih, J. Supercritical Fluids 12, 1998, 223

Colby 1986
    M.W. Colby et al J.Non-Cryst.Solids 82, 1986, 37

Craievich 1986
    A. Craievich, M. Agerter, D.I. Dos Santos, T. Woignier, J. Zarzycki, J. Non-Cryst. Solids
    86, 1986, 394

DAB 1997
    Deutsches Arzneibuch, Wiss. Verlag Stuttgart, 1997

Dai 2000
    C. Dai, Y.H. Ju, H.J. Gao, J.S. Lin, S.J. Pennycook, C.E. Barnes, Chem. Commun., 2000,
    243

DE 19653758 A1
    Offenlegungsschrift DE 19653758 A1, issued on 12.1996

Degussa 2001
    Technical Bulletin Aerosil & Silanes, 2001, Company publication, Degussa, Düsseldorf

Deshpande 1992
    R. Deshpande, D.W. Hua, D.M. Smith, C.J. Brinker J. Non-Cryst. Solids 144, 1992, 32

Deshpande 1996
    R. Deshpande, D. Smith, C.J. Brinker, US Patent 5,565,142 issued 15.10.1996

Dieudonne 2000
    A. Dieudonne, Hafidi Alaoui, P. Delord, L. Phalippou, J. Non-Cryst. Solids 262, 2000, 155

Domingo 2001
    C. Domingo, J. Garcia-Carmona, M.A. Fanovich, J. Llibre, R. Rodriguez-Clemente, J.
    Supercrit. Fluids 21, 2001, 147

Ehrburger-Dolle 1995
    F. Ehrburger-Dolle, J. Dallamano, E. Elaloui, G. Pajonk, J. Non-Cryst. Solids 186, 1995, 9

Einarsrud 2001
    M.-A. Einarsrud, E. Nilsen, A. Rigacci, G.M. Pajonk, J.Non-Cryst. Solids 285, 2001, 1

Fanelli 1989
    A.J. Fanelli, J.V. Burlew, G.B. Marsh, J. Catalysts. 116, 1989, 318

Ferrieri 1999
    R.A. Ferrieri, I. Garcia, J.S. Fowler, A.P. Wolf, Nuc.Drug&Med., 26, 1999, 443

Food and Drug Administration, HHS
    Food and Drug Administration, HHS, § 436.317, 21 CFR Ch.1 1998

Fricke 1986
    Aerogels, ed. J. Fricke, Springer, Berlin, 1986

Gash 2001
    A. Gash, T.M. Tillotson, J.H. Satcher, L.W. Hrubesh, R.L. Simpson, J.Non-Cryst.Solids
    285, 2001, 22

Gesser 1989
    H.D. Gesser, P.C. Goswami, Chem. Rev. 89, 1989, 765

Gohel 2000
    M.C. Gohel, M.K. Panchal, V.V. Jogani, AAPS PharmSciTech 1, 2000, 31

Golob 1997
    P. Golob, Journal of Stored Products Research 33, 1997, 69

Golov 1998
    A. Golov, J.V. Porto, J.M. Parpia, J.Low Temp.Physics 113, 1998, 329

Gross 1998
    J. Gross, P. Coronado, L. Hrubesh, J.Non-Cryst.Solids 225, 1998, 282

Haereid 1995
    S. Haereid, M. Dahle, S. Lima, M.-A. Einarsrud, J.Non-Cryst. Solids 186, 1995, 96

Hafidi 2000
    A. Hafidi et al., J. of Non-Cryst. Solids 265, 2000, 29

Haranath 1997
    D. Haranath, G.M. Pajonk, P.B. Wagh, A.V.Rao, Mat.Chem.and Phys. 49, 1997, 129

Hasegawa 1988
    I. Hasegawa, S. Sakka, Bull.Chem. Soc. Japan 61, 1988, 249

Heley 1995
    J.R.Heley, D.Jacson, P.F. James, J.Non-Cryst. Solids 186, 1995, 30

Henning 1981
    S. Henning, L. Svenson, Phys. Scr. 1981, 23, 697; US Patent 4,327,065

Henning 1990
    S. Henning, Airglass – Silica Aerogel, D7:1990

Higutchi 1963
    T. Higutchi, J.Pharm.Sci. 50, 1963, 1145

Hrubesh 2001
    L.W. Hrubesh, P.R. Coronado, J.H. Satcher Jr., J.Non-Cryst.Solids 285, 2001, 328

Hua 1995
    D.W. Hua, J. Anderson, J.Di Gregorio, D.M. Smith, G. Beaucage, J.Non-Cryst.Solids 186,
    1995, 142

Huang 1999
> W.L. Huang, K.M. Liang, S.R.Gu, J. of Non-Cryst. Solids 1258, 1999, 234

Hunt 1995
> A. Hunt, M. Ayers, W. Cao, J. of Non-Cryst. Solids 185, 1995, 227

Hunt 1998
> A. Hunt J.Non-Cryst.Solids 225, 1998, 303

Hüsing 1997
> N. Hüsing, Dissertation , Würzburg 1997

Hutter 1995
> R. Hutter, D.C.M. Dutoit, T. Mallat, M. Schneider and A. Baiker, J. Chem. Soc., Chem. Commun., 163, 1995.

Iler 1979
> R. Iler, "The chemistry of silica", Wiley, 1979

Kamiuto 1999
> K. Kamiuto, T. Miyamoto, S. Saitoh, Applied Energy 62, 1999, 113

Khaleel 1999
> A. Khaleel, P.N. Kapoor, K.J. Klabunde, NanoStructured Materials 11, 1999, 459

Kirkbir 1998
> F. Kirkbir, H. Murata, D. Meyers, S. Chaudhuri, J.Non-Cryst.Solids 225, 1998, 14

Kistler 1931
> S.S Kistler, Nature 127, 1931, 741

Kistler 1937
> S.S Kistler, US Patent 2,093,454; US Patent 2,188,007; US Patent 2,249,767

Klein 1985
> L.C. Klein, Ann.Rev.Mater.Sci. 15, 1985, 227

Knez 2001
> Z. Knez, Z. Novak, J.Chem.Eng.Data 46, 2001, 858

Koeppel 1998
> R.A. Koeppel, C. Stoecker, A. Baiker, J. Catal. 179, 1998, 515

Kordikowski 1995
> A. Kordikowski, A.P. Schenk, R.M. Van Nielen, C.J. Peters, J.Supercritical Fluids 8, 1995, 205

Lamb 1997
> L. Lamb, D. Huffman U.S Patent No.5,698,140 issued 16.12.1997

Land 2001
> V. Land, T. Harris, D. Teeters, J.Non-Cryst.Solids 283, 2001, 11

Lee 1995

    Kun-Hong Lee, Sun-Youg Kim, Ki-Pung Yoo, J.Non-Cryst.Solids, 186, 1995, 307

Leventis 2002

    N. Leventis, I.A. Elder, G.J. Long, D.R. Rollison, NanoLetters 2, 2002, 63

Loy 1997

    D.A. Loy, E.M. Russick, S.A. Yamanaka, B.M. Baugher, Chem. Nature. 9, 1997, 2264

Magnan 1996

    C. Magnan, C. Bazan, F. Charbit, J. Joachim, G. Charbit, in High Pressure Chemical
    Engineering, ed. Ph. Rudolph, Ch. Trepp, Elsevier, 1996

Martin 2001

    J. Martin, B. Hosticka, P. Norris .J Non-Cryst.Solids 285, 2001, 222

Maurer 1993

    S.M. Maurer, D. Ng, E.I. Ko, Catal.Today 16, 1993, 319

McHugh 1980

    McHugh, M.E. Paulaitis, J.Chem.Eng.Data 25, 1980, 326

Macnaughton 1996

    S.J. Macnaughton, I. Kikic, N.R. Foster, P. Alessi, A. Cortesi, I. Colombo, J. Chem. Eng.
    Data 41 1996 1083

Merzbacher 1999

    C.I. Merzbacher, J.G. Barker, J.W. Long, D.R. Rolison, NanoStructured Materials, 12, 1999,
    551

Micrometrics

    Paul A. Webb, Clyde Orr „Analytical Methods in Fine Particle Technology"
    Micromeritics Instrument Corporation, Norcross, GA USA, 1998

Moner-Girona 2000

    M. Moner-Girona, A. Roig, E. Molins, J. Llibre, Materials of ISA6, Albuquerque, N.M.,
    USA October 8-11, 2000

Morrison 1970

    R. Morrison, R. Boyd, Organic Chemistry, Eds. Allyn and Bacon, 8. Edition, 1970

Mrowiec-Bialon 1998

    J. Mrowiec-Bialon, A.B. Jarzebski, A.I. Lachowski, J.J. Malinowski, J.Non-Cryst. Solids
    225, 1998, 184

Nicolaon 1968-1

    G. Nicolaon, "Contribution on l'etude des aerogels des silice", Ph.D thesis, University of
    Lyon, 1968

Nicolaon 1968 -2
G. Nicolaon, S. Teichner, Bull.Soc.Chim.Fr., 1968, 8, 3107; ibid. 1968, 9, 3555; ibid. 1968, 11, 4343;

Nicolaon 1969
US Patent 3,672,833

NIST Databank
NIST Chemistry WebBook, NIST Standard Reference Database Number 69, Eds. P.J. Linstrom and W.G. Mallard, July 2001, National Institute of Standards and Technology, Gaithersburg MD, 20899 (http://webbook.nist.gov)

Novak 1997
Z. Novak, Z. Knez, J. Non-Cryst. Solids 221, 1997, 163

Novak 1999
Z. Novak, Z. Knez, M. Hadolin, Second European Congress of Chemical Engineering, Montpellier, 1999.

Orcel 1986
G. Orcel, J. Phalippou, L.L. Hench, J Non-Cryst.Solids 86, 1986, 114-130

Orlovic 2001
A.Orlovic, S.petrovic, D.Radivojevic, D.Skala, Chem. Ind. 55, 2001, 244

Pajonk 1986
G.M. Pajonk et al. J.Non-Cryst.Solids 81, 1986, 381

Pajonk 1997
G.M. Pajonk, Cat.Today 52, 1997, 319

Pajonk 1998
G.M. Pajonk, J. Non-Cryst. Solids 225, 1998, 307

Pajonk 1999
G.M. Pajonk, Cat.Today 52, 1999, 3

Peri 1966
J.B. Peri, J.Phys.Chem. 70, 1966, 2937

Pohl 1985
E.R Pohl, F.D.Osterholz in Molecular Characterization of Composite Interfaces, eds. H.Ishida and G.Kumar, Plenum, New York, 1985, p.157

Pope 1986
E.J.A. Pope and J.D. Mackenzie, J.Non-Cryst.Solids 87, 1986, 185

Posselt 1992
D. Posselt, J. Pedersen, K. Mortensen J. Non-Cryst. Solids 145, 1992, 128

Power 2001
M. Power, B. Hosticka, E. Black, C. Daitch, P. Norris .J Non-Cryst.Solids 285, 2001 303

Rao 1994
A. Venkateswara Rao, G.M. Pajonk, N.N. Parvathy, J. Mat. Sci. 29, 1994, 1807

Roethe 1986
K.P. Roethe, R. Gutsche, W. Richter, A. Roethe, J. Caro, J. Kärger,
Adsorption Sci. & Techn. 3, 1986, 65

Roig 1998
A. Roig et al. J. of Eu. Cer. Soc. 18, 1998, 1141

Rolison 2001
D.R. Rolison, B. Dunn, J. Mat. Chem. 11, 2001, 963

Scherer 1995
G.W. Scherer, D.M. Smith, X. Qiu, J.M. Anderson, J.Non-Cryst.Solids 186, 1995, 316

Schmid 1999
L. Schmid, M. Rohrer and A. Baiker, Chem. Commun 21, 1999, 2302

Schmidt 1998
M. Schmidt, F. Schwertfeger, J.Non-Cryst.Solids 225, 1998, 364

Schneider 1994 -1
M. Schneider, M. Wildberger, M. Maciejewski, D. Duff, T. Mallat and A. Baiker, J. Catal.,
148,1994, 625.

Schneider 1994-2
H. Schneider, S. Tschudin, M.Schneider, A. Wokaun, A. Baiker, J. Catal. 147, 1994, 5

Schneider 1994-3
M. Schneider, G.D. Duff, T. Mallat, M. Wildberger, A. Baiker, J. Catal. 147, 1994, 500

Schwertfeger 1996
F. Schwertfeger, A. Zimmermann, H. Krempel, WO 96/25850, issued 1996

Schwertfeger 1998
F. Schwertfeger, D. Frank, M. Schmidt , J.Non-Cryst.Solids 225, 1989, 18

Schwertfeger 2001
F. Schwertfeger, A. Zimmermann, H. Krempel, US Patent 6,280,744, issued 28.08.2001

Shaefer 1987
Physics and Chemistry of Porous Media II, Eds. AIP New York 1987

Shah 1987
M.V. Shah, M.D. de Gennaro, H. Suryakasuma, J. Microencapsul. 4, 1987, 223

Sharp 1993
K. Sharp, WO 93/23333, issued 1993

Sherer 1989
G.W. Sherer, J.Non-Cryst.Solids, 1989, 18

Sherer 1998
    G.W. Scherer, Adv. Coll. and Int. Sci. 76-77, 1998, 321

Sievers 1998
    W. Sievers, A. Zimmerman DE 19719395 A1 issued 12.11.1998

Sirisuth 2000
    N. Sirisuth, N.D. Eddington, Int. Journal Gen. Drugs, 2000

Smith 1998
    D. Smith, A. Maskara, U.Boes, J.Non-Cryst.Solids 225, 1998, 254

Stark 1998
    R.W. Stark, T.Drobek, M.Weth, J.Fricke, W.M.Heckl, Ultramicroscopy 75, 1998, 161

Stolarski 1999
    M. Stolarski, J. Walediewski, M. Steininger, B. Pniak, Applied Cat. A 177, 1999, 139

Stricker 1998
    H. Stricker, Physikalische Pharmazie, 3.rd edition,
    Wissenschaftliche Verlagsgesellschaft mbH Stuttgart, 1998

Suh 1999
    D.J. Suh, T.J. Park, J.H. Sonn, J.C. Lim, J. Mat. Sci. Lett. 18, 1999, 1473

Sun 1999
    N. Sun, K.J. Klabunde, J.Catal. 185, 1999, 506

Sun 2001
    J. Sun, J.P. Longtin, P.M. Norris, J.Non-Cryst.Solids 281, 2001, 39

Tajiri 1998
    K. Tajiri, K. Igarashi, Solar Energy Mat. And Solar Cells, 54 (1998) 189

Tan 2000
    H.W. Tan, J.R. Beamish, Physica B, 284-288, 2000, 389

Tewari 1985
    P.H. Tewari, A.J. Hunt, K.D. Lofftus, Materials Letters 3, 1985, 363

Tewari 1986
    P.H. Tewari, A.J. Hunt, US Patent No. 4,610,863, issued 09.09.1986

Tillotson 1992
    T.M. Tillotson, L.W. Hrubesh, J.Non-Cryst.Solids 145, 1992, 44

Tillotson 1995
    T.M. Tillotson, J.F. Poco, L.W. Hrubesh, I.M. Thomas US Patent 5,409,683, Issued
    15.04.1995

Tsou 1995
    P. Tsou, J.Non-Cryst.Solids 186, 1995, 415

Ullmann 1998

Ullmann's Encyclopedia of Industrial Chemistry, 6th Ed., 1998

Unsulu 2001

B. Unsulu, S. Sunol, A. Sunol , J. Non-Cryst. Solids 279, 2001, 110

van Bommel 1995

M. J.van Bommel, A.B. de Haan, J.Non-Cryst.Solids 186, 1995, 78

Vandana 1997

V. Vandana, A.S. Teja, Fluid Phase Equilibria 135, 1997, 83

Vetere 1998

A. Vetere, Fluid Phase Equilibria 148, 1998, 83

Wagh 1997

P.B. Wagh, G.M Pajonk, D. Haranath, A.V. Rao, Mat.Chem. and Phys. 50, 1997, 76

Wagh 1998

P.B. Wagh, A.V. Rao, D. Haranath, Mat.Chem. and Phys. 53, 1998, 41

Wagh 1999

P.B. Wagh, R. Begag, G.M. Pajonk, A.V. Rao, D. Haranath, Mat. Chem. and Phys. 57, 1999, 214

Wang 1993

P. Wang, PhD Thesis , Universität Würzburg, 1993

Wang 1994

P. Wang, A. Beck, W. Körner, H.Scheller, J.Fricke, J.Phys.D 27, 1994, 414

Westphal 1998

A.J. Westphal, M. Phillips, C. Keller, New Astronomy Reviews 42, 1998, 237

Woigner 1987

T. Woignier, J. Phalippou, J. Non-Cryst. Solids 93, 1987, 17

Woigner 1998-1

T. Woigner, J. Reynes, A. Hafidi Alaoui, I. Beurroies, J. Phalippou, J.Non-Cryst.Solids 241, 1998, 45

Woigner 1998-2

T. Woigner, J. Reynes, J. Phalippou, J.L. Dussussuy, N. Jacquet-Francillon, J.Non-Cryst.Solids 225, 1998, 353

Wong 1993

A.P.Y. Wong et al., Phys. Rev. Lett. 70, 1993, 954

Yao 2000

L.Z. Yao, C.H. Ye, C.M. Mo, W.L. Cai, L.D. Zhang, J.Non-Cryst.Solids 216, 2000, 147

Yoda 1996

S. Yoda et al. J.Non-Cryst.Solids 208, 1996, 191

Yoda 1999
    S. Yoda, S. Ohshima, J.Non-Cryst.Solids 248, 1999, 224

Yoda 2000
    S. Yoda, K. Ohtake, Y. Takebayashi, T. Sugeta, T. Sako, T.Sato, Materials Chemistry 10,
    2000, 2151

Yu 2002
    L.X. Yu, J.T.Wang, A.S.Hussain AAPS PharmSci 4, 2002, 1

Zegaoui 1996
    O. Zegaoui, C. Hoang-Van, M. Karroua, Appl.Catal.B 9, 1996, 211

ISA 1-6 (INTERNATIONAL SYMPOSIA ON AEROGELS)

1st ISA: Wurzburg, Germany, September 23-25 1985 Proceedings: "Aerogels" Ed. J. Fricke
        Springer Proceedings in Physics 6, Springer-Verlag (Berlin) 1986

2nd ISA: Montpellier, France, September 21-23, 1988Proceedings: Colloque de   Physique
        (Supplement au Journal de Physique, FASC. 4), C4-1989

3rd ISA: Wurzburg, Germany, September 30 - October 2, 1991; Proceedings: Journal of Non-
        Crystalline Solids vol. 145, 1992

4th ISA: Berkeley, California, USA. September 19-21, 1994; Proceedings: Journal of Non-
        Crystalline Solids vol. 185-6, 1995

5th ISA: Montpellier, France September 8-10, 1997; Proceedings: Journal of Non-Crystalline
        Solids vol. 225, 1998

7. Appendix
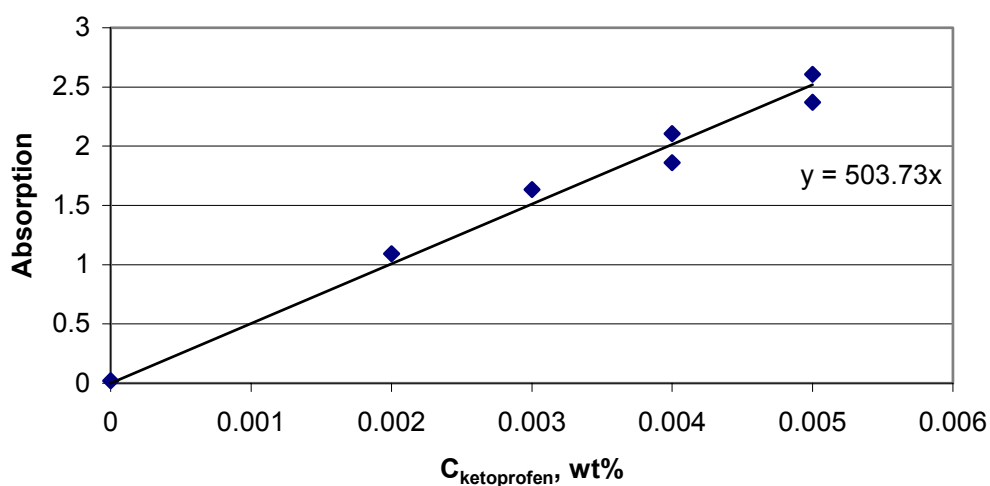
7.1. Calibration curves for UV Spectrometer

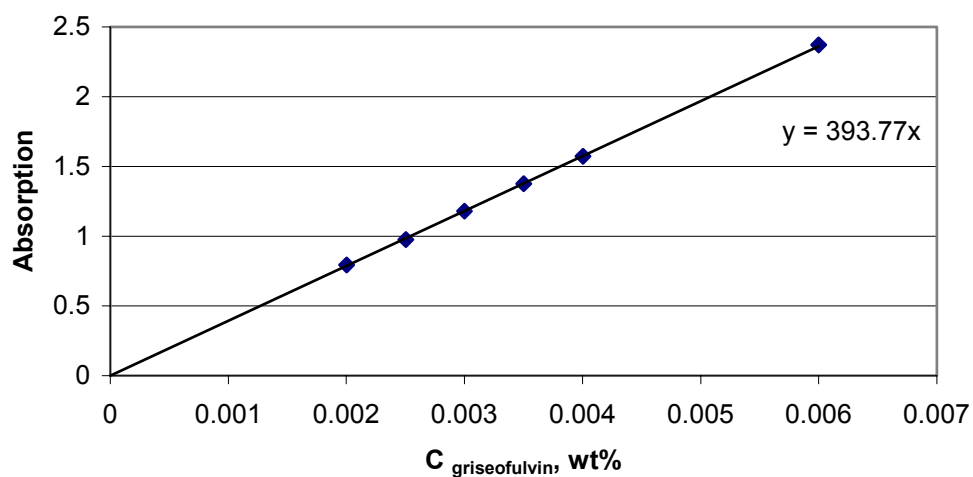**Figure 7-1 UV calibration curve for the system *ketoprofen* – acetonitrile**

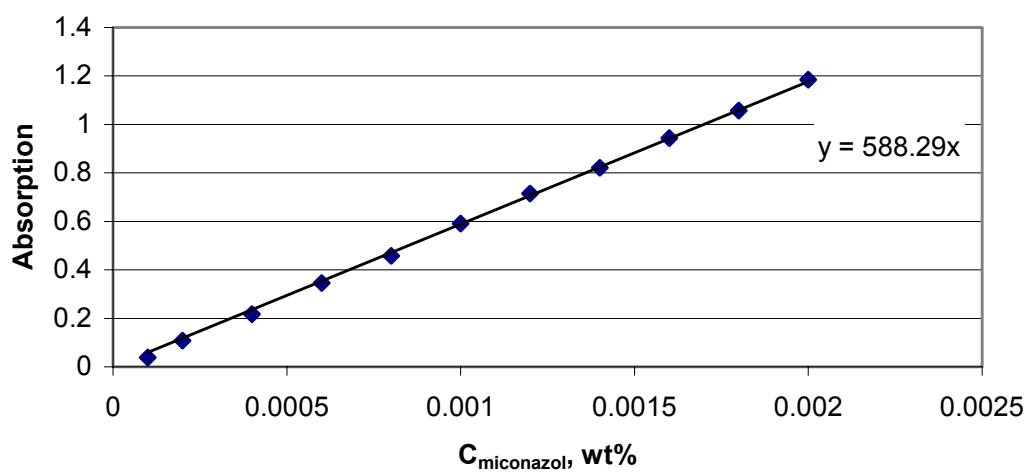**Figure 7-2 UV calibration curve for the system *griseofulvin* – acetonitrile**

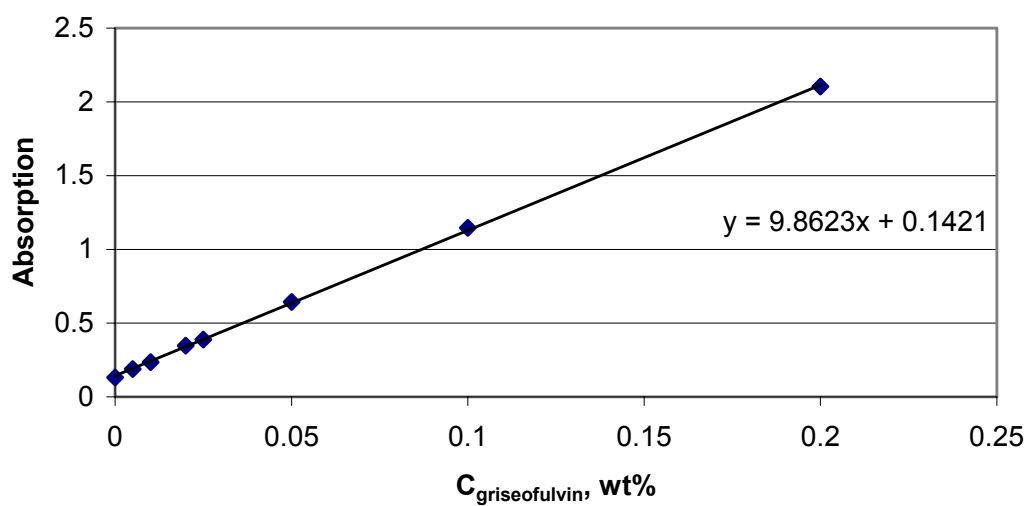**Figure 7-3 UV calibration curve for the system *miconazol* – acetonitrile**

Figure 7-4 UV calibration curve for the system *griseofluvin* – 0.1 N HCl
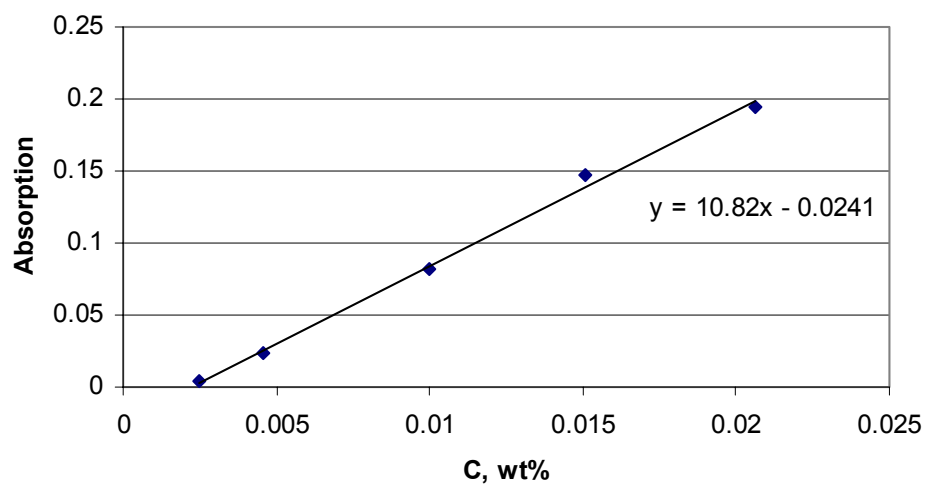
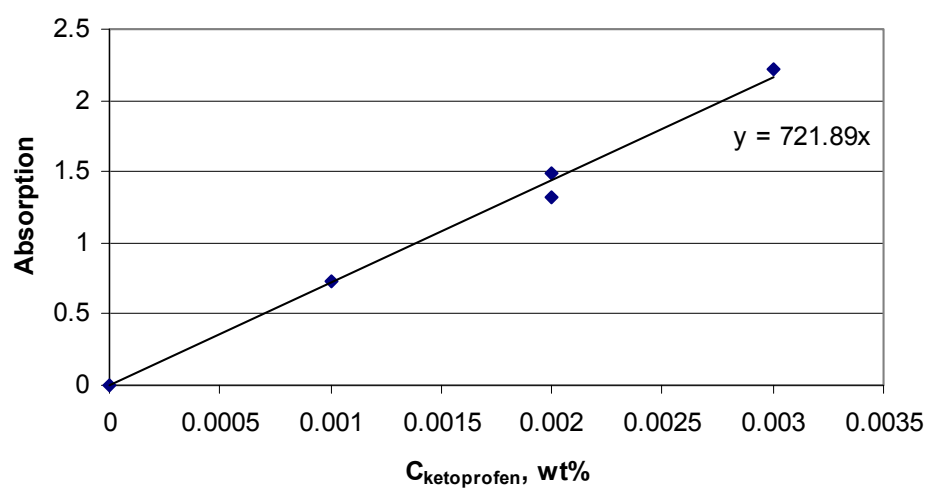**Figure 7-5 UV calibration curve for the system *miconazol* – 0.1 N HCl**

Figure 7-6 UV calibration curve for the system *ketoprofen* – 0.1 N HCl

7.2. Autoclave: technical drawings